COLLEGE OF ENGINEERING

VIRGINIA POLYTECHNIC INSTITUTE AND STATE UNIVERSITY

BLACKSBURG,
VIRGINIA

College of Engineering
Virginia Polytechnic Institute and State University
Blacksburg, Virginia 24061

VPI-E-74-3

STATISTICAL ANALYSIS OF LOW LEVEL
ATMOSPHERIC TURBULENCE

H. W. Tieleman*and W. W. L. Chen**

DEPARTMENT OF ENGINEERING SCIENCE & MECHANICS

January 1974

*Associate Professor
**Graduate Research Assistant
  Engineering Science & Mechanics Department
  Virginia Polytechnic Institute & State University
  Blacksburg, Virginia 24061

ABSTRACT

The statistical properties of low-level wind-turbulence data were obtained with the model 1080 total vector anemometer and the model 1296 dual split-film anemometer, both manufactured by Thermo-Systems Incorporated. The data obtained from the above fast-response probes were compared with the results obtained from a pair of Gill propeller anemometers.

The digitized time series representing the three velocity components and the temperature were each divided into a number of blocks, the length of which depended on the lowest frequency of interest and also on the storage capacity of the available computer. A moving-average and differencing high-pass filter was used to remove the trend and the low frequency components in the time series.

The degree of nonstationarity of each time series was determined by using a non-parametric statistical test on the statistical quantities calculated for each block in the time series. Besides the mean, the variances and the covariances of the fluctuating velocity components and the fluctuating temperature, spectral and cross-spectral estimates of each of the time series were obtained with the use of the fast Fourier transformation (F.F.T) technique. A special F.F.T. algorithmic with a no-bit reversal procedure for the analysis of series of long duration and high sampling rate (200 samples per second) has been developed.

In addition, a time series representing the streamwise fluctuating velocity component was simulated from the semi-empirical von Karman spectrum equation. The spectrum calculated from the simulated time series was compared with the original spectrum function from which the data was obtained.

The calculated results for each of the anemometers used are represented in graphical or tabulated form. The Fortran program for the entire data analysis procedure is listed in appendix B.

TABLE OF CONTENTS

LIST OF FIGURES

LIST OF TABLES

LIST OF SYMBOLS

$A_i(n)$	The ith time series consists of n finite samples
$\bar{A}_i^m$	The mean value of ith time series in block number m in sensor oriented coordinate system
$\bar{A}_i^{m*}$	The mean value of ith time series in block number m in probe oriented coordinate system
$\bar{A}_i$	Sample mean of the ith time series
A_t^I	Input data at time t before digital filtering
A_t^O	Output data at time t after digital filtering
$\tilde{A}_r$	Complex value defined by Eq. (3.5.13)
$a_i(n)$	The ith filtered time series of n finite samples
a_k	K^{th} sample of the discrete time series as defined by Eq. (3.5.21)
$\bar{a}_i^m$	Block mean value of the ith filtered time series as defined by Eq. (2.4.3)
$a_k^{'m}$	K^{th} sample of a discrete time series for block m as defined in Eq. (3.6.1)
$\tilde{a}_{1_r}, \tilde{a}_{2_r}$	Two real values defined in Eq. (3.5.13)
$\tilde{a}_r^m(f)$	Fourier transform defined in Eq. (3.6.1)
$\overline{a_i a_j}^m$	Variances (i = j) and covariances (i $\neq$ j) of the filtered time series for i,j = 1,2,...,4 in block m with near zero mean

ix

$\overline{a_i a_j}^{m*}$	Variances ($i = j$) and covariances ($i \neq j$) of the filtered time series for $i,j = 1,2,\ldots,4$ in block m with exact zero mean
$\overline{a_i a_j}$	Sample variances ($i = j$) and covariances ($i \neq j$) as defined in Eq. (2.4.4)
$\overline{a_i a_j}^{*}$	Sample variances ($i = j$) and covariances ($i \neq j$) as defined in Eq. (2.4.5)
B_e	Effective resolution bandwidth
B_k	Fourier coefficients for $k = 0,1,2,3$ defined in Eq. (3.5.25)
$\tilde{B}_r$	Complex value defined in Eq. (3.5.13)
b_ℓ	Decomposed time sequence consists of even-numbered samples for $\ell = 0,1,2,3$ defined in Eq. (3.5.24)
$b_k^{'m}$	K^{th} sample of a discrete time series in block m defined by Eq. (3.6.10)
$\tilde{b}_{1_r}, \tilde{b}_{2_r}$	Two real values defined by Eq. (3.5.13)
C_k	Fourier coefficients for $k = 0,1,2,3$ in Eq. (3.5.25)
$\tilde{C}_r$	A complex spectral series as defined in Eq. (3.5.12)
$\tilde{C}_r^m(f)$	Complex Fourier coefficients for block m calculated by Eq. (3.6.10)
$\tilde{C}_{N-r}^{*}$	Complex conjugate of $\tilde{C}_{N-r}$
$\tilde{C}_{r_1}^m(f), \tilde{C}_{r_2}^m(f)$	Complex Fourier coefficients calculated by Eq. (3.6.11) and (3.6.11) respectively
$\tilde{C}_{n-r}^{m*}(f)$	Complex conjugate of $\tilde{C}_{n-r}^m$

C_ℓ — Decomposed time series consists of odd-numbered samples for $\ell = 0,1,2,3$ in Eq. (3.5.24)

$\tilde{C}_r$ — A complex time series

$C_k'^m(t)$ — Kth sample of a complex time series defined by $C_k'^m = a_k'^m + j\, b_k'^m$ for block m and $j = \sqrt{-1}$

$C_{aa}(k)$ — Auto-correlation functions for lag k of time series a_i

$C_{ab}(k)$ — Cross correlation function for lag k between time series a_i and b_i

$CO_{ab}(f)$ — Cospectrum between time series a_i and b_i

$Coh^2_{abr}(f)$ — Smoothed squared coherence estimated as given by Eq. (3.6.17)

D_k — Fourier coefficients for $k = 0,1$ as defined by Eq. (3.5.27)

D_ℓ — Decomposed shorter time sequence for $\ell = 0,1$ as defined in Eq. (3.5.27)

$E[\ ]$ — Expected value of any argument inside the bracket

E_x, E_y — Gill anemometer output voltages

E_k — Fourier coefficients for $k = 0,1$ as defined in Eq. (3.5.27)

E_{ij} — 4 x 4 coordinate transformation matrix as defined in Eq. (2.4.3)

e_ℓ — Decomposed shorter time sequence for $\ell = 0,1$ as defined by Eq. (3.5.27)

F_k — Fourier coefficients for $k = 0,1$ as defined in Eq. (3.5.27)

f'_ℓ	Decomposed shorter time sequence for $\ell = 0,1$ as defined by Eq. (3.5.27)
f_i	Frequency
Δf	Frequency bandwidth
f_s	Nyquist frequency
f_{max}	Maximum frequency
$G(f)$	Defined by Eq. (3.2.9)
$G(f_i)$	Spectral value at i^{th} frequency
$G_p(f)$	Spectral density function with periodic function f in Eq. (3.2.12)
$\hat{G}_a(f)$	Power spectral estimate of discrete time series a_i
$\hat{G}_{ar}^{m}$	r^{th} power spectral estimate for block m of time series a_i
$\hat{G}_{ar}$	r^{th} power spectral estimate after smoothing
$\hat{G}_{abr}^{m}$	r^{th} cross spectral estimate for block m between time series a_i and b_i
$\hat{G}_{abr}$	r^{th} cross spectral estimate between time series a_i and b_i after smoothing
$G_k(f_i)$	Spectral values at i^{th} frequency in k blocks
$\overline{G}(f_i)$	Smoothed spectral estimates after applying segment averaging in Eq. (3.4.1)
$\hat{G}(f_k)$	Smoothed spectral estimates after applying frequency smoothing in Eq. (3.4.2)
$g_j^{(k)}$	Filter function used in Eq. (3.1.11)
$H(f)$	Frequency response function defined in Eq. (2.3.5)

$H_r(f)$	Spectral values defined by Eq. (3.5.1)
H_f	Discrete spectral values defined in Eq. (3.1.8)
H_f^*	Complex conjugate of H_f
$\hat{H}_r^m(f)$	Blocked spectral values as defined in Eq. (3.6.1)
H_0	The test hypothesis of no trend present
$I(f)$	Filter shape defined in Eq. (2.3.10)
j_ℓ, K_ℓ	Equal to 0 or 1 for all ℓ
K	Defined in Eq. (3.5.44)
K_r'	Fourier coefficients for $r = 0,1$ as defined in Eq. (3.5.27)
k_ℓ'	Decomposed shorter time sequence for $\ell = 0,1$ as defined in Eq. (3.5.27)
L	Number of data twice the total number in one block
ℓ	Average values used in frequency smoothing
M	Total of blocked time series
m	Block number
$N(0,1)$	Standard normal distribution
N	Total number of samples in a time series
n	Number of data points in the blocked time series
p	Integer value larger than one
P_T	Probability for event T
r	Defined in Eq. (3.5.30)
S_i	A set of block variables defined for $i = 1,2,\ldots,M-1$
S'	$T + \frac{1}{2}$, the normal variable
T	Total number of reverse arrangement

T_i	The number of reverse arrangements for given index i
T_{ij}	Defined in Eq. (2.2.1)
T_U	Upper limit of the confidence interval
T_L	Lower limit of the confidence interval
T^*	Defined in Eq. (2.2.5)
T^*_α	Percentile of the standard normal distribution as tabulated in Table 1
U'	Defined in Eq. (3.3.7)
$\overline{U_i}$	Mean velocity components when $i = 1,2,3$ and mean temperature when $i = 4$
$\overline{U_i}^m$	Mean velocity components when $i = 1,2,3$ and mean temperature when $i = 4$ in blocked time series m
u_i	Fluctuating velocity component when $i = 1,2,3$ and fluctuating temperature when $i = 4$
$\overline{u_i u_j}$	Variance $(i = j)$ and covariance $(i \neq j)$, $i,j = 1,2,\ldots4$ of the fluctuating components in the mean wind direction
VAR[ ]	Variance of the argument inside the bracket
W	Exp. $[-i2\pi/N]$
W(t)	Equally-weighted function defined in Eq. (2.3.4)
$w_1(t)$	Data window No. 1
$w_2(t)$	Data window No. 2
$W_1(f)$	Spectral window function of data window No. 1
$W_2(f)$	Spectral window function of data window No. 2
W_t	Cosine taper data window defined in Eq. (3.3.1)
X,Y,Z	Sensor oriented coordinate system

$x^* y^* z^*$ Probe oriented coordinate system

$x\ y\ z$ Coordinate system in the mean wind direction

α Probe pitch angle as shown in Figure 1-C or confidence level in statistical test

β Probe yaw angle as shown in Figure 1-C

β_m Probe yaw angle in block m

γ $2B_eT$, the number of degrees of freedom

μ $\dfrac{M(M-1)}{4}$, the normal variable

π 3.14159

σ $VAR[\ ]^{\frac{1}{2}}$, the standard deviation of the argument inside the bracket

$\Phi(\ )$ Standard normal cumulative distribution function of the argument inside the parenthesis

χ_γ^2 Chi-square distribution with γ degrees of freedom

CHAPTER I

INTRODUCTION

With the increasing necessity of understanding the effect of the turbulence on human activities in the atmospheric boundary layer, the knowledge of wind and temperature fluctuations becomes essential. This dissertation presents a statistical analysis of fluctuating wind data consisting of three velocity components for each of the three spatial directions and temperature in the time domain. Correlations and spectra will be calculated by using the experimental data obtained from T.S.I. split - film anemometers and a consequent data acquisition system as reported by Tieleman et. al. [95].

1.1 STATEMENT OF THE PROBLEM

Although geophysical flows provide much larger Reynolds numbers than wind tunnel flows, relatively few accurate results of the wind turbulence measurements in the atmospheric boundary layer are available because of the complexity and inadequacy of the required instrumentation. Existing measuring equipment usually cannot provide enough information for the three dimensional structure of the turbulence and its evolution with time. The selection of the three dimensional split-film anemometer (TSI-1080D) in this research program has many advantages over most of the presently used anemometers [95].

1

Insufficient knowledge of the ground wind structure is due to a lack of extensive experiments and due to large volumes of data necessary to obtain accurate and meaningful results. In order to understand the microstructure of turbulence, we must not only consider the energy spectrum but also several statistical quantities which are relevant to the basic mechanics of the motion of the air. The measurement of the ground wind structure and its statistical analysis becomes essential to the solution of such practical problems in the atmospheric boundary layer as low altitude operations of aircraft, design of many engineering structures, and atmospheric diffusion. It is therefore imperative to improve statistical calculation techniques of the measured quantities especially when dealing with large volumes of data even beyond the storage capacity of the existing computers.

The purpose of this dissertation is to analyse the data based upon the general aspects of time series analysis. First, the analysis in the time domain where the means, variances and covariances of blocked subseries are calculated. Second, the analysis in the frequency domain where the power- and cross- spectral density estimations are calculated.

The power spectrum which provides an insight to the spectral distribution of the kinetic energy of the turbulence, is basic to the understanding of the structure of the turbulence. The cross spectrum concerns itself primarily with the transport and conversion of energy and the transport of momentum and heat in the surface layer. All of these are fundamental in the understanding of micrometeorological processes in the atmosphere. The real part of the cross spectrum is

called cospectrum which for example, shows the effect of height above the ground on the scale of the eddies. The imaginary part of the cross spectrum is called quadrature spectrum which gives some information about the vertical extent of eddies. Therefore the spectral behavior of atmospheric turbulence is of considerable and practical importance.

Power and cross-spectral analysis of meteorological time series are generally based on the assumption that these series are stationary in the sense that their statistical properties are invariant with translations in time. At present, there exist techniques to analyse stationary time series records, but the techniques available for the analysis of non-stationary time series records are still inadequate and do not lend themselves to meaningful interpretations of physical problem. It is therefore necessary to use proper filtering techniques to adjust the non-stationary time series so that under certain circumstances the existing statistical analysis for stationary time series may be used on these non-stationary data. It is also assumed that the time series are ergodic which permits time averaging to be used in place of ensemble averaging.

Meteorological time series can mostly be represented as the sums of periodic (regular) and stationary (irregular) components since they almost always contain some definite periods, such as days, years or even decades etc. The longer than record length trends must be filtered out in order to eliminate the bias introduced in the spectral calculations. A moving-average and differencing high-pass filter is applied to our time series so as to create a new, mean free, time series.

There are methods available to calculate the correlation functions via the fast Fourier transform method and to apply the thoroughly studied lag window to obtain the smoothed spectrum. For large volumes of data this is not considered to be an economical and practical approach. Development of direct Fourier transform methods as applied to meteorological data and consequent smoothing techniques are still in their infant stages and have not been thoroughly studied. The reason for this is partly due to the potential flexibility of the fast Fourier transform, which is much greater than the indirect or Blackman-Tukey method.

The direct Fourier transform method or the periodogram approach is used for the calculations of power and cross spectra in this dissertation. A new algorithm is developed for the fast Fourier transformation which requires no bit-reversal procedures during the final stages of the calculations. A computer program based on non bit-reversal calculations is developed. Various time-domain smoothing functions have been applied to check the spectral variation. The calculated power and cross spectra agree fairly well with those reported in the literature of atmospheric turbulence.

1.2 REVIEW OF LITERATURE

The significance of correlation between the velocity of a fluid particle at one time and that of the same fluid particle at a later time or between simultaneous velocities at two fixed points was developed in 1921 by G. I. Taylor [90]. Taylor [91] further defined the scale of turbulence when it is applied either to the Lagrangian or to

the Eulerian concepts of fluid flow. The connection between the spectrum measured at a fixed point, and the correlation between simultaneous values of velocity measured at two points was also proposed by Taylor [92] in 1938. He pointed out that the correlation and the spectrum formed a Fourier transform pair.

In general there exist two methods for the digital spectral analysis of stationary time series. The method which requires to calculate the correlation function first before taking its Fourier transformation to obtain the spectral density function is called the indirect method. Instead of calculating all the correlation functions, the direct method of computing spectral-density estimates is achieved by squaring the quantity which is obtained directly from the Fourier transformation of the raw observations.

The spectral analysis using the indirect method has become a significant tool in the statistical analysis of stationary time series since the pioneer work of Daniel [22] and Bartlett [3,4]. They estimated consistent estimates of the spectral density function by modification of the classical periodogram (i.e. harmonic) analysis. Optimum consistent estimates of the spectrum of a stationary time series were studied by Parzen [74]. Most of the work involving spectral analysis was done primarily by mathematical statisticians in the fifties. The practical situation of designing a spectral analysis satisfying many specific conditions had not been studied until Blackman and Tukey [10] in 1958.

With the advent of the electronic computers and improvement in numerical calculation techniques in spectral analysis, many valuable papers were published in the earlier Sixties (Jenkins[49], Parzen [75], Tukey [96]). The users of the spectral analysis were still faced with the problem that if only a sample record of finite length is given, and no background information is available, there still existed no precise method of obtaining an estimate which could be considered the most accurate one. One can actually construct many estimates of the spectrum by using different smoothing techniques, yet the optimum one, relies on the role of the chosen bandwidth [84].

The spectral calculations via correlation functions or indirect method have been theoretically well established in the early Sixties. The periodogram approach or direct Fourier transform method in the time series analysis had been considered to be impractical because of the amount of computations involved. Actually, the periodogram as an estimate of the spectral density function of a stationary time series has had a long and controversial history starting with A. Schuster in 1898 when he was investigating the hidden oscillations in meteorological phenomena with periods of 26 days. In 1965, Jones [53] reappraised the periodogram in spectral analysis and pointed out some advantages over the indirect method for multiple dimensional processes.

During the controversy over the choice of direct or indirect approach to the calculation of the spectrum of stationary time series, the revolutionary paper on the Fourier transformation by Cooley and Tukey [19] was published in 1965. The algorithm they presented for the calculation of complex Fourier series permits the reduction of

operations by a factor of $N^2/(N \log_2 N)$ for a data sample length N. The latter should have a magnitude which is equal to an integer power of two. The operation consists of a complex multiplication followed by a complex addition. Numerous papers have been published to improve the algorithm or to explain the paper by Cooley and Tukey through different mathematical formulations. Ferrie [28] studied the relative advantages and disadvantages of various algorithms on the basis of execution time, storage and accuracy. He concluded that no single fast Fourier transform algorithm represents the best choice.

Following the discovery of the FFT (Fast Fourier Transform) algorithm, earlier methods [10,75] no longer can be relied upon for the best statistical and computational procedures. Bingham et. al. [9], Cooley et. al. [18] and Welsh [105] presented various techniques for the estimation of power and cross- spectra via FFT, whose applications in electronic engineering have been published in two exclusive issues in June 1967 and June 1969 of IEEE transactions on Audio and Electroacoustics.

The direct and indirect methods do not produce the same results though both have relative advantages [27]. For a spectrum with a large slope, the direct method permits more window leakage than the indirect method. The indirect or correlation function method is more effective than the direct FFT or periodogram method in computing the spectrum of short time series. For large data samples, the direct or FFT method seems to be the only feasible one. The indirect method has

been considered not practical to handle a time series exceeding 50,000 data points for spectral estimations.

Oort and Taylor [69] applied the FFT technique to analyse the spectrum of the horizontal wind speed and to investigate the diurnal variability in the kinetic energy. Ryznar [85] measured wind and temperature profiles and turbulent fluctuations of wind velocity and temperature under various stability conditions of horizontally homogeneous turbulence in the atmospheric surface layer. He concluded that the integration of the spectrum did not obtain the corresponding total variance prior to the spectral transformation. The reason is obviously due to the application of a "cosine bell" data window which reduced the variances of the spectral density estimate by a factor of 3/8 [43]. Kaimal et. al. [55] calculated power spectra and cospectra of turbulence in the surface layer using the fast-Fourier transform technique. A new short time series was generated from the original time series by averaging the neighboring data points to investigate the information in the lower frequency range.

Most of the books written on time series analysis such as Anderson [2], Grenander and Rosenblatt [41], Hannan [42], Wold [106] and the Brown symposium edited by Rosenblatt in 1963 [24] are concerned almost exclusively with theory. Practical applications of time series analysis started with Blackman and Tukey [10], though it was primarily from the point of view of the communication engineer. Books such as Brown [13], Fishman [31] and Granger and Hatanaka [39] provide a heuristic introduction to economic time series. The books

worthy of engineering applications are Bendat and Piersol [6], Jenkins and Watts [51], Otnes and Enochson [67] and the Wisconsin seminar edited by B. Harris [72] in 1966.

The problem of obtaining the best spectral estimate via the fast Fourier transform lies in the selection of the smoothing function which depends also on the type of the data to be analyzed. In dealing with different types of data such as atmospheric wind data, biological data, acoustical data or economical data, the selection of the same smoothing function could lead to different interpretable results. Only by the proper choice of a suitable smoothing function in spectral analysis can meaningful results be achieved.

CHAPTER II

DATA PROCESSING SYSTEM

The atmospheric wind turbulence data are collected through a three-dimensional split film anemometer (TSI-1080D) which consists of three split film sensors and a copper-constantan thermocouple for ambient temperature measurement. Each sensor consists of a 0.006 inch diameter quartz rod coated with a platinum film of approximately 1000 Å in thickness. The total sensor length is 0.200 inches with approximately 0.08 inches of active usage.

Data was sampled at a rate of 200 samples per second, and a special data acquisition and handling system has been developed to handle samples of half an hour duration. Detailed explanation of the data acquisition and handling system was presented in a report by Tieleman et. al. [95].

The data acquisition and data handling system was located in an instrumentation trailer positioned near the V.P.I. and S.U. low speed windtunnel. The instruments were used with a 350 ft. long connecting cable since mounting on the 300 ft. meteorological tower at NASA Wallops Station was proposed. After lengthy calibration in the low speed windtunnel, the probes were mounted in the atmosphere on top of the exchange section of this windtunnel. Since only a limited amount of time was available to test the probes in the atmosphere and

also since movement of the instrumentation trailer was a rather complicated operation, the instruments were tested in the atmosphere at the best location which could be reached with the 350 ft. cable from the position of the instrument trailer. The air flow on the top of the exchange section of the windtunnel (approximately 40 ft. above the ground) was a great deal influenced by surrounding buildings as well as the windtunnel and the exchange tower itself.

In addition to the fast response T.S.I. probes, two slower response Gill anemometers (see Appendix A) were positioned next to the T.S.I. probe so that comparisons could be made. The T.S.I. probes were positioned in a horizontal plane and could be rotated about a vertical axis by an antenna rotor into the prevailing wind direction. In the report by Tieleman et. al. [95] it was concluded among other things that the T.S.I. probes could operate with the best accuracy when they were directed into the mean wind.

The two Gill anemometers were mounted also on the antenna rotor so that the three sensors could be moved all simultaneously. One of the Gill anemometers was mounted parallel to the T.S.I. probe and the second Gill anemometer was mounted perpendicular to the first one in the horizontal plane. Only two Gill anemometers were available so that only statistics from the two horizontal components could be compared.

2.1 STATISTICAL ANALYSIS

Digitized data from the wind sensors were written on a 9-track magnetic tape in blocks with 209 samples in each block. Computer programs were developed [95] to convert the raw data from analog

voltages to velocity components and temperature by using IBM 370/155 digital computer.

The computed velocity components and temperature were again stored on a 9-track magnetic tape with the block size increased twice to 418 points in order that slight reduction in data-storage space on the tape and a saving of calculation time in the computer could be achieved.

The data was collected at a rate of 200 samples per second, and therefore 360,000 samples were recorded during a half hour period. The sample size N is determined by the total recording time T and by the sampling interval Δt through the following relationship

$$N = \frac{T}{\Delta t} \quad .$$ (2.1.1)

The sampling rate, f_s, of the collected data is considered as an important factor in the data reduction process. This rate is the key to the determination of the Nyquist frequency, f_n which is the highest frequency one can obtain without introducing aliasing. The sampling rate and the Nyquist frequency are related by the following expression

$$f_n = \frac{1}{2} f_s \quad .$$ (2.1.2)

Let $A_i(n)$, $i = 1,2,\ldots,4$ represent the three velocity components and the temperature recorded by the T.S.I. probe. The first three subscripts 1,2,3 denote the components of the instantaneous velocity vector in the coordinate system as determined by the directions of the sensors

on the T.S.I. probes (X, Y, Z). Subscript 4 represents the temperature at the point where the probe is located.

The time series are divided into many blocks. The determination of the number of data points in each block depends primarily on the storage capacity of the available digital computer. The maximum number of data points should be chosen so that enough spectral information may be obtained in each block during subsequent spectral analysis. The basic requirement is that the selected block size should be long compared to the random fluctuations of the time history. The sample mean and the sample probe yaw angle are calculated from the block mean and the block probe yaw angle. The mean value, the probe yaw angle, and the variance in each block may be used to test the sample for stationarity as described in section 2.2.

2.1.1 MEAN VALUES IN EACH BLOCK

The sample is broken into M non-overlapping blocks each of which contains n points, so that $Mn = N$. The wind turbulence data may be considered to be a combination of a mean component and a fluctuating component. For a given number of n data points of the i-th time series A_i (n) in each block, the mean component may be described if ergodicity is assumed by the average value of all n values,

$$\overline{A}_i^m = \frac{1}{n} \sum_{j=1}^{n} A_i(j), \quad i=1,\ldots,4, \tag{2.1.3}$$

where subscript i refers to the number of the time series and superscript

m denotes the block number and the bar describes mean value. By choosing n = 8192 and M = 44, we are analysizing 360,448 data points in approximately a sample of one half hour duration. The choice of 8192 data points for each block is to meet the requirement for appliation of the fast Fourier transform algorithm that the number of data points to be transformed must be a power of two. Also storage restrictions in the digital computer limits the block size.

2.1.2 PROBE YAW ANGLE IN EACH BLOCK

For each block of data points, a probe yaw angle β_m is calculated based on the previously obtained block mean values. The probe yaw angle is determined by the angle between the T.S.I. probes and the direction for which the lateral component of the mean velocity vanishes. This last direction fixes the so-called mean wind coordinate system. The x-direction is the direction of the mean wind, the y-direction (lateral direction) perpendicular to the x-direction in the horizontal plane and the z-direction is vertically upward.

The velocity components calculated initially in the coordinate system as determined by the directions of the sensors on the T.S.I. probes have to be transformed into components in the mean wind coordinate system for which the statistical quantities of the fluctuating velocities are of interest.

The transformation of the velocity components from one coordinate system to the other is carried out in two steps. First, one obtains the components in the probe oriented coordinate system by the following relationship

$$\bar{A}_j^{m^*} = E_{ij} \bar{A}_i^m , \qquad (2.1.3)$$

where E_{ij}, $i=1,2,3$ and $j=1,2,3$, are the direction cosines for the sensor oriented coordinate directions X Y Z and the probe oriented coordinate directions x*y*z*, the geometry of which is shown in Fig. (1a). It is seen that the x* coordinate direction coincides with the probe axis, the origin of which is located at the probe tip. The y*-axis is perpendicular to the probe in a horizontal plane while z*-axis is vertically upward.

Through geometric relations, Eq. (2.1.3) may be written in the following matrix form

$$\left\{ \begin{array}{c} \bar{A}_1^{m^*} \\ \bar{A}_2^{m^*} \\ \bar{A}_3^{m^*} \end{array} \right\} = \left[\begin{array}{ccc} 0.57735 & 0.57735 & 0.57735 \\ 0 & 0.70711 & -0.70711 \\ -0.8165 & 0.40824 & 0.40824 \end{array} \right] \left\{ \begin{array}{c} \bar{A}_1^m \\ \bar{A}_2^m \\ \bar{A}_3^m \end{array} \right\} \qquad (2.1.4)$$

The second step is to transform to the mean wind coordinates. This further transformation between the probe oriented coordinate system x*y*z* and the coordinate system in the mean wind direction x, y, and z, as shown in Fig. (1b), may be achieved by the following relationship

$$\bar{U}_j^m = E_{kj} \bar{A}_k^{m^*} \qquad j=1,2,3 \qquad (2.1.5)$$

or in matrix form

$$\begin{Bmatrix} \overline{U}_1^{-m} \\ \\ \overline{U}_2^{-m} \\ \\ \overline{U}_3^{-m} \end{Bmatrix} = \begin{bmatrix} \cos\beta & -\sin\beta & 0 \\ \\ \sin\beta & \cos\beta & 0 \\ \\ 0 & 0 & 1 \end{bmatrix} \begin{Bmatrix} \overline{A}_1^{m^*} \\ \\ \overline{A}_2^{m^*} \\ \\ \overline{A}_3^{m^*} \end{Bmatrix} \qquad (2.1.6)$$

By combining the Eqs. (2.1.4) and (2.1.6) one can determine the x component of the block mean as follows

$$\overline{U}_1^m = 0.57735 \cos\beta \cdot \overline{A}_1^m + (0.57735 \cos\beta - 0.70711 \sin\beta) \overline{A}_2^m$$

$$+ (0.57735 \cos\beta + 0.70711 \sin\beta) \overline{A}_3^m . \qquad (2.1.7)$$

Maximizing the mean wind component in the x-direction with respect to the probe yaw angle (i.e., $d\overline{U}_1^m/d\beta = 0$, or similarly vanishing of $\overline{U}_2^m$) one obtains an expression for the block yaw angle

$$\tan\beta_m = -1.22457 \frac{\overline{A}_2^m - \overline{A}_3^m}{\overline{A}_1^m + \overline{A}_2^m + \overline{A}_3^m} , \quad m=1,2,\ldots,M . \qquad (2.1.8)$$

The change of the probe yaw angle in each block indicates the shifting of the mean wind as averaged over 40.96 seconds (the latter is the total real time for each block). If there are significant changes in the block yaw angle from one block to the next, then we have reasons to believe the data to be nonstationary. The

same expressions 2.1.4, 2.1.6, and 2.1.8 may be used to determine the sample yaw angle and consequently the sample means, sample variances and sample covariances of the velocity components in the x,y,z coordinate directions.

2.1.3 Block Variances of the Time Series

The variances of the velocity components and temperature for each block are determined by the following equation

$$\overline{\sigma_i^2}^m = \frac{1}{n} \sum_{j=1}^{n} A_i(j) A_i(j) - (\overline{A}_i^m)^2 \ , \quad i=1,...,4 \qquad (2.1.9)$$

where the subscripts 1,2,3 represent the three velocity components and subscript 4 denotes the temperature. The positive square root of the variance is called the standard deviation and is calculated by

$$S_i^m = (\overline{\sigma_i^2}^m)^{1/2}, \quad i=1,...,4 \qquad (2.1.10)$$

where m again denotes the block number. The block standard-deviations calculated by Eq. (2.1.10) will also be used to determine the non-stationarity of the data by using a statistical test which will be discussed in section (2.2).

2.1.4 Sample Mean and Sample Probe Yaw Angle

The sample mean and the sample probe yaw angle are simply determined from the arithmetic averages of the block mean values and the block yaw angles in each sample by the following formulas

$$\bar{A}_i = \frac{1}{M} \sum_{m=1}^{M} A_i^m , \quad i=1,\ldots,4 \qquad (2.1.11)$$

and

$$\tan\beta = -1.22475 \left(\frac{\bar{A}_2 - \bar{A}_3}{\bar{A}_1 + \bar{A}_2 + \bar{A}_3}\right) , \qquad (2.1.12)$$

where M is the total number of blocks or subseries.

The sample mean value and the sample probe yaw-angle will be used to determine the velocity components in the mean wind coordinate system by the transformation (2.1.4) and (2.1.6).

Following the determination of the sample mean values for each of the three velocity components and the sample probe yaw angle in the data processing computer program called "DATP1", the trend and long period fluctuations will be removed through a program called "TREND". The theory of this filtering process will be described in section (2.3). The filtered data will be used to compute sample variances and co-variances as well as their respective values in the mean wind direc-tions through coordinate transformations. These computations will be included in another data processing computer program called "DATP2".

2.2 Statistical Test

The computed statistical properties for each block as described in the previous section 2.1 from a single sample record can be used to test the stationarity of the time series. The wide variations of the probe yaw angle may indicate relatively large angular shifts in the wind direction .

If the statistical properties thus calculated do not vary significantly from one block to the next, one may be assured to a certain degree stationarity of the time series. Otherwise, the data of interest might contain nonstationarities and are not fit for further analysis.

Without the detailed knowledge of the frequency composition of the calculated statistical properties, a non-parametric approach is necessary to determine whether or not the data are stationary [6]. A non-stationary trend test in either the mean or the variance is adapted from Kendall and Stuart [58]. The theoretical derivation is based on a paper written by Mann [65].

Suppose the block mean of each of the velocity components or the block yaw angle or their standard deviations are denoted by

$$S_1, S_2, S_3, \ldots, S_M,$$

where M denotes the total number of blocks in the sample.

Now, a reverse arrangement of such a set of block variables is defined as to occur every time

$$S_j > S_i, \qquad \text{for all } j > i$$

and $i = 1,2,3,\ldots, M-1$.

For a given value of index i, the number of reverse arrangements for this given i is denoted by T_i such that

$$T_i = \sum_{j=i+1}^{M} T_{ij}, \qquad (2.2.1)$$

where

$$T_{ij} = \begin{cases} 1 & \text{if } S_j > S_i \\ 0 & \text{if } S_j \leq S_i \end{cases}$$

20

Now, the total number of reverse arrangements is expressed by

$$T = \sum_{i=1}^{M-1} T_i = \sum_{i=1}^{M-1} \sum_{j=i+1}^{M} T_{ij} \ . \qquad (2.2.2)$$

In the case the set of block variables shows an upward trend as far as their magnitude is concerned, the total number of reverse arrangements can be expected to be some relatively large number. Conversely, if the set shows a downward trend the total number of reverse arrangements is relatively small. If no discernible trend is present the total number of reverse arrangements is some intermediate number.

The hypothesis H_0 of no trend present against the alternative of a trend being present at an α-level of significance can be expressed by

$$\text{Reject } H_0 \text{ if} \qquad T > (\tfrac{\alpha}{2}; M), \quad T < t(1 - \tfrac{\alpha}{2}; M)$$

$$(2.2.3)$$

$$\text{Accept } H_0 \text{ if} \qquad t(1 - \tfrac{\alpha}{2}; M) < T < t(\tfrac{\alpha}{2}; M).$$

In other words this hypothesis is similar to a symmetric 2-sided confidence interval for T, with a confidence coefficient, $1 - \alpha$, and a lower limit, $T_L = t(1 - \tfrac{\alpha}{2}; M)$. Therefore, for all T,

$$P_T \{ T_L < T < T_U \} = 1 - \alpha \ . \qquad (2.2.4)$$

For a large number of block variables (i.e. larger than 10), a normal distribution for the total number of reverse arrangements of each set of block variables can be assumed. So that, the estimated value of T, T^* can be given by [64]

$$T^* = \frac{T - E[T]}{[VAR(T)]^{1/2}} \quad , \tag{2.2.5}$$

where the average value and the variance of the total number of reverse arrangements of each set are found to be

$$E[T] = \frac{M(M - 1)}{4} \quad , \tag{2.2.6}$$

and

$$VAR[T] = \frac{2M^3 + 3M^2 - 5M}{72} \tag{2.2.7}$$

respectively. These expressions are only valid when the set of block averages does not show a trend.

The standard normal distribution function of the estimated values of T for an asymptotic $N(0,1)$ distribution when H_0 is true, is given by

$$\Phi[T^*] = \frac{1}{\sqrt{2\pi}} \int_{-\infty}^{T^*} e^{-\frac{S^2}{2}} \, dS \tag{2.2.8}$$

where

$$T^* = \frac{[T + \frac{1}{2} - \frac{M(M-1)}{4}]}{\sqrt{\frac{2M^3 + 3M^2 - 5M}{72}}} \qquad . \qquad (2.2.9)$$

The right hand side of eq. (2.2.9) is seen to be in the standarized form of $T^* = \frac{S' - \mu}{\sigma}$ where $S' = T + \frac{1}{2}$, $\mu = \frac{M(M-1)}{4}$, and $\sigma = \{VAR[T]\}^{1/2}$. If the normal variable S' is not "standard", its value must be standarized according to $T^* = \frac{S' - \mu}{\sigma}$ so that $P[T^* \le S'] = [\frac{S' - \mu}{\sigma}]$.

The probability that the value of T is less than T^* for a given α-level of significance can be written as

$$P[\ T < T^*_\alpha\ ] = \Phi\ [T^*_\alpha] = \alpha \qquad (2.2.10)$$

where T^*_α is the percentile of the standard Normal Distribution. By choosing different values of α, i.e. 0.95, 0.975, 0.99, the T^*_α value can be obtained from the standard distribution table [TABLE I]. For different values of T*, a table of reverse arrangement distribution has been generated by using eq. (2.2.9). For different α-level of significance, and different number of blocks M, the values of $t(\frac{\alpha}{2}; M)$ and $t(1 - \frac{\alpha}{2}; M)$ are given in Table II.

If the value of the total number of the reverse arrangements falls outside the range in our criterion eq. (2.2.4) for $\alpha = 0.05$, then a possible error of 5% can be made if the hypothesis that the data are

stationary is rejected. Clearly one wishes to commit such an error only rarely. If the value of T falls outside the range for $\alpha = 0.01$, then one will have less chance to make this error, and consequently one has more confidence to reject the hypothesis that the data are stationary.

This nonstationary trend test is generally effective in testing against linear or monotonic trends, as shown in Fig. 2 and ineffective against the type of nonstationarities as shown in Fig. 3 which show a reversal in the trend. The trend test is generally not successful in testing against the type of trends as shown in Fig. 4.

2.3 Removal of the Trend

Trend removal has been considered as an important step in the digital processing of random data. Large distortions can occur in the calculations of variances, covariances and spectral quantities if trends are not removed from the data.

Trend removal is a special case of a general filtering process. Filters are designed to pass either low or high frequencies of the signal while attenuating or eliminating respectively high or low frequency components. Filters, which pass low frequency components are called low-pass filters while others which pass high frequencies are called high pass filters. A third type of filters which passes a band of intermediate frequencies and attenuate both very low and very high frequencies in the signal are called band pass filter.

For meteorological time series, it is usually assumed that these series are statistically stationary and can be represented as sums of

regular (periodic) or irregular (stationary) components superimposed on each other. It is observed that these series almost always contain some definite periods that are due to certain external influences such as the time of day the data was taken and long periodic oscillations due to the presence of upstream obstacles. Since these periodic components may not enter into our statistical analysis of the observed time series some trend removal or filtering process is necessary.

2.3.1 Methods of Trend Removal

Different methods have been proposed for trend removal, the selection of an appropriate one depends largely on the practical situations. For small samples, plotting is the best way to compare the filtering effects upon the unfiltered time series. For samples with a large number of data points, calculation time becomes one of the essential factors to make the selection.

Dyer [25] suggested a modified difference filter applied to the meteorological data. However, the calculation of every auto-correlation coefficient between two neighboring values does not seem to be economical for the large volume of data encountered. Houbolt [47] proposed a high pass filter based on the idea of a symmetrical exponential filter. The requirement of making two passes in the calculation requires almost twice the computer time, which makes this method impractical.

It is generally known that the best way of estimating a trend is to use a polynomial of low order by the least square method, yet this method does not represent the trend satisfactorily. As a result, one frequently makes use of the method of moving average based on the

idea that although a low-order polynomial, say a cubic polynomial, may not approximate the trend very satisfactory over the whole time interval it may fit well over shorter intervals.

2.3.2 High Pass Filter

The high-pass filter applied to our data samples is obtained by first constructing the frequency response function of the equally-weighted moving-average low-pass filter which is the Fourier transform of the equally-weighted time function. The filter shape of the high-pass filter is obtained by squaring the frequency response function of the low-pass filter and then subtracted from unity. This particular high-pass filter is called the moving-average and differencing high-pass filter.

2.3.2.1 Weighting Function

Digital filtering is simply a process by which a set of input data A_t^I is transformed into a set of output data A_t^O by means of a linear expression

$$A_t^O = \sum_{k=-\frac{T}{2}}^{\frac{T}{2}} W_k \, A_{t+k}^I \, , \tag{2.3.1}$$

where W_k are the suitably chosen weights and T is called the filtering interval. Eq. (2.3.1) can be regarded as the numerical approximation of

$$A^O(t) = \int_{-\infty}^{\infty} W(\tau) \, A^I(t - \tau) \, d\tau \tag{2.3.2}$$

which states that the convolution of $W(t)$ and $A^I(t)$ produces $A^O(t)$.
The term $d\tau$ is usually absorbed in the following form

$$A^O_t = W_{-\frac{T}{2}} A^I_{t-\frac{T}{2}} + \ldots + W_{-1} A^I_{t-1} + W_0 A^I_t + W_1 A^I_{t+1} + \ldots$$

$$+ W_{\frac{T}{2}} A^I_{t+\frac{T}{2}} \qquad\qquad (2.3.3)$$

where T must be an even integer.

The weight W_0, which is multiplied by the observation A^I_t, is termed the central principal weight. It is seen that the greatest weight is placed on the most recent observation while both past and future observations receive symmetrically diminishing weights. In choosing an equally-weighted moving average filter, the weights selected are all equal to $\frac{1}{T}$, where T is the number of observations used in computing the mean or the filtering interval as described in Eq. (2.3.1). Therefore, the analytical form of the weighting function $W(t)$ may be expressed by

$$W(t) = \begin{cases} \frac{1}{T}, & |t| \leq \frac{T}{2} \\ 0, & |t| > \frac{T}{2} \end{cases} \qquad\qquad (2.3.4)$$

It is seen that the weighting function $W(t)$ is applied to the observations from $-\frac{T}{2}$ to $\frac{T}{2}$ so it is an even function of t. The frequency response of the filter, $H(f)$, is obtained from the Fourier

transformation of the weighting function W(t) by

$$H(f) = \int_{-\infty}^{\infty} W(t) \, e^{-i2\pi ft} dt \qquad (2.3.5)$$

or because of symmetry

$$H(f) = 2 \int_{0}^{\infty} W(t) \cos(2\pi ft) \, dt. \qquad (2.3.6)$$

For a finite filtering interval T, Eq. (2.3.6) may be written as

$$H(f) = 2 \int_{0}^{T/2} W(t) \cos(2\pi ft) \, dt. \qquad (2.3.7)$$

Substituting Eq. (2.3.4) into the Eq. (2.3.7), the frequency response function of the moving average filter may be written as

$$H(f) = \frac{\sin \pi ft}{\pi ft} \qquad (2.3.8)$$

which has a value of unity at f=0. This frequency response function is calculated from the equally-weighted moving average time-function. To obtain a high pass filter, it is necessary to subtract the moving average value from the original data.

The filtered data set for a moving average and differencing filter may be obtained by the following expression

$$A_t^O = A_t^I - \frac{1}{T+1} \sum_{i=-\frac{T}{2}}^{\frac{T}{2}} A_{t+i}^I, \quad t = \frac{T}{2} + 1, \frac{T}{2} + 2, \ldots, L - \frac{T}{2} \quad (2.3.9)$$

where A_t^O is the filtered value at time t, A_t^I is the original input

value, T is the filtering interval and L is the total number of data

points equal to twice the filtering interval. In this data processing

system, T is the total number of the data in one block (i.e. 8192)

while L = 16384.

2.3.2.2 Filter Shape for Moving-Average and Differencing High Pass
Filter

The filter shape for the moving-average and differencing high-

pass filter is obtained from Eq. (2.3.8) by subtracting from unity

$$I(f) = 1 - (\frac{\sin \pi ft}{\pi ft})^2 \quad (2.3.10)$$

which is shown in Fig. 5.

The moving average and differencing filter obviously has the draw-

back of failing to provide the trend values for the first half in the

first block of the sample and for the last half in the last block of

the sample. It is not a great loss to have to forego the initial

data values at the beginning of the first block, but the absence of

trend values at the end of the last block is a serious handicap if we

want to extrapolate into the future for forecasting.

2.4 Coordinate Transformation

Four new, mean-removed time series a_i, $i=1...,4$ have been created

after having applied the moving-average and differencing high pass

filter to the original raw observations. When $i = 1,2$ or 3, a_i repre-

sents the fluctuating velocity components in the sensor oriented co-

ordinate system, and when $i = 4$, a_i denotes the fluctuating temperature.

The sample probe yaw angle as calculated in Eq. (2.1.12) will be

used in the calculation of coordinate transformation of the values of

sample means, sample variances and covariances from the TSI or sensor

oriented coordinate system to the mean wind direction xyz. The x-

direction is the intersection of the vertical plane, which includes

the total wind vector, with the horizontal plane. The y-direction is

in the horizontal plane perpendicular to the x-direction and z-direc-

tion is vertically upward.

2.4.1 Variance and Covariance in each Block

The filtered time series should have a near zero mean value,

so variances and covariances in the blocked subseries m, m = $1,2,...$,

M-1 can be calculated by using the following definition

$$\overline{a_i a_j}^m = \frac{1}{n} \sum_{k=1}^{n} a_i(k)\, a_j(k), \quad i,j = 1,..4 \qquad (2.4.1)$$

where a_i, $i = 1,..,4$ represents the filtered time series. Equal subs-

cripts $i = j$ in the above equation represent the variances while unequal

subscripts $i \neq j$ denote the covariances. The total number of blocks

have decreased by one due to the application of moving-average and differencing high-pass filter.

In order to correct the values of the block variances and covariances of the time series, the filtered time series for each block should have exactly zero mean value. In this case, the following relationship should be used

$$\overline{a_i a_j}^m = \frac{1}{n} \sum_{k=1}^{n} a_i(k) \, a_j(k) - \bar{a}_i^m \, \bar{a}_j^m \, , \quad i,j=1,2,\ldots,4 \qquad (2.4.2)$$

where the block mean value of the filtered time series is calculated by

$$\bar{a}_i^m = \frac{1}{n} \sum_{k=1}^{n} a_i(k) \, , \qquad i = 1,2,\ldots 4 \qquad (2.4.3)$$

and m denotes the block number.

Covariances of two time series measures the covariation between the related time series. The covariance will have zero value if the two time series are not related.

2.4.2 Sample Mean Values

The values of the sample means for the four time series have been calculated previously in Eq. (2.1.11) by using the unfiltered observations. The sample variances and covariances are calculated from the filtered series a_i, $i = 1,2,\ldots,4$ by using arithmetic average of each blocked values as follows

$$\overline{a_i a_j} = \frac{1}{M-1} \sum_{m=1}^{M-1} \overline{a_i a_j}^m, \quad i,j=1,\ldots,4 \qquad (2.4.4)$$

where superscripts m = 1,.., M-1 denotes the number of blocks to be averaged.

The sample variances and covariances for the filtered time series a_i, i=1,..,4 with exactly zero mean value are calculated from

$$\overline{a_i a_j}^* = \frac{1}{M-1} \sum_{m=1}^{M-1} \overline{a_i a_j}^{m*} \quad . \quad i,j=1,2,..4. \qquad (2.4.5)$$

2.4.3 Mean Wind Direction Transformations

The statistical quantities of interest should be expressed in the mean wind direction, therefore transformation of all the values of sample mean, sample variances and covariances are to be performed from the sensor oriented coordinate system to the mean wind coordinate system. Since the covariances between fluctuating temperature and three fluctuating velocity components are also important, a new transformation 4 x 4 matrix is obtained by combining the relations in Eqs. (2.1.4) and (2.1.6) as follows

$$E_{ij} = \begin{pmatrix} E_{11} & E_{12} & E_{13} & 0 \\ E_{21} & E_{22} & E_{23} & 0 \\ E_{31} & E_{32} & E_{33} & 0 \\ 0 & 0 & 0 & E_{44} \end{pmatrix} \qquad (2.4.6)$$

where E_{11} = 0.57735 cosβ

E_{12} = 0.57735 sinβ

E_{13} = -0.8165

$$E_{21} = 0.57735 \cos\beta - 0.70711 \sin\beta$$

$$E_{22} = 0.57735 \sin\beta + 0.70711 \cos\beta$$

$$E_{23} = 0.40824$$

$$E_{31} = 0.57735 \cos\beta + 0.70711 \sin\beta$$

$$E_{32} = 0.57735 \sin\beta - 0.70711 \cos\beta$$

$$E_{33} = 0.40824$$

$$E_{44} = 1.0.$$

The values of mean velocity components and temperature, variances and covariances in the mean wind direction can be obtained by the following transformations

$$\overline{U}_i = E_{ki} A_k , \qquad i = 1,..,4 \qquad (2.4.7)$$

and

$$\overline{u_i u_j} = E_{ki} E_{\ell j} \overline{a_k a_\ell} , \qquad i,j = 1,\ldots,4 \qquad (2.4.8)$$

where the first three subscripts represent the three velocity components in the mean wind direction and the last subscript represents the temperature. The variance of temperature fluctuations in the sensor oriented coordinate system should be invariant under the coordinate transformations since temperature is a scalar quantity.

CHAPTER III

SPECTRAL ANALYSIS

The estimates of spectral density functions and other spectral characteristics associated with stationary multiple time series are considered necessary in order to study the physical properties of the phenomenon in terms of its behavior in the frequency domain. The power spectrum shows how the variance or average power of the time series is distributed over the entire frequency range. The cross-spectrum describes the relationship between two time series in the frequency domain through determining the coherence function. Since the cross-spectral density function is a complex function, it can be expressed in terms of a real part (co-spectral density function) and an imaginary part (quadrature spectral density function).

3.1 Methods of Analysis

In general, three different methods may be used to compute the power and the cross spectral densities. Each of the three methods is based on a different but asymptotically equivalent approach. These methods are

a. the indirect or Blackman-Tukey method which takes the Fourier transform of the auto- or cross-correlation functions of the time series to obtain the required spectral density functions.

b. the direct or fast Fourier transform method calculates a quantity

which is the direct Fourier transform of the time series. This quantity is then squared to obtain the spectral density functions.

c. the filtering method can be used either on a digital or analog computer to obtain these spectral density functions.

These three methods should turn out comparable results but these results are not necessarily identical, even if the same effective bandwidth at a given frequency is used. The three methods are suitable for computations of spectral density estimates, but they possess similar problems related to bandwidth, leakage, and statistical variability.

3.1.1 Indirect or Blackman-Tukey Method

This method requires the computation of the auto and the cross correlation functions before taking their Fourier transforms to obtain the spectral density functions. If the sampled observations $\{a_j\}$ and $\{b_j\}$ $j = 1,2,\ldots,n$ come from two discrete time series with zero means, then auto- and cross-correlation functions can be calculated respectively as follows

$$C_{aa}(k) = \frac{1}{n} \sum_{t=1}^{n-k} a_t \, a_{t+k}, \qquad k \geq 0 \tag{3.1.1}$$

and

$$C_{ab}(k) = \frac{1}{n} \sum_{t=1}^{n-k} a_t \, b_{t+k} \qquad k \geq 0 \ . \tag{3.1.2}$$

The power spectral density function of the discrete time series $\{a_j\}$, $j=1,2,\ldots,n$ is estimated by

$$G_a(f) = 2\Delta t \left\{ C_{aa}(0) + 2 \sum_{k=1}^{L-1} C_{aa}(k)W(k)\cos 2\pi f k\Delta t \right\},$$

$$0 \leq f \leq \frac{1}{2\Delta t} \qquad (3.1.3)$$

where $W(k)$ is the lag window with truncation point L. The selection of an optimum lag window and best truncation point is usually done by trial and error procedures.

The cross spectral density function for a stationary bivariate time series $\{a_j\}$ and $\{b_j\}$, $j=1,2,\ldots,n$ consists of a real part of the cross spectral density function called cospectrum and an imaginary part of the cross-spectral density function called quadrature spectrum. Respective estimates of these spectra can be calculated as follows

$$Co_{ab}(f) = 2\Delta t \left\{ \ell_{ab}(0) + 2 \sum_{k=1}^{L-1} \ell_{ab}(k)W(k)\cos 2\pi f k\Delta t \right\}$$

$$0 \leq f \leq \frac{1}{2\Delta t} \qquad (3.1.4)$$

and

$$Q_{ab}(f) = 4\Delta t \sum_{k=1}^{L-1} q_{ab}(k)w(k)\sin 2\pi f k\Delta t,$$

$$0 \leq f \leq \frac{1}{2\Delta t} \qquad (3.1.5)$$

where $\ell_{ab}(k)$ is the even part of the cross correlation function $C_{ab}(k)$.
That is

$$\ell_{ab}(k) = \frac{1}{2}(C_{ab}(k) + C_{ab}(-k)), \tag{3.1.6}$$

and $q_{ab}(k)$ is the odd part of the cross correlation function, namely

$$q_{ab}(k) = \frac{1}{2} (C_{ab}(k) - C_{ab}(-k)). \tag{3.1.7}$$

The cospectrum describes the in-phase relationship of the two time series, while the quadrature spectrum depicts the out-of-phase relationship. The quadrature spectrum assumes zero value if the cross correlation function is even. The occurrence of a maximum correlation between the two times series $\{a_j\}$ and $\{b_j\}$, at a non-zero lag will produce an odd function for $C_{ab}(k)$.

The calculations of auto- and cross-correlations in equations 3.1.1 and 3.1.2 involve a computational loop which is mainly a multiply-add operation, requiring execution time in modern high-speed digital computers of the order of seconds for just one single value for the time lag. In many physical applications, the number of time series to be analyzed can run into a fairly large number. Because of the time constraint, it is almost impossible to use this method to handle experimental records which run for half an hour and have a sample rate of 200 samples per second. As a result, alternative methods should be used for the spectral calculations of time series representing the ground level atmospheric turbulence.

3.1.2 Direct or Fast Fourier Transform Method

Instead of calculating the correlation functions, this method uses the Fourier transformation of the discrete time series $\{a_j\}$, $j = 1, 2, \ldots, n$ directly. First one has to obtain the following quantity

$$H_f = \Delta t \sum_{j=1}^{n} a_j e^{-i2\pi fj/n} W(j), \quad f = 0, 1, \ldots, n-1, \qquad (3.1.8)$$

where $W(j)$ is the data window. Hence the power spectral estimate is obtained as follows

$$\hat{G}_a(f) = \frac{2}{n\Delta t} H_f H_f^* \qquad (3.1.9)$$

where H_f^* is the complex conjugate of H_f. Equation (3.1.9) may also be written as

$$\hat{G}_a(f) = \frac{2}{n\Delta t} |H_f|^2, \quad f = 0, 1, 2 \ldots, \frac{n}{2} + 1. \qquad (3.1.10)$$

The introduction of the fast Fourier transform method makes the direct method extremely attractive in spectral density calculations. The detailed description of the application of the direct method in estimating power and cross spectral density functions is discussed in section 3.6.

3.1.3 Bandwidth Filtering Method

For a specific frequency index k, it is necessary to assign frequencies $\{f_k\}$ and bandwidth $\{B_k\}$ as follows

$$0 < f_0 < f_1 < \ldots < f_k \leq \frac{1}{2\Delta t}$$

where Δt is the sampling interval. The bandwidth $\{B_k\}$ of a narrow band-pass filter may be described in three different ways, namely, the half-power point bandwidth, the noise bandwidth, or the equivalent

statistical bandwidth. For the half-power point bandwidth $\{B_k\}$ used in this section, it is the frequency interval between the upper and lower frequencies where the filter attenuates an applied signal by 3 db below maximum transmissibility [6].

A separate bandpass filter, such as Chebyshev sine bandpass filter or Butterworth sine bandpass filter [67], is designed for each k. The filters have their half-power points at $(f_k - \frac{B_k}{2})$ and $(f_k + \frac{B_k}{2})$ hertz. More specifically, the distance between the two half-power points is set to be B_k hertz and f_k is located midway between them.

Let the output of the kth filter be denoted by $q_i^{(k)}$, $i=1,2,\ldots,n$ which is filtered by using each of the filter k, then

$$q_i^{(k)} = \sum_{j=1}^{\ell} h_j^{(k)} q_{i-j}^{(k)} + \sum_{j=1}^{\ell} g_j^{(k)} a_{i-j}, \quad (3.1.11)$$

where h_j and g_j for $j=1,2,\ldots,\ell$ are the chosen filtering functions with total number of ℓ weights. In practical numerical computations, it is noted that some input values a_{-i} and output values q_{-i} are necessarily set to zero initially. The power spectral density function is obtained by

$$G_k = \frac{1}{B_k n} \sum_{i=1}^{n} [q_i^{(k)}]^2 , \quad (3.1.12)$$

which means that the data are passed through a bandpass filter, squared, summed and finally normalized with the proper units.

3.2 Sampling Considerations for Random Data

For the purpose of statistical analysis, most continuous sample
records should be read at some fixed interval Δt and converted into
digitized records for numerical calculations. Sampling defines the
points at which the data are to be observed. Corresponding relation-
ships exist between a random time sample record $a(t)$ defined for the
time interval from 0 to T seconds and its Fourier transform $G(f)$ de-
fined over a range of frequencies from 0 to F. However, both sample
records $a(t)$ and its Fourier transform $G(f)$ are restricted by their
respective time and frequency properties. Proper considerations should,
therefore, be given to these problems in order to obtain better estimates
of the spectral density functions.

3.2.1 Resolution Difficulties

Resolution is defined as the degree to which the true spectrum
shows its narrow and tall peaks. Time and frequency are related inversely
as can be seen from their physical units. The actual record lengths
are finite instead of infinite in extent and the frequency bandwidth
Δf is also of finite width instead of near zero width. Due to this
resolution problem, additional errors will be encountered in the estimates
of the spectral density function.

For a fixed record time T, the estimate of the power spectral density
function might be improved by taking the frequency bandwidth Δf by the
following relationship

$$T \, \Delta f \geq C \qquad\qquad (3.2.1)$$

where C is a fixed constant. For a fixed record time T, values of Δf which are too small will violate this uncertainty principle. One should attempt to increase T and at the same time decrease Δf without corresponding increase in record length T will reduce the statistical reliability of the spectral density estimates. A decrease in bandwidth Δf will improve the resolution but has to trade for statistical reliability. A compromise between a reasonable bandwidth and statistical reliability is, therefore, necessary.

3.2.2 Aliasing Errors

The question of the "aliasing" error arises as a result of sampling the data $a(t)$ at equal intervals of time Δt and later confusing some of the higher frequency contents in the original frequency space with the lower frequencies as can be seen in Fig. 6. The aliasing can easily be avoided electronically in the experimental system by filtering the signal before sampling so that the power above the maximum frequency f_s is effectively removed. In digital data computations, care must be taken to avoid the occurrence of aliasing.

If a data sample $a(t)$ is sampled at equal intervals of time by

$$\Delta t = \frac{1}{2f_s} \qquad (3.2.4)$$

then f_s, which is called Nyquist frequency, is the highest frequency at which spectral data can be attained without introducing aliasing errors. Any frequencies present in the data which are integer multiples of Nyquist frequency f_s cannot be distinguished from f_s. For the frequency $f = nf_s$ and $\Delta t = \frac{1}{2f_s}$, it is seen that

$$\sin 2\pi f \Delta t = \sin 2\pi (nf_s)(\frac{1}{2f_s}) = 0, \text{ for all } n=1,2,\ldots . \qquad (3.2.5)$$

Similarly, the energy at an arbitrary frequency f cannot be separated from energies contributed by different frequencies such as

$$f \pm f_s, \quad f \pm 2f_s, \quad \ldots, \quad f \pm nf_s, \qquad (3.2.6)$$

and

$$\sin^2 2\pi f \Delta t = \sin^2 2\pi (f + nf_s)(\frac{1}{2f_s}), \text{ for all } n=1,2,\ldots . \qquad (3.2.7)$$

Thus, if frequencies higher than the Nyquist frequency f_s are actually presented in the data, they will contribute their energies to lower frequencies with consequent errors in power spectral density estimates at these lower frequencies.

To avoid this aliasing problem, one should choose the sampling frequency f_s and sampling rate Δt in such a way that

$$\Delta t = \frac{1}{2f_s} \leq \frac{1}{2f_{max}} , \qquad (3.2.7)$$

where f_{max} is the maximum frequency for which the data will be analyzed. It may also be written as

$$f_s \geq f_{max} . \qquad (3.2.8)$$

It is, therefore, concluded that the time interval between successive samples should be such that the sampled data contain at least two samples per cycle of the highest frequency of interest. In case extraneous noise is present in the data samples, ten to twenty

samples per cycle of this highest frequency are considered practical unless the high frequency noise can be filtered off before the data are sampled.

The effect of aliasing on the integral Fourier transform of a function a(t) can be shown as follows

$$G(f) = \int_{-\infty}^{\infty} a(t)e^{-i2\pi ft}dt \tag{3.2.9}$$

where $i = \sqrt{-1}$ and its inverse Fourier transform is

$$a(t) = \int_{-\infty}^{\infty} G(f)e^{i2\pi ft}df . \tag{3.2.10}$$

The effect of sampling at finite intervals, evaluated at the points $t_j = j\Delta t$, $j = 0, \pm 1, \pm 2, \ldots$ and $F = \frac{1}{\Delta t}$ can be seen as follows

$$a(t_j) = \int_{-\infty}^{\infty} G(f)e^{\frac{i2\pi fj}{F}}df = \sum_{K=-\infty}^{\infty} \int_{KF}^{(K+1)F} G(f)e^{\frac{i2\pi fj}{F}}df . \tag{3.2.11}$$

The exponential function in the integrand of Eq. (3.2.11) is a periodic function of frequency f in the region from f = 0 to f = F, so it may be written as

$$a(j\Delta t) = \int_{0}^{F} G_p(f)e^{\frac{-i2\pi jf}{F}}df \tag{3.2.12}$$

where $G_p(f)$ is the spectral density function with periodic function f such that

$$G_p(f) = \sum_{K=-\infty}^{\infty} G(f + Kf) . \qquad (3.2.13)$$

The $G_p(f)$ is different from the spectral density function $G(f)$ defined in Eq. (3.2.9) because $G_p(f)$ is the sum of the $G(f)$'s displaced by all multiples of F. This error is referred also as "aliasing" in the frequency domain.

3.3 Tapering Function - Time Domain

The selection of a tapering function is in many respects analogous to an engineering design of an electrical filter. Tapering is to multiply the time series by a data window, analogous to multiplying the correlation by a lag window in the indirect or Blackman-Tukey method. The method of using various lag windows to obtain smoothed spectral estimates have already been well established [77]. The problem of tapering the time series has not been thoroughly studied although different data window functions have been proposed [105].

By adopting the direct or FFT method for spectral estimation, emphasis will be placed on the use of data windows or tapering functions. The purpose of using a tapering function is to provide a slightly wider spectral window than would be obtained if a straightforward harmonic analysis is used. From the time domain viewpoint, tapering is to round off potential discontinuities at each end of the time series. In the frequency domain, tapering is to suppress large

negative side lobes in the power spectrum. In general, tapering will change the mean and variances of the data sample since unequal weights are given to different portions of the time series. In effect, some data are lost and as a result degrees of freedom are lost. A scale factor is therefore necessary to compensate this difference in order to obtain the accurate spectral estimates.'

3.3.1 Cosine Taper Data Window

It is essential that the mean is removed from the data before the data window function is applied. Bingham et. al. [9] proposed a data smoothing function consisting of a short left-half cosine bell, a long constant and a short right-half cosine bell. Later they proposed a data window to taper both ends of the time series with the cosine bell each of which contains one tenth the time of the total sample time. The data between these cosine bells are multiplied by unity. This data window is called cosine taper data window and may be expressed in the following form

$$
\left.
\begin{array}{ll}
W_t = (\frac{1}{2})\ (1 - \cos \frac{\pi t}{0.1T}) & 0 \le t \le 0.1T \\[2mm]
W_t = 1 & 0.1T < t \le 0.9T \\[2mm]
W_t = (\frac{1}{2})\ (1 - \cos \frac{\pi(T-t)}{0.1T}) & 0.9T < t \le T \\[2mm]
& (\text{or } 0 < T-t \le 0.1T)
\end{array}
\right\} \quad (3.3.1)
$$

where T is the total sample time. The corresponding smoothed filter shape $C_T(f)$ which can be used in conjunction with FFT, is shown in Fig. 8. This function is the Fourier transform of the data window W_t, as is shown in Fig. 7. The $C_T(f)$ has a wider main lobe with

suppressed side lobes so as to reduce any possible power leakage and to prevent negative power estimates.

The general form of the cosine-taper data window of Eq. (3.3.1) may be written as

$$W_t = \frac{1}{2}(1 - \cos\frac{10\pi t}{T})$$ (3.3.2)

or

$$W_t = \frac{1}{2} - \frac{1}{2}[\frac{1}{2}(e^{\frac{10\pi t}{T}} + e^{-\frac{10\pi t}{T}})]$$

or

$$W_t = [-\frac{1}{4} + \frac{1}{2}e^{\frac{10\pi t}{T}} - \frac{1}{4}e^{\frac{20\pi t}{T}}]e^{-\frac{10\pi t}{T}}.$$ (3.3.3)

From the numerical coefficients inside the bracket of the above equation, it is seen that the cosine-bell data window is simply an extension of the Hanning weighting function with coefficients $(\frac{1}{4}, \frac{1}{2}, \frac{1}{4})$ for frequency domain smoothing.

3.3.2 Other Data Windows

There are few other proposed data windows [105] but they have not received wide attention. Their application in any practical problem has not been attempted. In applying these windows to the atmospheric turbulence data, the results predicted are generally lower in value as compared to those using cosine-taper data window which was discussed in the previous section. A brief discussion of these windows is presented in the following section.

3.3.2.1 Window No. 1

Welsh [105] proposed a data window which is expressed by the following function

$$W_1(t) = 1 - \left[\frac{t - \frac{n-1}{2}}{\frac{n+1}{2}}\right]^2 , \quad t = 0,1,2,\ldots,n-1. \qquad (3.3.5)$$

The resulting spectral window corresponding to the data window (3.3.5) is given approximately by

$$W_1(f) = \frac{1}{nU'} \left\{\frac{2}{\pi^2(n+1)f^2} \left[\frac{\sin(n+1)\pi f}{(n+1)\pi f} - \cos(n+1)\pi f\right]\right\}^2 \qquad (3.3.6)$$

where

$$U' = \frac{1}{n} \sum_{t=0}^{n-1} W_1^2(t) \qquad (3.3.7)$$

and n is the total number of data points used in the computation and can be considered as a scale factor. To change n will mean a variation of the shape of the spectral window, $W_1(f)$, by expansion or compression of the extent of the independent variable f.

The half-power width is given by

$$\Delta_1 f = \frac{1.16}{n+1} \qquad . \qquad (3.3.8)$$

When the same half-power width is used for comparison, the spectral window, $W_1(f)$ turns to be almost identical to the spectral window as proposed by Hanning [10].

3.3.3.2 Window No. 2

Welsh [105] also proposed another data window but it has a different shape as compared to window No. 1.

$$w_2(t) = 1 - \left| \frac{t - \frac{n-1}{2}}{\frac{n+1}{2}} \right| \quad t = 0,1,2,111,n-1 \ . \tag{3.3.9}$$

The resultant spectral window $W_2(f)$ is again obtained by applying Fourier transform to the data window $w_2(t)$ and can be expressed as follows

$$W_2(f) = \frac{1}{nU'} \left[\frac{n+1}{2} \frac{\sin^2\{(n+1)\frac{\pi f}{2}\}}{\{(n+1)\frac{\pi f}{2}\}^2} \right]^2 \tag{3.3.10}$$

where

$$U' = \frac{1}{n} \sum_{t=0}^{n-1} w_2^2(t) \ . \tag{3.3.11}$$

Changing the total length of the data set will again result in the change of the shape of the spectral window function $W_2(f)$ by expansion or compression of the extent of the independent variable f.

The half-power width is found to be

$$\Delta_2 f = \frac{1.28}{n+1} \ . \tag{3.3.12}$$

When this half-power width is used to compare the shapes of the spectral windows, $W_2(f)$ is found to be very close to Parzen's spectral window [51], which possesses large negative side lobes. The presence of

negative side lobes in the spectral window function has great dis-
advantages since prediction of negative power spectral density function
may occur.

3.4 Smoothing Function - Frequency Domain

The smoothing of the spectral estimates in the frequency domain
may be achieved by either averaging the estimates at the corresponding
frequency points of segmented subseries in a time series (segment
averaging) or averaging the spectral estimates among neighboring points
in the spectrum function (frequency smoothing). The combination of
both segment averaging and frequency smoothing may be applied to obtain
a smooth spectral estimate. This type of smoothing is referred to as
combined averaging.

A plot of the individual power estimates versus frequency for a
one half hour sample will be next to impossible. Even the plotting
of spectrum functions which are smoothed using the segment averaging
method will show many small individual peaks. These small peaks and
valleys are insignificant in the explanation of the turbulence
structure, because they may represent sampling fluctuations rather
than any systematic physical variations. Frequency smoothing may
average out these peaks in order to obtain a more useful representation
of the spectrum but has limitations as far as the resolution is con-
cerned. However, for a long time series covering nearly four decades
on the frequency scale, the resolution is generally two or more orders
of magnitude greater than actually required [69].

3.4.1 Segment Averaging

The data sample of one half hour duration has been previously blocked into M different subseries each of which has n data points. The total number of blocks has been reduced by one as a result of applying the moving-average and differencing high-pass filter. By using the fast Fourier transformation technique, there will be M-1 number of blocked spectral estimates each of them of length n. The M-1 spectral estimates are averaged over corresponding frequencies to obtain a smoothed spectral estimate given by

$$\overline{G}(f_i) = \frac{1}{M-1} \sum_{K=1}^{M-1} G_K(f_i) \qquad i = 1,2,\ldots,n . \qquad (3.4.1)$$

The application of segment-average smoothing will increase the effective resolution bandwidth B_e depending on the number of blocks to be averaged. The spectral window before applying the segment averaging was triangular in shape with $B_e = \frac{1}{T}$. After applying the segment averaging, the spectral window is still triangular in shape except the effective resolution bandwidth B_e will be wider (i.e. $B_e = \frac{M-1}{T}$) as shown in Fig. 9. The spectral estimate $\overline{G}(f_i)$ in Eq. (3.4.1) may be considered as representing the midpoint of the frequency interval covered by B_e. A total of n spectral estimates can be obtained.

3.4.2 Frequency Smoothing

After averaging the ℓ neighboring spectral estimates of the power spectrum, the new spectral function can be expressed in terms of the original one as follows

$$\hat{G}(f_K) = \frac{1}{\ell} \sum_{i=1}^{\ell} G(f_i) \qquad K = 1,2,\ldots,\frac{n}{\ell}$$

where ℓ is the number of neighboring frequency components to be averaged and n is the total number of original spectral estimates. The spectral window before frequency smoothing was triangular in shape with the effective resolution bandwidth $B_e = \frac{1}{T}$. After frequency smoothing, the spectral window will be trapezoidal in shape with much wider effective resolution bandwidth (i.e. $B_e = \frac{\ell}{T}$) as shown in Fig. 10. The spectral estimate may be considered as representing the midpoint of the frequency interval from f_K to $f_{K+\ell-1}$, where K denotes interval number.

3.4.3 Combined Averaging

The smoothing of spectral estimates can be achieved more effectively by first applying segment averaging followed by frequency smoothing which is known as combined averaging. As a result of applying the combined averaging technique for smoothing of the spectral density estimates, the final effective resolution bandwidth becomes much wider and can be approximated by

$$B_e = \frac{M\ell}{T} \qquad (3.4.3)$$

where M is the number of blocks to be averaged and ℓ is the number of averaged spectral estimates and T is the total sample time. The number of degrees of freedom γ is

$$\gamma = 2B_e T = 2M\ell, \qquad (3.4.4)$$

which can be interpreted as the total number of real and imaginary components within the bandwidth, B_e. Since each of the spectral estimates is in itself a Gaussian random variable, the squaring and

adding of them will produce a Chi-square distribution. The broader effective resolution bandwidth gives the reduced normalized standard error which will be explained in the next chapter.

3.4.3 Proposed Frequency Smoothing Technique

The frequency smoothing is usually done by choosing an equal number of neighboring frequency components of the spectral estimates to be averaged. This technique is effective only if the power spectral density estimates are distributed evenly throughout the whole frequency range of interest. If the power spectral density estimates are concentrated either in the low or in the high frequency range, a new frequency smoothing technique is proposed in order that more information is to be obtained in the range of interest.

In order to obtain more spectral information in the lowest frequency range of the atmospheric turbulence spectrum, it is proposed that the total number of spectral estimates after segment averaging be separated into different averaging regions.

Since the power spectral estimate at zero frequency is of no significance for reliable analysis, the smoothing starts with the second value of the spectral estimates after zero frequency.

The power spectral density estimates at the lowest frequency range have been obtained by only going through segment averaging (i.e. $\ell = 1$, $n = 8$ in Eq. (3.4.2)). The average value ℓ used in the frequency smoothing method is chosen in a manner of geometric progression (i.e. $\ell = 2^0, 2^2, 2^4, \ldots$). For different values of ℓ different spectral estimates will be obtained as expressed by the following

$\ell = 1$,

$$\hat{G}(f_k) = \frac{1}{\ell} \sum_{i=1}^{\ell} G_i(f_k) \qquad k = 1,2,\ldots,8 \ , \qquad (3.4.5)$$

$\ell = 4$,

$$\hat{G}(f_k) = \frac{1}{\ell} \sum_{i=1}^{\ell} G_i(f_k) \qquad k = 9,10,\ldots,38 \ , \qquad (3.4.6)$$

$\ell = 16$,

$$\hat{G}(f_k) = \frac{1}{\ell} \sum_{i=1}^{\ell} G_i(f_k) \qquad k = 39,40,\ldots,62 \ , \qquad (3.4.7)$$

$\ell = 64$,

$$\hat{G}(f_k) = \frac{1}{\ell} \sum_{i=1}^{\ell} G_i(f_k) \qquad k = 63,64,\ldots,86 \ , \qquad (3.4.8)$$

and $\ell = 256$,

$$\hat{G}(f_k) = \frac{1}{\ell} \sum_{i=1}^{\ell} G_i(f_k) \qquad k = 87,88,\ldots,94 \ . \qquad (3.4.9)$$

In this case, 4097 unique values of spectral density estimates $G_i(f_k)$ have been used to obtain 94 final smoothed spectral density estimates $\hat{G}(f_k)$. The overall filter spacing for this proposed frequency smoothing technique is shown in Figure 11.

3.5 Fast Fourier Transform

The fast Fourier transform (FFT) is an efficient and time saving algorithm for the computation of the harmonic amplitudes in the frequency domain from uniformly spaced input data points. It is used to analyse the periodic phenomena of a time series as it converts to

a frequency function. The time savings of this algorithm will permit the reduction of operations by a factor of $N^2/N \log_2 N$ if the number of data points in the sample is a power of two.

Many widely used FFT algorithms involved bit-reversal procedures to sort the Fourier coefficients into the proper order in the final stages of the transformation. The bit-reversal procedures can also be avoided if the input data have been sorted into different orders so the output coefficients will be in the proper order.

Uhrich [99] developed a Fortran program without requiring bit-reversal procedures but lacked a supporting theory. His algorithm requires a 2xN array for variable storage in the computer rather than a 1xN storage for bit-reversal sorting. The required computation time, therefore, is almost twice as long as is necessary.

A different algorithm for FFT calculations without bit-reversal and sorting procedures together with complete mathematical formulations will be presented in the following sections.

3.5.1 Properties of Fourier Transform

In order to understand the fantastic time savings involved in FFT computations, some basic properties of the Fourier transformation need to be explained. In processing digitized signals or samples, the attention will be focused on the properties of the discrete finite Fourier transform (DFFT). Some useful properties related to the development of the fast Fourier transform will also be discussed.

Property 1: The Fourier transform transfers the N data points of the time series $(a_0, a_1, a_2, \ldots, a_{N-1})$ to the N-spectral values

$(H_0, H_1, H_2, \ldots, H_{N-1})$ in the frequency domain, as defined by

$$H_r(f) = \sum_{n=0}^{N-1} a_n(t) \, W^{rn} \qquad r = 0,1,2,\ldots,N-1 \qquad (3.5.1)$$

where $W = e^{\frac{-i2\pi}{N}}$. A very similar equation defining the inverse finite Fourier transform, which transforms the discrete spectral values back to the original discrete time series can be written as

$$a_n(t) = \frac{1}{N} \sum_{r=0}^{N-1} H_r(f) \, W^{-rn} \qquad n = 0,1,2,\ldots,N-1 \; . \qquad (3.5.2)$$

In case the digitally recorded data points $a_0, a_1, \ldots, a_{N-1}$ are finite but non-periodic (random), the sample values as defined by Eq. (3.5.2) can be proven to be periodic and infinite as follows

$$a_{n+N}(t) = \frac{1}{N} \sum_{r=0}^{N-1} H_r(f) \, W^{-r(n+N)}$$

or

$$a_{n+N}(t) = \frac{1}{N} \sum_{r=0}^{N-1} H_r(f) \, W^{-rn} \, (W^N)^{-r} \qquad (3.5.3)$$

where W is the Nth root of 1 or $W^N = 1$, so $(W^N)^{-r} = 1$ and it follows that

$$a_{n+N}(t) = \frac{1}{N} \sum_{r=0}^{N-1} H_r(f) \, W^{-rN} = a_n(t) \; . \qquad (3.5.4)$$

Similarly one can prove that $H_{r+N}(f) = H_r(f)$.

Property 2: If the time series $(a_0, a_1, \ldots, a_{N-1})$ is real, then the second part of its finite Fourier transform is equal to the complex conjugate of the first part. The spectral values $H_0, H_1, \ldots,$ H_{N-1} can be separated into two parts

$$\underbrace{H_0, H_1, H_2, \ldots, H_{\frac{N}{2}-1}}_{\text{First Part}}, \underbrace{H_{\frac{N}{2}}, H_{\frac{N}{2}+1}, H_{\frac{N}{2}+2}, \ldots, H_{N-1}}_{\text{Second Part}}$$

It is necessary to prove that

$$H_{N-j}(f) = H_j^*(f) \qquad \text{for } 0 < j \leq N-1, \qquad (3.5.5)$$

where the star superscript refers to the complex conjugate. From Eq. (3.5.1), one can write

$$H_{N-j}(f) = \sum_{n=0}^{N-1} a_n(t) \, W^{(N-j)n} . \qquad (3.5.6)$$

Using the property 1, Eq. (3.5.6) reduces to

$$H_{N-j}(f) = \sum_{n=0}^{N-1} a_n(t) \, W^{-jn} . \qquad (3.5.7)$$

Now,

$$W^{-1} = \frac{1}{W} = \frac{1}{\cos\frac{2\pi}{N} - i \sin\frac{2\pi}{N}} \qquad (3.5.8)$$

or

$$W^{-1} = \cos\frac{2\pi}{N} + i \sin\frac{2\pi}{N} = W^* . \qquad (3.5.9)$$

Hence Eq. (3.5.6) can be written as

$$H_{N-j}(f) = \sum_{n=0}^{N-1} a_n^*(t)(W^{jn})^* \ . \tag{3.5.10}$$

For a real valued time series, $a_n(t) = a_n^*(t)$ and Eq. (3.5.10) can be written as

$$H_{N-j}(f) = \left[\sum_{n=0}^{N-1} a_n(t) \ W^{jn}\right]^* = H_j^*(f) \ . \tag{3.5.11}$$

<u>Property 3</u>: The atmospheric turbulence data are always a sequence of real numbers. By applying Fourier transformation we usually store the actual (real) input in the real-part array of the computer and zeros in the imaginary-part array of the computer. This requires storage length of 2N and produces 2N components of N complex Fourier coefficients. In fact, we used only N Fourier coefficients which should take much less storage in the computer. By forming a complex time series $(\tilde{c}_0, \tilde{c}_1, \ldots, \tilde{c}_{N-1})$ from two real input time series $(\tilde{a}_0, \tilde{a}_1, \ldots, \tilde{a}_{N-1})$ and $(\tilde{b}_0, \tilde{b}_1, \ldots, \tilde{b}_{N-1})$, one can perform Fourier transformation utilizing complex input in a form of $\tilde{c}_r = \tilde{a}_r + i \ \tilde{b}_r$ for $r = 0,1,2,\ldots,N-1$ and $i = \sqrt{-1}$. Then the combined spectral series will be in the form of

$$\tilde{c}_r = \tilde{A}_r + i \ \tilde{B}_r \qquad r = 0,1,2,\ldots,N-1 \tag{3.5.12}$$

where $\tilde{A}_r$ and $\tilde{B}_r$ are both complex. Let

$$\tilde{A}_r = \tilde{a}_{1_r} + i\ \tilde{a}_{2_r}$$

and   (3.5.13)

$$\tilde{B}_r = \tilde{b}_{1_r} + i\ \tilde{b}_{2_r}$$

where $\tilde{a}_{1_r}, \tilde{a}_{2_r}, \tilde{b}_{1_r}$, and $\tilde{b}_{2_r}$ are real numbers.

By using property 2, one can write

$$\tilde{C}_{N-r} = \tilde{A}_r^* + i\ \tilde{B}_r^*$$ (3.5.14)

where $\tilde{A}_r^*$ and $\tilde{B}_r^*$ are complex conjugate of $\tilde{A}_r$ and $\tilde{B}_r$ respectively.

Both Eqs. (3.5.12) and (3.5.14) can be written in form of

$$\tilde{C}_r = (\tilde{a}_{1_r} + i\ \tilde{a}_{2_r}) + i\ (\tilde{b}_{1_r} + i\ \tilde{b}_{2_r})$$

and

$$\tilde{C}_{N-r} = (\tilde{a}_{1_r} - i\ \tilde{a}_{2_r}) + i\ (\tilde{b}_{1_r} - i\ \tilde{b}_{2_r}) \ .$$

Hence it follows that

$$\tilde{C}_r = (\tilde{a}_{1_r} - \tilde{b}_{2_r}) + i\ (\tilde{a}_{2_r} + \tilde{b}_{1_r})$$ (3.5.15)

and

$$\tilde{C}_{N-r} = (\tilde{a}_{1_r} + \tilde{b}_{2_r}) + i\ (\tilde{a}_{2_r} - \tilde{b}_{1_r})$$ (3.5.16)

By combining Eqs. (3.5.15) and (3.5.16) one obtains

$$\frac{\tilde{C}_r + \tilde{C}_{N-r}^*}{2} = \tilde{a}_{1_r} + i\ \tilde{a}_{2_r} = \tilde{A}_r$$ (3.5.17)

$$\frac{\tilde{C}_r - \tilde{C}_{N-r}^*}{2i} = \tilde{b}_{1_r} + i\,\tilde{b}_{2_r} = \tilde{B}_r \qquad\qquad (3.5.18)$$

where $\tilde{A}_r$ and $\tilde{B}_r$, for $r = 0,1,2,\ldots,N-1$ are the Fourier transform values of the two real time series $\tilde{a}_n$ and $\tilde{b}_n$ respectively. Both Eqs. (3.5.17) and (3.5.18) can be written in more easily perceptive forms as follows

$$\tilde{A}_r(f) = \mathrm{Re}\left[\frac{(\tilde{C}_r(f) + \tilde{C}_{N-r}(f))}{2}\right] + i\,\mathrm{Im}\left[\frac{(\tilde{C}_r(f) - \tilde{C}_{N-r}(f))}{2}\right]$$

$$(3.5.19)$$

and

$$\tilde{B}_r = \mathrm{Im}\left[\frac{(\tilde{C}_r(f) + \tilde{C}_{N-r}(f))}{2}\right] - i\,\mathrm{Re}\left[\frac{(\tilde{C}_r(f) - \tilde{C}_{N-r}(f))}{2}\right].$$

$$(3.5.20)$$

There are many other properties (i.e. circular convolution of two time series) which may be found in most of the standard textbooks on Fourier transformation.

3.5.2 Basic Theory of Fast Fourier Transform (FFT)

The basic theory of FFT was developed by Cooley and Tukey [19] in a subtle way so that it was somewhat difficult to understand. The main idea involved in the entire development was to continuously reduce a time series into two final point functions. It may also be illustrated by the principle of matrix factorization [34]. The theory presented here is to illustrate in a simple mathematical form the reasons for the time-saving capacities of this algorithm.

In the sampled-data case, the discrete Fourier transform (DFT) is defined previously by

$$H_r = \sum_{k=0}^{N-1} a_k e^{-i2\pi kr/N} \qquad r = 0,1,2,\ldots,N-1 \qquad (3.5.21)$$

where H_r is the rth coefficient of the DFT and a_k denotes the kth sample of the time series which consists of N samples and $i = \sqrt{-1}$. The definition of DFT is not consistent throughout the literature. Some authors prefer to use H_r/N as DFT coefficients, others use $H_r/\sqrt{N}$. Therefore, care should be exercised in doing the numerical computations. The a_k's in expression 3.5.21 can be either real or complex but the H_r's are almost always complex. Eq. (3.5.21) may be written in a simplified form

$$H_r = \sum_{k=0}^{N-1} a_k W^{rk} \qquad r = 0,1,2,\ldots,N-1 \qquad (3.5.22)$$

where $W^{rk} = e^{-i2\pi rk/N}$ or $W = e^{-i2\pi/N}$.

3.5.2.1 Illustrated Example

To become more familiar with the discrete fast Fourier transformation as defined in Eq. (3.5.22), an example will be used to describe this technique for 8 data points. For a random digitized time series a_k, $k = 0,1,2,\ldots,7$ the Fourier transform of Eq. (3.5.22) may be written as follows

$$H_0 = a_0 + a_1 + a_2 + a_3 + a_4 + a_5 + a_6 + a_7$$

$$H_1 = a_0 + a_1 W + a_2 W^2 + a_3 W^3 + a_4 W^4 + a_5 W^5 + a_6 W^6 + a_7 W^7$$

$$H_2 = a_0 + a_1 W^2 + a_2 W^4 + a_3 W^6 + a_4 W + a_5 W^2 + a_6 W^4 + a_7 W^6$$

$$H_3 = a_0 + a_1 W^3 + a_2 W^6 + a_3 W^1 + a_4 W^4 + a_5 W^7 + a_6 W^2 + a_7 W^5$$

$$H_4 = a_0 + a_1 W^4 + a_2 + a_3 W^4 + a_4 + a_5 W^4 + a_6 + a_7 W^4$$

$$H_5 = a_0 + a_1 W^5 + a_2 W^2 + a_3 W^7 + a_4 W^4 + a_5 W^1 + a_6 W^6 + a_7 W^3$$

$$H_6 = a_0 + a_1 W^6 + a_2 W^4 + a_3 W^2 + a_4 + a_5 W^6 + a_6 W^4 + a_7 W^2$$

$$H_7 = a_0 + a_1 W^7 + a_2 W^6 + a_3 W^5 + a_4 W^4 + a_5 W^3 + a_6 W^2 + a_7 W^1$$

(3.5.23)

where use has been made of the relations $W^0 = 1$, $W^{8+n} = W^n$ and $W^4 = -1$.
It is clear that the complete calculations of Eq. (3.5.23) requires 64
complex multiplications and additions. Samples which consist of
thousands of data points would require an extremely large number of
computer computations and also require a large storage. But from Eq.
(3.5.23) some basic characteristics of the Fourier transform may be
recognized. Obviously, symmetry in the right hand side of these
expressions can be observed. The first equation in (3.5.23) is simply
the sum of all the data points.

The FFT method is essentially to divide the total number of data
points in half which gives two sequences and then dividing these
sequences in half again to give four short sequences each consisting
of two terms. It will be shown that the shorter sequences require
fewer operations than the longer sequences. It is profitable to
separate the original data points into two shorter sequences b_ℓ,
$\ell = 0,1,2,\ldots,\frac{N}{2}$ composed of only the even-numbered data points, and

c_ℓ, $\ell = 0,1,2,\ldots,\frac{N}{2}$ composed of only the odd-numbered samples. Now the discrete Fourier transform of the shorter sequences for the 8-data points sample is given by

$$B_r = \sum_{k=0}^{3} b_k W^{2rk} \qquad r = 0,1,2,3$$

and
$$(3.5.24)$$

$$C_r = \sum_{k=0}^{3} c_k W^{2rk} \qquad r = 0,1,2,3 \ ,$$

where $W^2 = \cos(\frac{2\pi}{4}) - i \sin(\frac{2\pi}{4})$. The computing time for obtaining the Fourier coefficients B_r and C_r, $r = 0,1,2,3$ is now reduced to $2(4)^2 = 32$. By expanding Eq. (3.5.24) one should see more clearly the advantages of separation of the long sequence,

$$
\begin{aligned}
B_0 &= b_0 + b_1 + b_2 + b_3 &= a_0 + a_2 + a_4 + a_6 \\
B_1 &= b_0 + b_1 W^2 + b_2 W^4 + b_3 W^6 \\
B_2 &= b_0 + b_1 W^4 + b_2 + b_3 W^4 \\
B_3 &= b_0 + b_1 W^6 + b_2 W^4 + b_3 W^2 \\
C_0 &= c_0 + c_1 + c_2 + c_3 &= a_1 + a_3 + a_5 + a_7 \\
C_1 &= c_0 + c_1 W^2 + c_2 W^4 + c_3 W^6 \\
C_2 &= c_0 + c_1 W^4 + c_2 + c_3 W^4 \\
C_3 &= c_0 + c_1 W^6 + c_2 W^4 + c_3 W^2 \ .
\end{aligned}
$$

$$(3.5.25)$$

To illustrate the advantages of FFT more clearly, the spectral values H_k, $k = 0,1,2,\ldots,N-1$ can be expressed in terms of spectral values B_ℓ and C_ℓ, $\ell = 0,1,\ldots,\frac{N}{2}$ as follows

$$H_0 = B_0 + C_0$$

$$H_1 = B_1 + WC_1$$

$$H_2 = B_2 + W^2C_2$$

$$H_3 = B_3 + W^3C_3$$

$$H_4 = B_0 + W^4C_0$$

$$H_5 = B_1 + W^5C_1$$

$$H_6 = B_2 + W^6C_2$$

$$H_7 = B_3 + W^7C_3 \ .$$

(3.5.26)

Now the sequences b_ℓ and c_ℓ, $\ell = 0,1,2,3$ can be further halved to obtain four short sequences of two terms each. They may be written as follows

$$D_r = \sum_{j=0}^{1} d_j W^{4rj} \qquad r = 0,1$$

$$E_r = \sum_{j=0}^{1} e_j W^{4rj} \qquad r = 0,1$$

$$F_r = \sum_{j=0}^{1} f_j' W^{4rj} \qquad r = 0,1$$

$$K_r' = \sum_{j=0}^{1} k_j' W^{4rj} \qquad r = 0,1$$

(3.5.27)

By expanding Eq. (3.5.27), they are given as follows

$$D_0 = d_0 + d_1 \quad = a_0 + a_4$$

$$D_1 = d_0 + d_1 W^4 = a_0 + a_4 W^4$$

$$E_0 = e_0 + e_1 \quad = a_2 + a_6$$

$$E_1 = e_0 + e_1 W^4 = a_2 + a_6 W^4$$

$$F_0 = f_0' + f_1' \quad = a_1 + a_5$$

$$F_1 = f_0' + f_1' W^4 = a_1 + a_5 W^4$$

$$K_0' = k_0' + k_1' \quad = a_3 + a_7$$

$$K_1' = k_0' + k_1' W^4 = a_3 + a_7 W^4$$

(3.5.28)

Combining Eqs. (3.5.25) and (3.5.28), the spectral values B_r and C_r, $r = 0,1,2,3$ may be expressed in terms of the four short spectral sequences as follows

$$B_0 = D_0 + E_0$$

$$B_1 = D_1 + E_1 W^2$$

$$B_2 = D_0 + E_0 W^4$$

$$B_3 = D_1 + E_1 W^6$$

$$C_0 = F_0 + K_0'$$

$$C_1 = F_1 + K_1' W^2$$

$$C_2 = F_0 + K_0' W^4$$

$$C_3 = F_1 + K_1' W^6$$

(3.5.29)

where relations $W^8 = 1$ and $W^{10} = W^2$ are used. Therefore, the basis to calculate the finite Fourier transform of a time series a_k, $k = 0,1,2, \ldots,7$ is to use the sets of equations (3.5.28), (3.5.29) and (3.5.26) in this order.

The example illustrated above gives the basic reduction procedures needed to calculate the finite Fourier transform of a time series with eight data samples. From Eqs. (3.5.26), (3.5.28) and (3.5.29), each one of them requires 8 complex multiplications and additions. Thus the finite Fourier transform calculations can be achieved in a total of 24 complex multiplications and additions. Using the straight forward calculations in Eq. (3.5.23), a total of 64 complex multiplications and additions are required.

The reduction of the time sequence can be carried on as long as each reduced data sequence has a number of data points that is divisible by two. This FFT technique can be generalized to handle a time series of any length N as long as $N = 2^p$, where p is any integer larger than 1. The number of complex multiplications and additions is pN instead of N^2, and therefore since always $p \ll N$ the number of calculations is drastically reduced.

In summary, the basic steps for using FFT algorithm to perform spectral calculations for a time series with $N = 8$ may be written as follows:

1. Use Eq. (3.5.28) to calculate the spectral values (D_0, D_1, E_0, E_1, F_0, F_1, K_0', K_1'). These eight values may be stored in the position (complex) occupied by the original data values for they are no longer needed.

2. Use Eq. (3.5.29) to calculate the new set of spectral values (B_0, B_1, B_2, B_3, C_0, C_1, C_2, C_3).

3. Use Eq. (3.5.26) to obtain the required finite Fourier transform set of spectral values (H_0, H_4, H_2, H_6, H_1, H_5, H_3, H_7). It is seen that these spectral values are not arranged in the required order. A bit-reversal procedure is therefore necessary to align them in the proper order.

3.5.2.2 Mathematical Formulations

There is a large number of fast Fourier transform algorithms and computer programs available, the details of their computations are difficult to understand. It is therefore advantageous to develop a new algorithm based on the original theory presented by Cooley and Tukey [19]. The general mathematical formulations for FFT without bit-reversal procedure are presented in this section. A computer program based upon the mathematical formulations of FFT is developed and presented in the appendix.

From the definition of the discrete Fourier transform in Eq. (3.5.22), r may be expressed in the form of

$$r = j_{p-1}2^{p-1} + j_{p-2}2^{p-2} + \ldots + j_2 2^2 + j_1 2 + j_0 \qquad (3.5.30)$$

where $j_\ell = 0$ or 1 for all ℓ.

The time series a_k, $k = 0,1,2,\ldots,N-1$ can be separated into two time sequences each containing half of the total number of data points, thus Eq. (3.5.22) becomes

$$H_r = \sum_{k=0}^{N_1-1} a_k W_0^{\frac{kr}{N}} + \sum_{k=N_1}^{N-1} a_k W_0^{\frac{kr}{N}} \qquad (3.5.31)$$

where $W_0 = e^{-i2\pi}$, $i = \sqrt{-1}$, $N_1 = \dfrac{N}{2} = 2^{p-1}$ and p is the total number of times necessary to reduce the time series into two-point functions. By changing the summation limits in the second term on the right hand side of Eq. (3.5.31), it may be written as

$$H_r = \sum_{k=0}^{N_1-1} [a_k + a_{k+N_1} W_0^{\frac{r}{2}}] W_0^{\frac{rk}{2N_1}} . \qquad (3.5.32)$$

Furthermore, Eq. (3.5.30) can be rearranged as follows

$$\frac{r - j_0}{2} = j_{p-1} 2^{p-2} + j_{p-2} 2^{p-3} + \ldots + j_2 2 + j_1 \equiv r_1 . \quad (3.5.33)$$

Substituting the newly defined value r_1 in Eq. (3.5.33) into the Eq. (3.5.32) one obtains

$$H_r = \sum_{k=0}^{N_1-1} \left[\left\{ a_k + a_{k+N_1} W_0^{\frac{j_0}{2}} \right\} W_0^{\frac{j_0 k}{N}} \right] W_0^{\frac{r_1 k}{N_1}} , \qquad (3.5.34)$$

where use has been made of the fact that $W^n = 1$ for the integers n = 1,2,...,p. Eq. (3.5.32) may again be written as

$$H_r = \sum_{k=0}^{N_1-1} a_{2k+j_0}^{(1)} W_0^{\frac{r_1 k}{N_1}} \qquad k = 0,1,2,\ldots,N_1-1 \qquad (3.5.35)$$

where

$$a_{2k+j_0}^{(1)} = \{ a_k + a_{k+N_1} W_0^{\frac{j_0}{2}} \} W_0^{\frac{j_0 k}{N}} . \qquad (3.5.36)$$

By using similar procedures, Eq. (3.5.35) can be further reduced into another set of time sequences as follows

$$H_r = \sum_{k=0}^{N_2-1} a_{2k+j_0}^{(1)} W_0^{\frac{r_1 k}{N_1}} + \sum_{k=N_2}^{N_1-1} a_{2k+j_0}^{(1)} W_0^{\frac{r_1 k}{N_1}}$$

$$= \sum_{k=0}^{N_2-1} a_{2k+j_0}^{(1)} W_0^{\frac{r_1 k}{N_1}} + \sum_{k=0}^{N_2-1} a_{2k+j_0+N_1}^{(1)} W_0^{\frac{r_1(k+N_2)}{N_1}} ,$$

or

$$H_r = \sum_{k=0}^{N_2-1} \left[\left\{ \left(a_{2k+j_0}^{(1)} + a_{2k+j_0+N_1}^{(1)} W_0^{\frac{j_1}{2}} \right) W_0^{\frac{j_1 k}{N_1}} \right] W_0^{\frac{r_2 k}{N_2}} , \quad (3.5.37)$$

where $N_2 = \dfrac{N_1}{2} = 2^{p-2} = \dfrac{N}{4}$

$r_2 \equiv \dfrac{r_1 - j_1}{2} = j_{p-1} 2^{p-3} + j_{p-2} 2^{p-4} + \ldots + j_3 2 + j_2$

$W_0^{\frac{j_1}{2}} = (-1)^{j_1} .$

Eq. (3.5.37) can again be written as

$$H_r = \sum_{k=0}^{N_2-1} a_{4k+2j_1+j_0}^{(2)} W_0^{\frac{r_2 k}{N_2}} \qquad\qquad k = 0,1,2,\ldots,N_2-1 \quad (3.5.38)$$

where

$$a_{4k+2j_1+j_0}^{(2)} = \{ a_{2k+j_0}^{(1)} + a_{2k+j_0+N_1}^{(1)} (-1)^j \} W_0^{\frac{j_1 k}{N_1}} . \qquad (3.5.39)$$

By employing similar halfing procedures, a general form may be developed through induction as follows

$$H_r = \sum_{k=0}^{N-1} a_k W_0^{\frac{rk}{N}}$$

$$= \sum_{k=0}^{N_1-1} a_{2k+j_0}^{(1)} W_0^{\frac{r_1 k}{N_1}}$$

$$= \sum_{k=0}^{N_2-1} a_{4k+2j_1+j_0}^{(2)} W_0^{\frac{r_2 k}{N_2}}$$

$$= \sum_{k=0}^{N_3-1} a_{8k+4j_2+2j_1+j_0}^{(3)} W_0^{\frac{r_3 k}{N_3}}$$

$$= \quad . \quad . \quad . \quad . \quad . \quad . \quad . \quad . \quad . \quad . \quad . \quad .$$

$$= \sum_{k=0}^{N_{p-1}-1} a_{2^{p-1}k+2^{p-2}j_{p-2}+2^{p-3}j_{p-3}+\ldots+2j_1+j_0}^{(p-1)} W_0^{\frac{r_{p-1} k}{N_{p-1}}}$$

$$(3.5.40)$$

where p is the number of times the data sequences are decomposed into shorter sequences.

By employing halfing procedures a total of p times, one obtains the following expression

$$H_r = \sum_{k=0}^{N_p-1} a_{2^p k+2^{p-1} j_{p-1}+2^{p-2} j_{p-2}+\ldots+2j_1+j_0}^{(p)} W_0^{\frac{r_p k}{N_p}} \, ,$$

$$k = 0,1,2,\ldots,N_p-1 \qquad (3.5.41)$$

where

$$a^{(p)}_{2^p k + 2^{p-1} j_{p-1} + 2^{p-2} j_{p-2} + \ldots + 2j_1 + j_0}$$

$$= \sum_{q=0}^{1} (-1)^{j_{p-1} q} \; a^{(p)}_{2^{p-1} k + 2^{p-2} j_{p-2} + 2^{p-3} j_{p-3} + \ldots 2j_1 + j_0 + q N_{p-1}} \; W_{N_{p-1}}^{j_{p-1} k} \quad ,$$

$$N_p = \frac{N_{p-1}}{2} = 2 \; .$$

The summation limit in Eq. (3.5.41) is no longer in existence if the time series of 2^p data samples is halved continuously a total of p times. Thus, Eq. (3.5.41) can be written as

$$H_r = a^{(p)}_{2^{p-1} j_{p-1} + 2^{p-2} j_{p-2} + \ldots + 2j_1 + j_0} = a_r^{(p)} \tag{3.5.42}$$

which is the final result of a single point transformation.

The previous mathematical developments may also be written in another form of notation so as to be able to grasp more clearly the ideas involved in developing the FFT computer program. In general, Eq. (3.5.22) may be written in the following form

$$H(r) = \sum_{k=0}^{N-1} a(k_{p-1}, k_{p-2}, \ldots, k_1, k_0) W_0^{\frac{rk}{N}} \quad r = 0,1,2,\ldots,N-1$$

$$\tag{3.5.43}$$

where r and k is expressed by

$$r = 2^{p-1}j_{p-1} + 2^{p-2}j_{p-2} + \ldots + 2j_1 + j_0 \;,$$

$$(3.5.44)$$

$$k = 2^{p-1}k_{p-1} + 2^{p-2}k_{p-2} + \ldots + 2k_1 + k_0$$

and k_ℓ and j_ℓ take on values for 0 and 1 only, for all ℓ.
Expanding the exponential term on the right hand side of Eq. (3.5.43),
it gives

$$W_0^{\frac{rk}{N}} = W_0^{r2^{p-1}k_{p-1}/N} \; W_0^{rk^{(1)}/N}$$

$$= W_0^{j_0 k_{p-1}/2} \; W_0^{(2^{p-1}j_{p-1}+\ldots+2j_1)2^{p-1}k_{p-1}/N} \; W_0^{\frac{rk^{(1)}}{N}}$$

$$= W_0^{j_0 k_{p-1}/2} \; W_0^{r_1 k_{p-1}} \; W_0^{j_0 k^{(1)}/N} \; W_0^{r_1 k^{(1)}/N_1} \quad (3.5.45)$$

where $\qquad N_1 = \dfrac{N}{2} = 2^{p-1} \;,$

$$r_1 = \frac{r-j_0}{2} = 2^{p-2}j_{p-1} + 2^{p-3}j_{p-2} + \ldots + 2j_2 + j_1$$

and

$$(3.5.46)$$

$$k^{(1)} = 2^{p-2}k_{p-2} + 2^{p-3}k_{p-3} + \ldots + 2k_1 + k_0 \;.$$

Equation (3.5.43) may be expanded into the following form

$$H(r) = \sum_{k_0=0}^{1} \sum_{k_1=0}^{1} \sum_{k_2=0}^{1} \ldots \sum_{k_{p-1}=0}^{1} a(k_{p-1}, k_{p-2}, \ldots, k_1, k_0)$$

$$W_0^{j_0 k_{p-1}/2} \; W_0^{j_0 k^{(1)}/N} \; W_0^{r_1 k^{(1)}/N_1} \quad (3.5.47)$$

where $W_0^{r_1 k_{p-1}}$ is unity due to the fact that both r_1 and k_{p-1} assume
an integer value.

Equation (3.5.47) may be written as follows

$$H(r) = \sum_{k_0=0}^{1} \sum_{k_1=0}^{1} \sum_{k_2=0}^{1} \cdots \sum_{k_{p-2}=0}^{1} a_1(k_{p-2},k_{p-3},\ldots,k_1,k_0;j_0)$$

$$W_0^{\frac{r_1 k(1)}{N_1}}$$

$$(3.5.48)$$

where $\quad a_1(k_{p-2},k_{p-3},\ldots,k_1,k_0;j_0)$

$$= \sum_{k_{p-1}=0}^{1} a(k_{p-1},k_{p-2},\ldots,k_1,k_0)W_0^{j_0 k_{p-1}/2} W_0^{j_0 k^{(1)}/N}$$

$$(3.5.49)$$

Similarly, by letting

$$a_2(k_{p-3},k_{p-4},\ldots,k_1,k_0;j_1,j_0)$$

$$= \sum_{k_{p-2}=0}^{1} a_1(k_{p-2},k_{p-3},\ldots,k_1,k_0,j_0)W_0^{j_1 k_{p-2}/2} W_0^{j_1 k^{(2)}/N_1} \qquad (3.5.50)$$

Eq. (3.5.47) may be further reduced to

$$H(r) = \sum_{k_0=0}^{1} \sum_{k_1=0}^{1} \cdots \sum_{k_{p-3}=0}^{1} a_2(k_{p-3},k_{p-4},\ldots,k_1,k_0;j_1,j_0)$$

$$W_0^{r_2 k^{(2)}/N_2}$$

$$(3.5.51)$$

where $\quad N_2 = \dfrac{N_1}{2} = 2^{p-2},$

$$r_2 = \frac{r_1 - j_1}{2} = 2^{p-3}j_{p-1} + 2^{p-4}j_{p-2} + \ldots + 2j_3 + j_2 \qquad (3.5.52)$$

and

$$k^{(2)} = 2^{p-3}k_{p-3} + 2^{p-4}k_{p-4} + \ldots + 2k_1 + k_0 .$$

In general, by letting

$$a_q(k_{p-q-1}, k_{p-q-2}, \ldots, k_1, k_0; j_{q-1}, j_{q-2}, \ldots, j_1, j_0)$$

$$= \sum_{k_{p-q}=0}^{1} a_{q-1}(k_{p-q}, k_{p-q-1}, \ldots, k_1, k_0; j_{q-2}, j_{q-3}, \ldots, j_1, j_0) W_0^{j_{q-1}k_{p-q}/2}$$

$$W^{j_{q-1}k^{(q)}/N_{q-1}}, \qquad \text{for } q < p \qquad (3.5.53)$$

the general form of the Fourier coefficients may be written as

$$H(r) = \sum_{k_0=0}^{1} \sum_{k_1=0}^{1} \cdots \sum_{k_{p-q-1}=0}^{1} a_q(k_{p-q-1}, k_{p-q-2}, \ldots, k_1, k_0;$$

$$j_{q-1}, j_{q-2}, \ldots, j_1, j_0) W_0^{r_q k^{(q)}/N_q} \qquad (3.5.54)$$

where $\quad N_q = \dfrac{N_{q-1}}{2} = 2^{p-2},$

$$r_q = \frac{r_{q-1} - j_{q-1}}{2} = 2^{p-q-1}j_{p-1} + 2^{p-q-2}j_{p-2} + \ldots$$

$$+ 2j_{q+1} + j_q \qquad (3.5.55)$$

and

$$k^{(q)} = 2^{p-q-1}k_{p-q-1} + 2^{p-q-2}k_{p-q-2} + \ldots + 2k_1 + k_0 .$$

For the case $p = q + 1$, Eq. (3.5.54) may be written as

$$H(r) = \sum_{k_0=0}^{1} a_{p-1}(k_0;j_{p-2},j_{p-3},\ldots,j_1,j_0)W_0^{r_{p-1}k^{(p-1)}/N_{p-1}} \qquad (3.5.56)$$

where p is the largest integer value of the time series with sample length $N = 2^p$. Further reduction of Eq. (3.5.56) gives

$$H(r) = a_p(j_{p-1},j_{p-2},\ldots,j_1,j_0) \qquad (3.5.57)$$

which is simply the transformation into a single data sample.

3.6 Computing Techniques

The computational procedures using the FFT method for power and cross spectra of multiple stationary time series is based on the requirement that the total number of data points transformed to be integer powers of two. If the blocked time series do not have this required number of data points, zeros must be added to fill up the series to the required number before applying Fourier transformation.

In case the calculated spectrum will be used to obtain the correlation function, then the time series should be filled up with zeros to obtain a total data points of 2^{p+1} to start with. This new approach of obtaining correlation functions by using two passes of Fourier transformation has been considered to be more economical in comparison with the direct multiply-add operations in obtaining the correlation functions. These correlation functions can further be used to obtain smoothed spectral estimates by applying the properly chosen lag windows whose characteristics are more generally discussed in time series analysis [51].

The general procedures used in computing power and cross spectral estimates via FFT are listed in the following two sections.

3.6.1 Power Spectrum

Reasonable power spectral estimates can be obtained for a time series of length $n = 2^p$ by the following procedures:

1. Either truncate the excessive data or add zeros so the number of data points for blocked time series $a_i'^m$, $i = 1,2,\ldots,n$, $m = 1,2,\ldots$, M-1, to be transformed is $n = 2^p$, where p is an integer and M is the total number of blocks.

2. Taper the blocked time series with a cosine taper data window as discussed in section 3.3.1 or with another appropriate tapering function as presented in section 3.3.2.

3. Compute the finite Fourier transform of each blocked subseries by

$$\hat{H}_r^m(f) = \sum_{k=0}^{n-1} a_k'^m(t)W^{rk} \qquad r = 0,1,2,\ldots,n-1 \qquad (3.6.1)$$

where $W = e^{-i2\pi/n}$ and $m = 1,2,\ldots,$M-1 is the block number.

4. Compute the absolute squared value scaled appropriately to obtain the power spectral estimates by

$$\hat{G}_{ar}^m = \frac{2\Delta t}{n}\left|\hat{H}_r^m\right|^2 \qquad r = 0,1,2,\ldots,n-1 \qquad (3.6.2)$$

where subscript a in $\hat{G}_{ar}^m$ refers to blocked time series $a_i'^m$ for i = 1,2,\ldots,n and $m = 1,2,\ldots,$M-1.

5. Adjust the power spectral estimates for a scale factor due to the cosine data window tapering by

$$\hat{G}_{ar}^{\ m} = \frac{1}{0.875} \ \hat{G}_{ar}^{\ m} \qquad\qquad r = 0,1,2,\ldots,n-1 \ . \qquad (3.6.3)$$

6. Adjust the segment average for M-1 blocked spectral estimates each of length n by

$$\hat{G}_{ar} = \frac{1}{M-1} \sum_{m=1}^{M-1} \hat{G}_{ar}^{\ m} \qquad\qquad r = 0,1,2,\ldots,n-1 \ . \qquad (3.6.4)$$

7. Apply the frequency smoothing for segmently smoothed spectral estimates of length n = 8192. The spectral estimates are unique only up to the point where $r = \frac{n}{2} + 1$. This is due to the result of the application of the Fourier transform. At this point the Nyquist cut-off frequency occurs. The smoothing is performed for 4096 spectral estimates without including the zero frequency point.

Looking at the printed-out spectral estimates of 4096 values, the energy is more concentrated in the lower frequency range. The proposed frequency smoothing technique as discussed in section 3.4.4 is therefore adopted. The frequency smoothed spectral estimates may be considered as representing the midpoint of the frequency interval from f_k to $f_{k+\ell-1}$, $k \geq 1$, where ℓ is the chosen average value except when ℓ equals unity. The value of the frequency associated with different values of ℓ and which corresponds to the spectral estimate in Eqs. (3.4.5) to (3.4.9) is calculated as follows

$\ell = 1$

$$f_k = k\Delta f \qquad\qquad k = 1,2,\ldots,8 , \qquad\qquad (3.6.5)$$

$\ell = 4$

$$f_k = [4(k-7) + 2.5]\Delta f \qquad k = 9,10,\ldots,38 , \qquad (3.6.6)$$

$\ell = 16$

$$f_k = [16(k-31) + 9.5]\Delta f \qquad k = 39,40,\ldots,62 , \qquad (3.6.7)$$

$\ell = 64$

$$f_k = [64(k-54) + 33.5]\Delta f \qquad k = 63,64,\ldots,86 , \qquad (3.6.8)$$

and $\ell = 256$

$$f_k = [256(k-79) + 129.5]\Delta f \qquad k = 87,88,\ldots,94 , \qquad (3.6.9)$$

where $\Delta f = \frac{1}{n\Delta t}$. The number of the spectral estimates was reduced to 94 as a result of the application of the segment average and frequency smoothing technique in section 3.4.4. The frequency points represented in Equations (3.6.5) to (3.6.9) are corresponding to these smoothed spectral estimates.

3.6.2 Cross Spectrum

The computations for the cross spectral estimates between two discrete time series a_i and b_i, $i = 0,1,2,\ldots,n-1$ seem to be more involved due to the requirement of obtaining the coherence function and phase angles between the two time series. The general procedures for calculating cross spectral estimates via FFT can be written as follows

1. Either truncate the excessive data or add enough zeros in the two discrete time series $a_i^{'m}$ and $b_i^{'m}$, $i = 0,1,2,\ldots,n-1$ so that $n = 2^p$ as discussed in step 1 in section 3.6.1.

2. Taper both blocked time series $a_i^{'m}$ and $b_i^{'m}$, $i = 0,1,2,...,n-1$ with the cosine taper data window or other appropriate data windows as presented in section 3.3.2.

3. Let $a_i^{'m}$ be the real part and $b_i^{'m}$ be the imaginary part of a newly created complex time series $c_i^{'m} = a_i^{'m} + jb_i^{'m}$, $i = 0,1,2,...,n-1$ and $j = \sqrt{-1}$.

4. Compute the finite Fourier transform of each blocked complex time series by

$$\tilde{C}_r^m(f) = \sum_{k=0}^{n-1} c_k^{'m}(t) \, W^{rk} \qquad r = 0,1,2,...,n-1 \qquad (3.6.10)$$

where $W = e^{-\frac{2\pi}{n}}$ and $m = 1,2,...,M-1$ is the block number.

5. Obtain the respective spectral values of both $a_i^{'m}$ and $b_i^{'m}$, $i = 0,1,2,...,n-1$ by using the properties of the Fourier transformation as discussed in section 3.5.1 as follows

$$\tilde{C}_{r_1}^m(f) = \frac{\tilde{C}_r^m(f) + \tilde{C}_{n-r}^{m*}(f)}{2} \qquad (3.6.11)$$

and

$$\tilde{C}_{r_2}^m(f) = \frac{\tilde{C}_r^m(f) - \tilde{C}_{n-r}^{m*}(f)}{2j} \qquad (3.6.12)$$

where $\tilde{C}_{n-r}^{m*}(f)$ represents complex conjugate of $\tilde{C}_{n-r}^{m*}(f)$ and $j = \sqrt{-1}$.

6. Compute the cross spectral estimate $\hat{G}_{abr}^m$, $r = 0,1,2,...,n-1$ for block m by

$$\hat{G}_{abr}^m = \frac{2\Delta t}{n} \left| \tilde{C}_{r_1}^{m*}(f) \, \tilde{C}_{r_1}^m(f) \right| . \qquad (3.6.13)$$

7. Adjust the cross spectral estimates by a scale factor due to cosine data window tapering in each block

$$\hat{G}_{abr}^{m}(f) = \hat{G}_{abr}^{m}\left(\frac{1}{0.875}\right) \qquad r = 0,1,2,\ldots\frac{n}{2} + 1 \qquad (3.6.14)$$

8. Apply the segment average smoothing for M-1 blocks of spectral estimates each of length n by

$$\hat{G}_{abr}(f) = \frac{1}{M-1} \sum_{m=1}^{M-1} \hat{G}_{abr}^{m} \qquad r = 0,1,2,\ldots,\frac{n}{2} + 1 \qquad (3.6.15)$$

9. Pick up the real and imaginary part of $\hat{G}_{abr}$ by

$$\hat{G}_{abr}(f) = Co_{abr}(f) - j\ Q_{abr}(f) \quad r = 0,1,2,\ldots\frac{n}{2} + 1 \qquad (3.6.16)$$

where $Co_{abr}(f)$ is called the cospectral density function and $Q_{abr}(f)$ is called the quadrature spectral density function.

10. In order to apply the proposed frequency smoothing technique for cross spectral density estimate, two different ways can be taken as the following

a. Smooth the cross spectral estimate $\hat{G}_{abr}(f)$ and then obtain the Co- and quadrature-spectral density function.

b. Smooth the real and imaginary parts of $\hat{G}_{abr}(f)$ individually and then obtain the final smoothed cross spectral estimates.

These two prcoedures can give different results, since the linear smoothing operation, the non-linear operations of the square root of squared value, and division are not commutative. In meteorological applications, it is the co- and quadrature-spectral density functions that are of interest instead of the positively valued cross spectral density function. Thus, the procedure of smoothing the real

and imaginary parts of the cross-spectral estimates separately is
used in this case. The final smoothed cross spectral density esti-
mates are obtained by

$$\hat{G}_{abr}(f) = \sqrt{Co^2_{abr}(f) + Q^2_{abr}(f)} \quad r = 1,2,\ldots,94 \ . \quad (3.6.17)$$

11. The phase angle contained in the smoothed cross spectral
estimate $\hat{G}_{abr}(f)$ is calculated by

$$\Theta_{abr} = \tan^{-1} \left[\frac{Q_{abr}(f)}{Co_{abr}(f)} \right] \quad r = 1,2,\ldots,94 \ . \quad (3.6.18)$$

12. The smoothed squared coherence estimate is given by

$$Coh^2_{abr}(f) = \frac{\hat{G}^2_{abr}(f)}{\hat{G}_{ar}(f) \cdot \hat{G}_{br}(f)} \quad r = 1,2,\ldots,94 \quad (3.6.19)$$

where $\hat{G}_{ar}(f)$ and $\hat{G}_{br}(f)$ are calculated by Eq. (3.6.4). The frequency
smoothing technique of $\hat{G}_{ar}(f)$ and $\hat{G}_{br}(f)$ was presented in the previous
section.

CHAPTER IV

STATISTICAL ERRORS

Errors in calculations of statistical quantities of digitized time series are quite uncertain because of the large amount of data collected, the underlying probabilistic nature of the data and the method in deriving the desired statistical parameters.

The random nature of the data makes it almost impossible to know the deterministic characteristics of a physical phenomenon. It is only possible to know the average level and to obtain some estimate of the reliability or accuracy of this average level.

In representing an estimate of a statistical parameter, no indication of the reliability of the estimate is found from the simple calculations of the estimated value. Given the size of the sample does not provide the means to interpret the accuracy of the estimate as a function of the sample size. A more direct indication of the accuracy is desirable.

The standard error of any estimate is used to indicate the reliability or precision of the calculation of this estimate. What one really wants is a range of values within which the estimates should fall. Therefore, the notion of confidence interval for a parameter is commonly used to serve this purpose.

This chapter will investigate the validity of estimating the blocked mean and blocked variances in the blocked time series in relation to the sample mean and sample variances of the total sample. The confidence interval of spectral density estimates as a result of using the FFT technique will be determined in this chapter.

4.1 Mean Value Estimate

The block mean value for n data points of the ith time series in the mth block may be calculated by

$$\overline{A}_i^m = \frac{1}{n} \sum_{j=1}^{n} A_i(j) \qquad i = 1,2,\ldots,4 \qquad (4.1.1)$$

where bar denotes the mean value and i indicates the number of the time series.

The sample mean of the time series is simply the arithmetic average of the block mean values as obtained by

$$\overline{A}_i = \frac{1}{M} \sum_{m=1}^{M} \overline{A}_i^m \qquad i = 1,2,\ldots,4 \qquad (4.1.2)$$

where M is the total number of blocks in the time series.

In case the time series has not been blocked, then the sample mean is calculated by

$$\overline{A}_i^* = \frac{1}{N} \sum_{j=1}^{N} A_i(j) \qquad i = 1,2,\ldots,4 \qquad (4.1.3)$$

where N is the total number of samples in the time series (i.e. N = nM).

Combining Eqs. (4.1.1) and (4.1.2), one obtains

$$\bar{A}_i = \frac{1}{Mn} \sum_{m=1}^{M} \sum_{j=1}^{n} A_i(j)$$

$$= \frac{1}{Mn} \left\{ \sum_{j=1}^{n} A_i(j) + \sum_{j=n+1}^{2n} A_i(j) + \ldots + \sum_{j=(M-1)n+1}^{Mn} A_i(j) \right\}$$

$$= \frac{1}{Mn} \sum_{j=1}^{Mn} A_i(j) \qquad\qquad i = 1,2,\ldots,4 \qquad\qquad (4.1.4)$$

Comparing Eqs. (4.1.3) and (4.1.4), it is seen that the sample mean of the sample can be calculated from the average of the block mean values in each subseries. The only possible difference between the calculated sample mean value of Eq. (4.1.2) and (4.1.3) is the summation of large numbers by floating-point representation in the computer without using double precision. In fact, the sample mean values calculated from Equation 4.1.2 should be more accurate than using Equation 4.1.3 directly.

4.2 Variance and Covariance Estimates

The sample variance and covariance are calculated from the filtered series with exactly zero mean by Eq. (2.4.2) as follows

$$\overline{a_i a_j} = \frac{1}{M-1} \sum_{m=1}^{M-1} \overline{a_i a_j}^m \qquad\qquad i,j = 1,2,\ldots,4 \qquad\qquad (4.2.1)$$

where block variances and covariances are calculated from Eq. (2.4.1)

$$\overline{a_i a_j}^m = \frac{1}{n} \sum_{k=1}^{n} a_i(k)a_j(k) \qquad\qquad i,j = 1,2,\ldots,4 \qquad\qquad (4.2.2)$$

where a_i, $i = 1,2,\ldots,4$ represents filtered time series. Equal subscripts $i = j$ in Eq. (4.2.1) denote the variances while unequal subscripts $i \neq j$ represent the covariances.

In case the filtered subseries has a near zero mean but not exactly zero mean, then the values of block variances and covariances calculated by Eq. (4.2.2) will be overestimated. The variance and covariance of the total sample with near zero mean values for the subseries are calculated as follows

$$\overline{a_i a_j}^* = \frac{1}{M-1} \sum_{m=1}^{M-1} \left[\frac{1}{n} \sum_{k=1}^{n} (a_i(k) - \overline{a_i}^m)(a_j(k) - \overline{a_j}^m) \right]$$

$$= \frac{1}{M-1} \sum_{m=1}^{M-1} \left[\frac{1}{n} \sum_{k=1}^{n} a_i(k)a_j(k) - \frac{\overline{a_i}^m}{n} \sum_{k=1}^{n} a_j(k) \right.$$

$$\left. - \frac{\overline{a_j}^m}{n} \sum_{k=1}^{n} a_i(k) - \frac{1}{n} \sum_{k=1}^{n} \overline{a_i}^m \overline{a_j}^m \right]$$

$$= \frac{1}{M-1} \sum_{m=1}^{M-1} \left[\overline{a_i a_j}^m - \overline{a_i}^m \overline{a_j}^m \right]$$

$$= \overline{a_i a_j} - \frac{1}{M-1} \sum_{m=1}^{M-1} \overline{a_i}^m \overline{a_j}^m \qquad (4.2.3)$$

where

$$\overline{a_i}^m = \frac{1}{n} \sum_{k=1}^{n} a_i(k) \qquad i = 1,2,\ldots,4 \ . \qquad (4.2.4)$$

Consequently, $\overline{a_i}^m$ is the mean value of the subseries after the moving average filter has been applied to the total sample. The reason we

chose the number of blocks to be M-1 here is because the data samples were filtered and the ends were lost. Now, the sample variances and covariances based on the total filtered sample can be calculated as follows

$$\overline{a_i a_j}^{**} = \frac{1}{N} \sum_{k=1}^{N} (a_i(k) - \overline{a_i})(a_j(k) - \overline{a_j}) , \qquad (4.2.5)$$

where $\overline{a_i}$ is defined by

$$\overline{a_i} = \frac{1}{N} \sum_{k=1}^{N} a_i(k) \qquad i = 1,2,\ldots,4 \qquad (4.2.6)$$

and N is the total number of data points in the filtered sample. In this case, N is equal to n(M-1) data samples.

Expanding the terms in the right hand side of Eq. (4.2.5) and combining, one obtains

$$\overline{a_i a_j}^{**} = \overline{a_i a_j} - \overline{a_i}\,\overline{a_j} \quad i,j = 1,2,\ldots,4 \qquad (4.2.7)$$

where the Equations 4.2.1 and 4.2.2 have been used.

The error E(m) in variances and covariances as a result of the subdivision of the original time series in blocks may be obtained by combining the Equations 4.2.3 and 4.2.7 as follows

$$E(m) = \overline{a_i a_j}^{**} - \overline{a_i a_j}^{*}$$

$$= \frac{1}{M-1} \sum_{m=1}^{M-1} \overline{a_i^m a_j^m} - \overline{a_i}\,\overline{a_j} \qquad (4.2.8)$$

or

$$E(m) = \frac{1}{M-1} \sum_{m=1}^{M-1} (\overline{a_i} - \overline{a_i}^m)(\overline{a_j} - \overline{a_j}^m) \ . \tag{4.2.9}$$

The value of this error $E(m)$ can be discussed by the following two limiting cases:

1. In the limit when $m = 1$, the total sample consists of one block only, the error is zero.

2. In the limit when m approaches infinity and the sample contains a finite number of data points, then each block contains only one data point. In this case, the block mean value is simply the value of the data point itself in the block. It is obvious that the error $E(m)$ is again zero.

In case when the number of blocks is chosen to be a finite value as in most practical situations, the error $E(m)$ can be significant since it depends on the time of the subseries. The time of the subseries will affect the shape of the moving average filter as can be seen from Figure 5. The effective cut-off frequency in the filter with different time interval is different. One should choose the block length of the subseries to be comparable to the period of the minimum frequencies of interest. The storage limitation in the computer for numerical calculations imposed another restriction in the selection of the block length in the subseries.

4.3 Spectral Density Estimate

For a stationary Gaussian random process $\{a(t)\}$, the power spectrum for a sample record $a_k(t)$, $k=0,1,..,n-1$ of finite length n is defined by

$$G_a(f) = 2 \lim_{n \to \infty} \frac{1}{n} E\left[|H(f,n)|^2\right] \tag{4.3.1}$$

where

$$H(f,n) = \Delta t \sum_{k=0}^{n-1} a_k(t) e^{-j2\pi fk\Delta t} . \tag{4.3.2}$$

The estimate of power spectrum can be obtained by omitting the limiting and expectation operations in the Eq. (4.3.1) to yield the following

$$\hat{G}_a(f) = \frac{2}{n\Delta t} |H(f,n)|^2 \tag{4.3.3}$$

with the narrowest possible resolution $B_e = \frac{1}{n\Delta t}$.

For the discrete frequency values, the Fourier components are defined by

$$H_k = \frac{H(f,n)}{\Delta t} = \sum_{k=0}^{n-1} a_k(t) e^{-j2\pi fk\Delta t} \tag{4.3.4}$$

and the spectral estimate is given by

$$\hat{G}_a(f) = \frac{2\Delta t}{n} |H_k|^2 \tag{4.3.5}$$

The estimate of the spectral density function $G_a(f)$ is denoted by $\hat{G}_a(f)$ and is unbiased if

$$E[\hat{G}_a(f)] = G_a(f) . \tag{4.3.6}$$

The mean square error of the power spectral density estimate is defined by

$$\text{m.s.e.} = E[(\hat{G}_a(f) - G_a(f))^2] . \tag{4.3.7}$$

In general, the power spectral density estimate is a function of the number of data samples n. In order that $\hat{G}_a(f)$ is the consistent estimate of the power spectral density function $G_a(f)$, it is required that

$$\lim_{n \to \infty} E[(\hat{G}_a(f) - G_a(f))^2] = 0 . \qquad (4.3.8)$$

By assuming the random process $\{a_i\}$, $i = 1,2,\ldots,n$ to be uncorrelated white noise. Otnes and Enochson [67] proved that the power spectral density estimate $\hat{G}_a(f)$ is an unbiased but not a consistent estimate of the power spectral density function $G_a(f)$.

4.3.1 Chi-Square Distribution

The Fourier components H(f,n) computed by Eq. (4.3.2) are complex with real and imaginary parts, $H_R(f,n)$ and $H_I(f,n)$ which are uncorrelated random variables with zero mean and unit variance [6]. Both $H_R(f,n)$ and H (f,n) will be Gaussian random variables if the data sample $a_i(t)$, $i = 0,1,2,\ldots,n-1$ is Gaussian as a result of the linear operation of the Fourier transformation. It is seen that the quantity

$$|H(f,n)|^2 = H_R^2(f,n) + H_I^2(f,n) \qquad (4.3.9)$$

is the sum of the squares of two independent Gaussian variables. From the definition of Chi-square distribution, each frequency component of the power spectral density $\hat{G}_a(f)$ will have a sampling distribution given by

$$\frac{2\hat{G}(f)}{G(f)} = \frac{\chi_2^2}{2} \qquad (4.3.10)$$

88

where χ_2^2 is the Chi-square variable with two degrees of freedom. The number of degrees of freedom, γ, represents the number of independent or "free" squares summing in the expression (4.3.9). The mean and variance of the chi-square variable are γ and 2 , respectively. The normalized mean square error can be obtained by

$$\epsilon^2 = \frac{E[(\hat{G}_a(f) - G_a(f))^2]}{[G_a(f)]^2} = \frac{2}{\gamma} \tag{4.3.11}$$

where use has been made of Equation 4.3.6.

For $\gamma = 2$, the normalized standard error is given by

$$\epsilon = \sqrt{\frac{2}{\gamma}} = \pm 1 \tag{4.3.12}$$

which means that the standard deviation of the pSD estimate is as great as the quantity being estimated. To reduce the error of the pSD estimate as calculated by Eq. (4.3.5), smoothing the estimates is necessary. By smoothing either segmentally or frequency smoothing as discussed in chapter three, the number of degrees of freedom γ can be increased. It is seen, from Eq. (4.3.12) that the normalized standard error can be reduced if γ is increased.

The $(1 - \alpha)$ confidence interval for the power spectral density function $G_a(f)$ around the frequency f based upon an estimate $\hat{G}_a(f)$ measured with a resolution bandwidth B_e and a record length n is given by

$$\left[\frac{\gamma\hat{G}_a(f)}{\chi^2_{\gamma;\frac{\alpha}{2}}} \le G_a(f) < \frac{\gamma\hat{G}_a(f)}{\chi^2_{\gamma;1-\frac{\alpha}{2}}}\right] = 1 - \alpha . \tag{4.3.12}$$

and
$$\gamma = 2B_e n .$$
(4.3.13)

The term, $1 - \alpha$, is a fixed confidence level which commonly is taken to be 0.80, 0.90 or 0.95. The true value $G_a(f)$ lies between the two values in the bracket of Eq. (4.3.12). The Chi-square distribution $\chi^2_{\gamma;\alpha}$ is tabulated in Table III and defined by

$$\chi^2_{\gamma;\alpha} = [b \text{ such that } \int_b^\infty P(\chi^2_r)d\chi^2_\gamma = \alpha]$$
(4.3.14)

For degrees of freedom where $\gamma > 30$, the following expression may be used to obtain the χ^2 distributions.

$$\chi^2_{1-\alpha} = \frac{1}{2} \left[T^*_\alpha + \sqrt{2\gamma - 1} \right]$$
(4.3.15)

where T^*_α is the corresponding percentile of the standard normal distribution (Table I).

4.3.2 Numerical Example

An example will illustrate the application of Equations 4.3.12 and 4.3.15.

The total number of data points used for the estimation of the spectral density for 43 blocks each of which contains 8192 data points is

$$N = 8192 \times 43 = 352,256 .$$

The effective bandwidth for a sampling rate of 200 samples per second is

$$B_e = \frac{1}{N\Delta t} = 0.000567 \text{ HZ} .$$

The number of the degrees of freedom is

$$\gamma = 2B_e T \simeq 2 .$$

The 95% confidence interval for two degrees of freedom in Chi-square distribution is found from Table 3 to be

$$\left. \begin{array}{l} \chi^2_{2; \ .975} = .051 \\ \\ \\ \chi^2_{2; \ .025} = 7.38 \end{array} \right\} \qquad\qquad (4.3.16)$$

If $\hat{G}_a(f)$ is the spectral density estimate, then the 95% confidence interval of the true spectral density function $G_a(f)$ is given by

$$\left[\frac{2}{7.38} \hat{G}_a(f) \leq G_a(f) \leq \frac{2}{0.051} \hat{G}_a(f) \right]$$

or

$$[0.271 \ \hat{G}_a(f) \leq G_a(f) \leq 39.215 \ \hat{G}_a(f)] . \qquad (4.3.17)$$

It is seen from Eq. (4.3.17) that the true spectrum lies in a wide range of values and that little confidence can be placed on the estimate. The range of the confidence interval can be reduced by increasing the number of degrees of freedom. The number of degrees of freedom can be increased greatly when the segment average technique is applied. By averaging over 43 blocks of spectral density estimates, the resulted smoothed spectral density estimate has the number of degrees of freedom as follows

$$\gamma = 43 \times 2 = 86$$

The 95% confidence bands for 86 degrees of freedom in Chi-square distribution is formed by using Equation 4.3.15 as follows

$$\left. \begin{array}{l} \chi^2_{86;\ .975} = 61.68 \\[2ex] \chi^2_{86;\ .025} = 113.2 \end{array} \right\} \tag{4.3.18}$$

and the true spectrum lies in the interval

$$[.76\ \hat{G}_a(f) \le G_a(f) \le 1.39\ \hat{G}_a(f)] \tag{4.3.19}$$

It is seen that the range of values in between which the true spectrum lies has been reduced as a result of applying the segment smoothing technique in the spectral density estimates. The application of frequency smoothing on the spectral density estimates may give a much better representation in the range of estimated values.

The analysis shown above was based upon the assumption that the data samples were both Gaussian and white. In general, the data are colored (i.e. correlated) in some manner. This has the effect of reducing the number of the degrees of freedom in the Chi-square distribution. The standard practice is to use the white noise results as a guideline in the spectral density estimates [67].

CHAPTER V

DISCUSSION OF THE RESULTS

The data used for the statistical analysis in this dissertation
were measured with either the Model 1080D Total Vector Anemometer
probe (triple split films) or the Model 1296L dual split film
probe both manufactured by Thermo-Systems, Inc. The operation and
the analysis of the data from these probes are discussed in detail
in references [95] and [108] respectively. In conjunction with the
two types of TSI probes a set of Gill propeller anemometers was used.
These propeller anemometers were mounted in such a way that one was
parallel to the TSI probe and the other perpendicular to the first
one and both in a horizontal plane and located adjacent to the TSI
probe. A detailed discussion of the operation of the Gill anemometers
and data analysis can be found in Appendix A. The Gill anemometers
were used mainly for comparison of results with those obtained from
both types of TSI probes. The anemometers were located on the top of
the air exchanger of the low speed wind tunnel at Virginia Polytechnic
Institute and State University. This was the best location available
in the neighborhood of this wind tunnel in which the anemometers were
calibrated. The connecting cable between the probe and the anemo-
meter was 350 feet long, and since it was not feasible to move the
trailer in which the data acquisition system was located, the above

described location for the probes was the best available within
a 350-foot radius from the trailer.

It turned out that the winds measured in this location as mentioned
above were mainly from a north-west direction. However, due to the
presence of upstream buildings and due to the location of the anemo-
meters on top of the wind tunnel a flow was measured with an appreciable
vertical component and with relatively large fluctuations in magnitude
and lateral direction. As a result of the type of data measured, a
great deal of effort was used in the proper analysis of the data with
respect to stationarity, filtering and smoothing of the calculated
statistical quantities. Mean values, variances, covariances, power
spectral estimates, cross spectral estimates, coherence functions and
phase angles of the three turbulent wind components in the mean wind
oriented coordinate system were calculated.

During the period in time that these data were taken, considerable
troubles were still encountered with the data acquisition system
(see reference [95] for a detailed description of the data acquisition
system). Specifically, the PDP-11/20 mini-computer had an intermittent
problem which was extremely difficult to pin down. Also, the data
acquisition as well as the consequent digitizing of the data was
affected by the simultaneous operation of the wind tunnel. It was
found that fluctuations in line voltage as a result of the starting of
the wind tunnel often erased the recorded time of day or the recorded
voltages of the anemometers.

Due to the fact that two different anemometers (TSI and Gill) were used simultaneously, the data from the Gill had to be recorded on an F.M. tape recorder first and consequently played back at a later time in order to be digitized. The data received from either TSI - anemometer was fed directly into the multiplexer and directly stored on the digital tape. It often occurred that bad data or no data were recorded on the digital tape or that tape marks disappeared and as a result the data were useless. Since this period, the entire data acquisition and data handling system has been moved to NASA - Wallops Station for data gathering from the meteorological tower at Wallops Island. The Wallops Island data will be analyzed at a later date, only data taken at the Virginia Polytechnic Institute and State University location will be discussed in this dissertation. The data acquisition and data handling system while in operation at Wallops Island did not experience the breakdown and problems as were en-countered when in operation at Virginia Polytechnic Institute and State University. Consequently, the data discussed in this report are somewhat sketchy, but adequate to indicate that very good results can be obtained with the system.

The accuracy and the efficiency of the computer program which was developed in order to calculate the statistical quantities of a digitized time series, was tested against a simulated time series. The theory and the processing of digital simulation of random processes is described in detail by Sinha [87]. If the power-spectral density

function is known, a sample of the corresponding time series can be developed by inverse fast Fourier transformation.

In order to simulate the streamwise turbulence component in the atmosphere, use was made of the semi-empirical von Karman spectrum given by the following expression in dimensionless form

$$\frac{fG(f)}{\overline{u^2}} = \frac{4\frac{Lf}{\overline{U}}}{\left[1 + 70.78 \left(\frac{Lf}{\overline{U}}\right)^2\right]^{5/6}}$$

A 20% intensity of the turbulence was assumed so that $\sqrt{\overline{u^2}} = 0.20\ \overline{U}$. Here, $G(f)$ is the power spectral density function of the streamwise turbulence component so that

$$\int_0^\infty G(f)df = \overline{u^2}\ ,$$

and L is the longitudinal integral scale which varies with height but which was chosen to be 360 feet.

Based on this information a value for the simulated time series was calculated at intervals of .05 seconds. In this manner $(2)^{15}$ data points were generated which represents the digitized time series sampled at a rate of 20 samples per second and of 27.31 minutes duration (Figure 12). This simulated, digitized time series was then used as the input to the computer program which was developed for the statistical analysis of time series of long duration. The calculated power spectral density function was then compared with the original semi-empirical von Karman spectrum from which the time series was

developed. As can be seen from Figure 13, the similarity is very good, especially at higher frequencies. At lower frequencies, the estimates of the power spectral density function seem to deviate a great deal from the expected values which is due to the limited sample length of the simulated time series.

Because of the way the fast Fourier transformation works, only a few points at the lower frequency range are calculated and as a result one can only resort to the so-called segment smoothing of the spectral estimates in this range. At the high frequency range the density of calculated spectral estimates is much higher and as a result the so-called combined smoothing process can be applied with the result that the estimates show much less scattering.

The statistical quantities are calculated from the data measured by three different wind measuring sensors, namely, Gill anemometers, TSI Model 1080-D total vector anemometer and the TSI Model 1296, dual split-film probe for four separate runs. Mean values, variances and the covariances are all listed and compared in Tables IV through VII. The smoothed spectral density estimates are plotted versus frequencies in Figures 14 through 25.

In Table IV, the block means, samples means and the number of reverse arrangements of the block means used for statistical test are listed for each velocity component in the sensor oriented coordinate system. Mean wind velocity, variances and covariances of the velocity components and temperature in the mean wind coordinate system are also tabulated. The calculated numbers of reverse arrangements of

the block means of the velocity components show that the hypothesis of nonstationarity as far as the trend in the data is concerned is acceptable at the 10 percent level of significance for the A and B components of the veloicty. The reverse arrangements of the block means of the C component shows that some trend is present. However, for this run the results of the trend test are in general acceptable. If the number of reverse arrangements would be significantly different from the expected numbers given in Table II, the hypothesis of acceptable nonstationarity would be rejected and the data would be rejected for further analysis.

The results of run 10 show that an appreciable vertical mean velocity component is present and the turbulence intensities are between 20 and 25 percent for all three components.

The smoothed power spectral density estimates of each velocity component of run 10 are plotted against frequency in Figures 14 through 16. The area under the curves correspond closely to the respective variances and at the high frequency range the spectrum functions vary as expected as the frequency to the -5/3 power. Due to the limitation of core storage in the IBM 360/155 digital computer, the number of data points selected in the subseries restricts the computation of the spectrum functions at frequencies above 0.0244 hertz (period of 40.96 seconds). Due to the chosen sample rate of 200 samples per second the maximum frequency at which the spectrum function can be analyzed is 100 hertz.

The cospectrum between the longitudinal and vertical velocity components is plotted in Figure 17, and the shape of the spectrum agrees fairly well with that which was observed at Brookhaven, Long Island and and reported by Panfsky [72].

In Table V, the results calculated from the data of run 11 as measured by the TSI #1192 total vector anemometer and the Gill anemometers are compared. In order that the results calculated from the data as measured by these two different sensors are comparable, the block means calculated from the velocity components measured by TSI #1192 probe are transformed into the probe oriented coordinate system. The number of reverse arrangements of the block means for measurements from the TSI #1192 probe are calculated based on the velocity components in the sensor oriented coordinate system. The number of reverse arrangements of the block means for Gill anemometers are calculated based on the data obtained in the probe oriented coordinate system.

The number of reverse arrangements for the block means of the lateral velocity component is very high and after examination of the data one can see that this is due to a gradual change in wind direction or due to the gradual change from positive to negative lateral velocity components. The longitudinal component of the velocity does not show any trend and is not very much affected by the gradual change in wind direction. Comparison of the block means and the sample mean shows that the longitudinal component measured by the Gill anemometer is consistently higher than that measured by the TSI probe. The block means and the sample mean of the lateral velocity component and the angle the mean wind makes with the direction of the instruments compare very well.

Due to the limited response characteristics of the Gill anemometers, the turbulence quantities obtained from the Gill anemometer are consistently lower than those obtained from the TSI probe. Due to the presence of some high frequency noise during the data runs, the smoothed spectral estimates

have folded in the high-frequency range and as a result the graphs for the smoothed spectral estimates for run 11 are not shown.

In Tables VI and VII, the results calculated from the data of both runs 12 and 14 as measured by the dual split-film anemometer and Gill anemometers are tabulated and compared. Both these anemometers measure the velocity components in the same probe oriented coordinate system. Since the shafts of the propellers of the Gill anemometers are parallel to each of the two perpendicular coordinate axes in the horizontal plane, only the block means of the longitudinal and lateral velocity components can be compared in Tables VI and VII. The block means calculated from the vertical velocity components as measured by the dual split-film probe are tabulated only for completeness not for comparison.

The number of reverse arrangements for the block means of the longitudinal and lateral velocity components for both run 12 and 14 show that the data are free of abnormal trends. Again the Gill anemometer overestimates the block means of the longitudinal velocity component by as much as 15 percent. The variances $\overline{u^2}$ and $\overline{v^2}$ are estimated lower by the Gill anemometers as before. For this particular type of flow the values for the covariance $\overline{uw}$ are very low and compare reasonably well. The horizontal angles of attack between the mean wind and the instruments compare quite well for both runs.

In both Tables VI and VII, comparisons are also made for the values of the sample means, the variances, and the covariances of the velocity components in the mean wind coordinate system for the cases with either the near-zero block-mean values removed or not removed. These near-zero

block means are the mean values remaining in the data samples of each block after having applied the moving-average and differencing high-pass filter to the origional time series as discussed in chapter two. The small near-zero mean values do not have any effect upon the values of the mean velocity components in either the probe oriented coordinate system or the mean wind coordinate system since the mean velocity components are calculated from the unfiltered original time series. The effects of these near-zero means upon the estimated values of the variances and covariances in the mean wind direction are not very significant. They do have significant effects upon the estimated values of the spectral density function at low frequencies.

Figures 18 through 20 show the plots of the power spectrum of the longitudinal, lateral, and vertical velocity components measured by TSI #122 in run 12, respectively. The power spectrum of the longitudinal and lateral velocity components measured by the Gill anemometers in the same run 12 are plotted in Figures 21 and 22. It is quite evident when like spectra form the TSI probe and the Gill anemometers are superimposed, the difference at frequencies higher than one hertz are considerable; expecially when one realizes that the ordinate of these spectrum functions has a logarithmic scale. For both spectrum functions of the longitudinal as well as the lateral turbulence components the Gill anemometers show a too rapid decrease with frequency in the range from 0.5 to 100 hertz. In the low frequency range the comparison is quite good.

The power spectrum of the longitudinal velocity component measured by the TSI #122 probe in run 14 is plotted in Figure 23. In order to obtain some spectral properties in the lower frequency range below 0.024 hertz, two new time series were generated from the data samples in run 14.

The first one (series A) is generated by taking a 10-point non-over-lapping average from the original time series. The second one (series B) is obtained by containing every 10th point from the original time series. The two newly generated time series have a reduced number of data points to one-tenth of the original number. The sampling rate is also decreased from 200 samples per second to 20 samples per second. The spectral density estimates for the newly generated time series are calculated by following the similar procedures used in computing the estimates from the original time series except the segment average is taken over the corresponding estimates of the four blocked subseries.

The power spectra calculated from the time series A and B are plotted in the Figures 25 and 24 respectively and can be compared with the original power spectrum of run 14 plotted in Figure 23. The power spectra of the newly created time series show a greater deal of scatter in the low and intermediate frequency range. The spectrum of the time series B shows some frequency folding in the high-frequency range since the data were not filtered at 10 hertz. The spectrum of the time series does not show this folding since the averaging procedure act as a low-pass filter at approximately 10 hertz. At the low-frequency range the scatter of the spectrum data for both time series A and B is more severe than for the spectrum data of the original time series. The limited segment averaging results in a reduction of the number of degrees of freedom which will give a broad confidence interval in the spectral density estimates. The data in each block sampled at a rate of 20 samples per second allows calculation of spectral estimates

down to a frequency of 0.00244 hertz (period of 409.6 seconds) since the number of data per block is limited to 2^{13} or 8192. However, only four blocks can be obtained from time series A and B, and in the low-frequency range where only segment averaging can be applied the spectral data can only be averaged over four values as compared to 44 values in the original time series. In order to get more reliable spectrum estimates at frequencies lower than 0.0244 hertz, the total sample time should be increased ten times if spectral information down to 0.00244 hertz is required. However, with time series A and B we can get some idea how the spectrum varies at frequencies lower than 0.0244 hertz.

CHAPTER VI

CONCLUSIONS

The statistical analysis of a discrete time series with a large number of data points representing a random process can be achieved successfully by the procedures as outlined in this report. It is necessary that these time series are subdivided into a certain number of sample records each containing an equal number of data points. The number of data points in each sample record depends largely on the storage capacity of the available digital computer. The total number of data points in each sample record should be chosen such that it is an integer power of two in order to satisfy the requirements for the fast Fourier Transformation. The statistical quantities calculated from each sample record or data block can be used to determine the degree of stationarity of the total sample by application of the nonparametric statistical test. The existence of any trends in the time series can be removed successfully by using the moving-average and differencing high-pass filter. This type of statistical analysis was used to obtain statistical information from long time series representing low-level atmospheric winds and temperature. These quantities were measured with fast response split-film anemometers developed by Thermo-Systems Inc. A set of propeller-type Gill anemometers was used simultaneously to measure wind velocities in the horizontal plane in order to compare their results with the results from the TSI probes.

The digitized data obtained from the TSI probes are stored on digital tape as voltages. Seven voltages are necessary to obtain three velocity components and temperature if the triple split-film probe is

used, and five voltages are necessary to obtain the same information
when the dual split-film probe is used. The following steps are re-
quired to obtain the statistical information for each data set.

A. The first step is to calculate for each sample point the three
velocity components and the temperature. This information is obtained
through calculations as outlined in reference 95, and it is consequently
stored on another digital tape in blocks of 418 sample points each. The
velocity components are calculated in the so-called sensor-oriented co-
ordinate system.

B. In the second step, the block size is changed from 418 sample
points to 2^{13} = 8192 sample or data points. First the means of each ve-
locity component and the magnitude of the mean velocity for each block
are calculated. Also the mean temperature and the average horizontal
angle the mean velocity for each block makes with the probe axis is
obtained. In addition, the block variances and covariances for the three
velocity components and the temperature are calculated. The number of
blocks depends on the recording length of the data, but for a run of
about one half hour the number of blocks is 44. In addition to the block
means, the sample means of the velocity components, the temperature as
well as the horizontal angle between the sample mean-wind and the axis
of the probe are calculated. Also the number of reverse arrangements of
the block means of the velocity components and the temperature and those
of the block standard deviations of velocity components and temperature
are calculated. The latter calculations are made in order to check for
nonstationarities such as time-varying mean values or time-varying standard
deviations or a combination of these two. At this point further analysis

of the data would be stopped if the number of reverse arrangements would be significantly different from the expected numbers as given in Table II.

C. The third step of the data analysis consists of the removal of the mean and low frequency components of the four time series. This is accomplished with the use of the moving-average and differencing high-pass filter. After this filter has been applied to the data four new time series with new sample mean and without low-frequency components are established. The cutoff frequency for this type of filter with a filtering interval of 40.96 seconds (the length of one block) is approximately .0108 hertz.

D. In the fourth step the sample variances and covariances of the four filtered time series are calculated and consequently transformed into the mean-wind coordinate system.

E. In this step the data representing the filtered velocity components in the sensor oriented coordinate system are transformed into components of the mean-wind coordinate system. As a result four time series with zero mean are created representing the fluctuating temperature and, the fluctuating velocity components in the mean-wind coordinate system.

F. In this step the power spectral densities of the four time series obtained in step E are calculated using the newly developed fast Fourier transform method with the no-bit reversal procedure and also using the appropriate combined smoothing techniques.

G. In the last step the coincident spectral density function and the quadrature spectral density function of two different time series are calculated using the newly developed fast Fourier transform method and in addition using both the segment as well as frequency averaging method

In order to check the accuracy of the calculated power spectral density extimates of any time series, spectral densities were calculated from a simulated time series which was generated from a known spectrum function. The calculated spectral densities correspond quite well with the spectrum function from which the simulated time series was generated. This indicates that with the newly developed computer program using the fast Fourier transform with a no-bit reversal procedure and with proper smoothing procedures, accurate spectral information can be obtained in the frequency range between 0.0244 and 100 hertz. Spectral density estimates of a lower degree of accuracy for frequencies less than 0.0244 hertz can be obtained by creating a new time series by taking as an example a 10-point non-overlapping average of the original time series. Mean values, variances as well as covariances of the two horizontal wind components measured with the TSI probe were compared with the same quantities measured simultaneously with the Gill propellor anemometers. The discrepancies in these quantities can be attributed to the varying and limiting response characteristics of the Gill propeller anemometers.

As a result of carefully carried out calibration procedures and the application of the newly developed computer program, accurate statistical estimates of long time series describing the fluctuating wind components can be obtained with either the dual or the triple split film TSI probes.

REFERENCES

1. Alavi, A. S. and G. M. Jenkins, "An Example of Digital Filtering", Appl. Stat., Vol. 14, 1965, pp. 70-74.

2. Anderson, T. W., The Statistical Analysis of Time Series, John Wiley and Sons, Inc., New York, 1971.

3. Bartlett, M.S., "Smoothing Periodogram from Time Series with Continuous Spectra", Nature, Vol. 161, May, 1948, p. 686.

4. Bartlett, M.S., "Periodogram Analysis and Continuous Spectra", Biometrika, Vol. 37, part I and II, June, 1950, pp. 1-16.

5. Bendat, J. S., "Principles and Applications of Random Noise Theory", John Wiley and Sons, Inc., New York, 1958.

6. Bendat, J. S. and A. G. Piersol, "Measurement and Analysis of Random Data", John Wiley and Sons, Inc., New York, 1971.

7. Bertram, S., "Frequency Analysis Using the Discrete Fourier Transform", IEEE Trans. on Audio and Electroacoustics, Vol. AU-15, No. 2, June 1967, pp. 495-500.

8. Bertram, S., "On the Derivation of the Fast Fourier Transform", IEEE Trans. on Audio and Electroacoustics, Vol. AU-18, No. 1, March 1970, pp. 55-58.

9. Bingham, C., M. D. Godfrey, and J. W. Tukey, "Modern Technique of Power Spectrum Estimation", IEEE Trans. on Audio and Electroacoustics, Vol. AU-15, No. 2, June 1967, pp. 56-66.

10. Blackman, R. B. and J. W. Tukey, "The Measurement of Power Spectra", Dover Publications, New York, 1958.

11. Bowne, N. E. and G. E. Anderson, "Take-Off and Landing Critical Atmospheric Turbulence (TOLCAT) Analytical Investigation", Air Force Flight Dyn. Lab. - Tech. Rept. - 68-23, April, 1968.

12. Brigham, E. O. and R. E. Morrow, "The Fast Fourier Transform", IEEE Spectrum, Vol. 4, Dec. 1967, pp. 63-70.

13. Brown, R. G., "Smoothing, Forecasting and Prediction of Discrete Time Series", Prentice-Hall, Inc., Englewood Cliffs, N.J., 1963.

14. Chatfield, C. and M. P. G. Pepper, "Time Series Analysis: An Example from Geophysical Data", Appl. Stat., Vol. 20, No. 3, 1971, pp. 217-238.

15. Cochran, W. T., Cooley, J. W., et. al., "What is the Fast Fourier Transform", IEEE Trans. on Audio and Electroacoustics, Vol. AU-15, No. 2, June 1967, pp. 45-55.

16. Cooley, J. W., P. A. W. Lewis and P. D. Welsh, "The Finite Fourier Transform", IEEE Trans. on Audio and Electroacoustics, Vol. AU-17, No. 2, June 1969, pp. 77-85.

17. Cooley, J. W., P. A. W. Lewis and P. D. Welsh, "The Fast Fourier Transform Algorithm: Programming Considerations in the Calculation of Sine, Cosine and Laplace Transforms", J. of Sound and Vib., Vol. 12, No. 3, 1970, pp. 315-317.

18. Cooley, J. W., P. A. W. Lewis, and P. D. Welsh, "The Application of the Fast Fourier Transform Algorithm to the Estimation of Spectra and Cross Spectra", J. of Sound and Vib., Vol. 12, No. 3, 1970, pp. 339-352.

19. Cooley, J. W., and J. W. Tukey, "An Algorithm for the Machine Calculation of Complex Fourier Series", Maths. of Comput., Vol. 19, April 1965, pp. 297-301.

20. Craddock, J. M., "An Analysis of the Slow Temperature Variations at Kew Observatory by means of Mutually Exclusive Bandpass Filters", J. R. Stat. Soc., Ser. A, Vol. 120, 1957, pp. 387-397.

21. Cramer, H. E., and F. A. Record, Properties of Turbulent Energy Spectra and Cospectra at the Atmospheric Surface Layer, Res. and Dev. Tech. Rep., ECOM-64GI-F, 1969.

22. Daniell, P. J., Discussion on "Symposium on Autocorrelation in Time Series", J. Roy. Stat. Soc., Vol. 8, Ser. B, 1946, pp. 88-90.

23. Davenport, A. G., "The Spectrum of Horizontal Gustiness near the Ground in High Winds", Q. J. Roy. Meteor. Soc., Vol. 87, 1961, pp. 194-211.

24. Drinkrow, R., "A Solution to the Paired Gill-Anemometer Response Function", J. of Appl. Meteor., Vol. 11, No. 1, Feb. 1972, pp. 76-80.

25. Durbin, J., "Trend Elimination by Moving Average and Variate Difference Filters", Bull. Int. Stat. Inst., Vol. 19, 1964.

26. Dyer, R. M., "Method for Filtering Meteorological Data", Monthly Weather Review, Vol. 99, No. 5, May 1971, pp. 435-438.

27. Edge, B. L., and P. C. Liu, "Comparing Power Spectra Computed by Blackman-Tukey and Fast Fourier Transform", Water Resources Research, Vol. 6, No. 6, Dec. 1970, pp. 1601-1610.

28. Ferrie, J. F., et. al., "Comparison of Four Fourier Transform Algorithms", Naval Underwater Systems Center Report No. 4113, June, 1971.

29. Fichtl, G. H. and G. E. McVehil, "Longitudinal and Lateral Spectra of Turbulence in the Atmospheric Boundary Layer", NASA Tech. Note D-5584, Feb. 1970.

30. Fisher, J. R., "Fortran Program for Fast Fourier Transform", NRL Report No. 7041, April 1970.

31. Fishman, G. S., "Spectral Methods in Econometrics", Harvard Univ. Press. Cambridge, Mass., 1969.

32. Foster, F. G., and A. Stuart, "Distribution-Free Tests in Time Series on the Breaking of Records", J. R. Stat. Soc., B, Vol. 16, No. 1, 1954, pp. 1-13.

33. Foster, M. R., and N. J. Guinzy, "The Coefficient of Coherence: Its Estimation and Use in Geophysical Data Processing", Geophysics, Vol. 32, No. 4, Aug. 1967, pp. 602-616.

34. Gentleman, W. M., "Matrix Multiplication and Fast Fourier Transform", The Bell System Tech. Journal, July 1968, pp. 1099-1103.

35. Gentleman, W. M., and G. Sande, "Fast Fourier Transform for Fun and Profit", 1966 Fall Joint Computer Conference, AFIPS Proc., Vol. 29, 1966, pp. 563-578.

36. Gibbons, J. D., "Nonparametric Statistical Inference", McGraw Hill Book Co., Inc., New York, 1971.

37. Gibson, C. H., G. R. Stegen, and R. B. Williams, "Statistics of the Fine Structure of Turbulent Velocity and Temperature Fields Measured at High Reynolds Number", J. Fluid Mechanics, Vol. 41, part 1, 1970, pp. 153-167.

38. Glisson, T. H., C. I. Black, and A. P. Sage, "The Digital Computation of Discrete Spectra Using the Fast Fourier Transform", IEEE Trans. on Audio and Electroacoustics, Vol. AU-18, No. 3, Sept. 1970, pp. 271-280.

39. Granger, C. W. J., and M. Hatanaka, "Spectral Analysis of Economic Time Series", Princeton Univ. Press, Princeton, N.J., 1964.

40. Granger, C. W. J., and A. O. Hughes, "Spectral Analysis of Short Series -- a Simulation Study", J. R. Stat. Soc., A, Vol. 131, 1968, pp. 83-99.

41. Grenander, U., and M. Rosenblatt, "Statistical Analysis of Stationary Time Series", John Wiley and Sons, Inc., New York, 1970.

42. Hannan, E. J., "Multiple Time Series", John Wiley and Sons, Inc., New York, 1970.

43. Hinich, M. J., and C. S. Clay, "The Application of Discrete Fourier Transform in the Estimation of Power Spectra, Coherence, and Bispectra of Geophysical Data", Review of Geophysics, Vol. 6, No. 3, Aug. 1968, pp. 347-363.

44. Hinze, J. O., "Turbulence", McGraw Hill Book Co., Inc., New York, 1959.

45. Hollander, M., and D. A. Wolfe, "Nonparametric Statistical Methods", John Wiley and Sons, New York, 1973.

46. Holloway, J. C., Jr., "Smoothing and Filtering of Time Series and Space Fields", Adv. in Geophysics, Vol. 4, 1958, pp. 351-390.

47. Houbolt, J. C., G. G. Williamson, and B. H. Jones, "Effect of Filtering on Statistical Properties of Random Functions", AFOSR Scientific Report 69-3036 TR, 1969.

48. Hyson, P., "Cup Anemometer Response to Fluctuating Wind Speeds", J. of Appl. Meteor., Vol. 11, No. 5, August 1972, pp. 843-848.

49. Izumi, Y., and M. L. Barad, "Wind Speeds as Measured by Cup and Sonic Anemometers and Influenced by Tower Structure", J. of Appl. Meteor., Vol. 9, Dec. 1970, pp. 851-856.

50. Jenkins, G. M., "General Considerations in the Analysis of Spectra", Technometrics, Vol. 3, 1961, pp. 133-166.

51. Jenkins, G. M., "A Survey of Spectral Analysis", Appl. Statistics, Vol. 14, 1965, pp. 2-32.

52. Jenkins, G. M., and D. G. Watts, "Spectral Analysis and Its Applications", Holden-Day, San Francisco, 1969.

53. Jones, R. H., "A Reappraisal of the Periodogram in Spectral Analysis", Technometrics, Vol. 1, No. 4, Nov. 1965, pp. 531-542.

54. Kahaner, D., "Matrix Description of the Fast Fourier Transform", IEEE Trans. on Audio and Electroacoustics, Vol. AU-18, No. 4, Dec. 1970, pp. 442-450.

55. Kaimal, J. C., J. C. Wyngaard, Y. Izumi, and O. R. Cote, "Spectral Characteristics of Surface Layer Turbulence", O. J. Roy. Meteor. Soc., Vol. 98, 1972, pp. 563-589.

56. Kendall, M. G., "Oscillatory Time Series", Nature, Vol. 161, No. 4084, Feb. 1948, p. 187.

57. Kendall, M. G., "A Theorem in Trend Analysis", Biometrika, Vol. 48, 1961, pp. 224-227.

58. Kendall, M. G., and A. Stuart, "The Advanced Theory of Statistics", Hafner Publishing Co., New York, Vol. III, 1966.

59. Krause, F. R., J. A. Jones, M. J. Fisher, and J. C. Pooley, "Digital Analysis of Random Data Records by Piecewise Accumulation of Time Averages", NASA TN D-6073, Dec. 1970.

60. Lindgren, B. W., "Statistical Theory", The MacMillan Co., New York, 2nd edition, 1968.

61. Lumley, J. L., and H. A. Panofsky, "The Structure of Atmospheric Turbulence", Interscience Publishers, New York, 1964.

62. MacCready, P. B., Jr., "Mean Wind Speed Measurements in Turbulence", J. of Appl. Meteor., Vol. 5, 1966, pp. 219-225.

63. MacCready, P. B., Jr., and H. R. Jex, "Response Characteristics and Meteorological Utilization of Propeller and Vane Wind Sensors", J. of Appl. Meteor., Vol. 3, 1964, pp. 182-193.

64. Maling, G. C., W. T. Morrey, and W. W. Lang, "Digital Determination of Third-Octave and Full-Octave Spectra of Acoustical Noise", IEEE Trans. on Audio and Electroacoustics, Vol. AU-15, No. 2, June 1967, pp. 98-104.

65. Mann, H. B., "Non-Parametric Tests Against Trends", Econometrica, Vol. 13, 1954, pp. 245-259.

66. Maynard, H., "A Radix-2 Fast Fourier Transform Program", U.S. Army Electronic Command, Atmospheric Sciences Laboratory, White Sands Missile Range, N.M., ECOM-5363, March 1971.

67. Otnes, R. K., and L. Enochson, "Digital Time Series Analysis", John Wiley and Sons, Inc., New York, 1972.

68. Olin, J. G., and R. B. Kiland, "Split-Film Anemometer Sensor for Three-Dimensional Velocity-Vector Measurements", Report of Thermo-Systems, Inc., St. Paul, Minn., 1970.

69. Oort, A. H., and A. Taylor, "On the Kinetic Energy Spectrum near the Ground", Monthly Weather Review, Vol. 97, No. 9, Sept. 1969, pp. 623-636.

70. Ormsby, J. F. A., "Design of Numerical Filters with Applications to Missile Data Processing", J. Ass. Computing Mach., July 1961, pp. 440-466.

71. Owen, D. B., "Handbook of Statistical Tables", Addison-Wesley Publishing Co., Inc., Reading, Mass., 1962.

72. Panofsky, H. A., "Meteorological Applications of Cross-Spectrum Analysis", Spectral Analysis of Time Series, edited by B. Harris, John Wiley and Sons, Inc., New York, 1967, pp. 109-132.

73. Panofsky, H. A., and G. W. Brier, "Some Applications of Statistics to Meteorology", The Penn. State Univ. Press, University Park, Penn., 1958.

74. Parzen, E., "On Consistent Estimates of the Spectrum of a Stationary Time Series", Ann. Math. Stat., Vol. 28, 1957, pp. 329-348.

75. Parzen, E., "Mathematical Considerations in the Estimation of Spectra", Technometrics, Vol. 3, 1961, pp. 167-190.

76. Parzen, E., "Time Series Analysis Papers", Holden-Day, San Francisco, 1967.

77. Parzen, E., "On Empirical Multiple Time Series Analysis", Proc. Fifth Berkeley Symp., Vol. 1, edited by L. LeCam, Univ. of California, 1966, pp. 305-340.

78. Parzen, E., "The Role of Spectra Analysis in Time Series Analysis", Review of the Intern. Stat. Inst., Vol. 35, 1967, pp. 125-141.

79. Parzen, E., "Multiple Time Series Modeling", Multivariate Analysis II, edited by P. R. Krishnaiah, Academic Press, New York, 1969, pp. 389-409.

80. Parzen, E., "Some Recent Advances in Time Series Analysis", Tech. Report No. 18, Stanford Univ., Stanford, Calif., July 1971.

81. Payne, F. R., and J. L. Lumley, "One-Dimensional Spectra Derived from the Airborne Hot-Wire Anemometer", Q. J. Roy. Meteor. Soc., Vol. 92, No. 39, 1966, pp. 397-401.

82. Priestley, C. H. B., "Turbulent Transfer in the Lower Atmosphere", Univ. Chicago Press, Chicago, 1959.

83. Priestley, M. B., "Basic Considerations in the Estimation of Spectra", Technometrics, Vol. 4, No. 4, Nov. 1962, pp. 551-564.

84. Priestley, M. B., "The Role of Bandwidth in Spectral Analysis", Appl. Statistics, Vol. 14, 1965, pp. 33-47.

85. Ryznar, E., "Wind and Temperature Structure in the Surface Layer of the Atmosphere", Report of U.S. Army Research Office - Durham, Contract DAGCO 4-67-C-0027, Dec. 1971.

86. Sheik, C. M., H. Tennekes, and J. L. Lumley, "Airborne Hot-Wire Measurements of the Small-Scale Structure of Atmospheric Turbulence", The Physics of Fluids, Vol. 14, No. 2, Feb. 1971, pp. 201-215.

87. Sinha, A. K., "On Digital Simulation of Multicorrelated Random Processes and Its Application", Ph.D. dissertation, Dept. of Engineering Science and Mechanics, Virginia Polytechnic Institute and State University, July, 1973.

88. Sitaraman, V., "Spectra and Cospectra of Turbulence in the Atmospheric Surface Layer", Quart. J. Roy. Meteor. Soc., Vol. 96, 1970, pp. 744-749.

89. Sloane, E. A., "Comparison of Linearly and Quadratically Modified Spectral Estimate of Gaussian Signals", IEEE Trans. of Audio and Electroacoustics, Vol. AU-17, No. 2, June 1969, pp. 133-137.

90. Taylor, G. I., "Diffusion by Continuous Movements", Proc. of the London Math. Soc., Vol. 20, Ser. 2, 1921, pp. 196-211.

91. Taylor, G. I., "Statistical Theory of Turbulence", Proc. of Royal Soc., Vol. 151, Parts I and IV, Ser. A, 1935, pp. 421-478.

92. Taylor, G. I., "The Spectrum of Turbulence", Proc. of Royal Soc., Vol. 164, Ser. A, 1938, pp. 476-490.

93. Theilheimer, F., "A Matrix Version of the Fast Fourier Transform", IEEE Trans. on Audio and Electroacoustics, Vol. AU-17, No. 2, June 1969, pp. 158-161.

94. Tick, L. J., "Estimation of Coherency", Spectral Analysis of Time Series, edited by B. Harris, John Wiley and Sons, Inc., New York, 1967, pp. 133-152.

95. Tieleman, H. W., K. P. Fewell, and H. L. Wood, "An Evaluation of the Three-Dimensional Split-Film Anemometer for Measurement of Atmospheric Turbulence", VPI-E-73-9, March 1973.

96. Tukey, J. W., "Discussion Emphasizing the Connection Between Analysis of Variance and Spectrum Analysis", Technometrics, Vol. 3, No. 2, May 1961, pp. 191-219.

97. Tukey, J. W., "Data Analysis and the Frontiers of Geophysics", Science, Vol. 148, 1965, pp. 1282-1289.

98. Tukey, J. W., "An Introduction to the Calculation of Numerical Spectral Analysis", Spectral Analysis of Time Series, edited by B. Harris, John Wiley and Sons, Inc., New York, 1967, pp. 25-46.

99. Uhrich, M. L., "Fast Fourier Transform Without Sorting", IEEE Trans. on Audio and Electroacoustics, Vol. AU-17, No. 2, June 1969, pp. 170-172.

100. Uhrig, R. E., "Random Noise Techniques in Nuclear Reactor System", The Ronald Press Co., New York, 1970.

101. Villasenor, A. J., "Digital Spectral Analysis", NASA TN D-4510, 1968.

102. Walker, A. M., "Some Asymptotic Results for the Periodogram of a Stationary Time Series", J. of Aust. Math. Soc., Vol. 5, 1965, pp. 107-128.

103. Walsh, J. E., "Handbook of Nonparametric Statistics", D. Van Nostrand Co., Inc., Princeton, N.J., 1962.

104. Welsh, P. D., "A Direct Digital Method of Power Spectrum Estimation", IBM J. Res. Dev., Vol. 5, April 1961, pp. 141-156.

105. Welsh, P. D., "The Use of Fast Fourier Transform for the Estimation of Power Spectrum: A Method Based on Time-Averaging Over Short, Modified Periodograms", IEEE Trans. on Audio and Electroacoustics, Vol. AU-15, No. 2, June 1967, pp. 70-73.

106. Wold, H., "A Study in the Analysis of Stationary Time Series", Almquist and Wiksell, Stockholm, 1938.

107. Young, E. F., "Calibration of a Three-Dimensional Split-Film (Two Sensor) Anemometer for Measurement of Atmospheric Turbulence", Senior Project Report, Engineering Science and Mechanics Dept., Virginia Polytechnic Institute and State University, May, 1973.
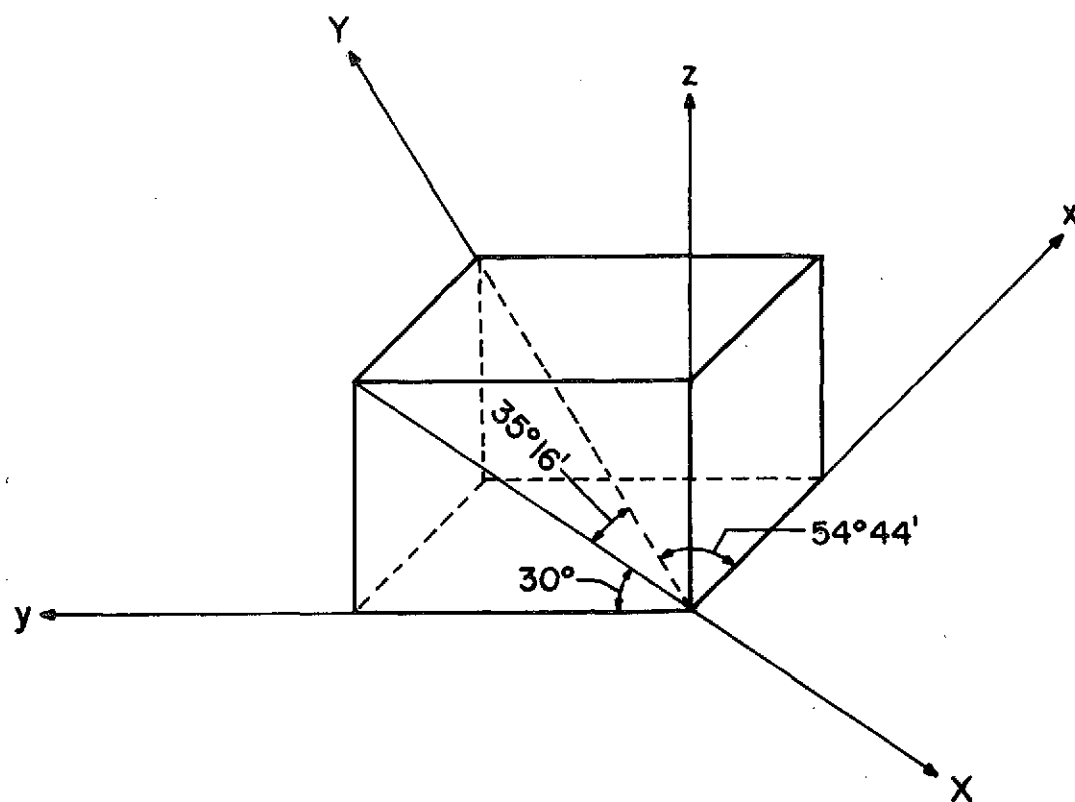
Figure 1-a. Schematic Diagram of the Sensor Oriented Coordinate System
XYZ and the Probe Oriented Coordinate System x*y*z*.
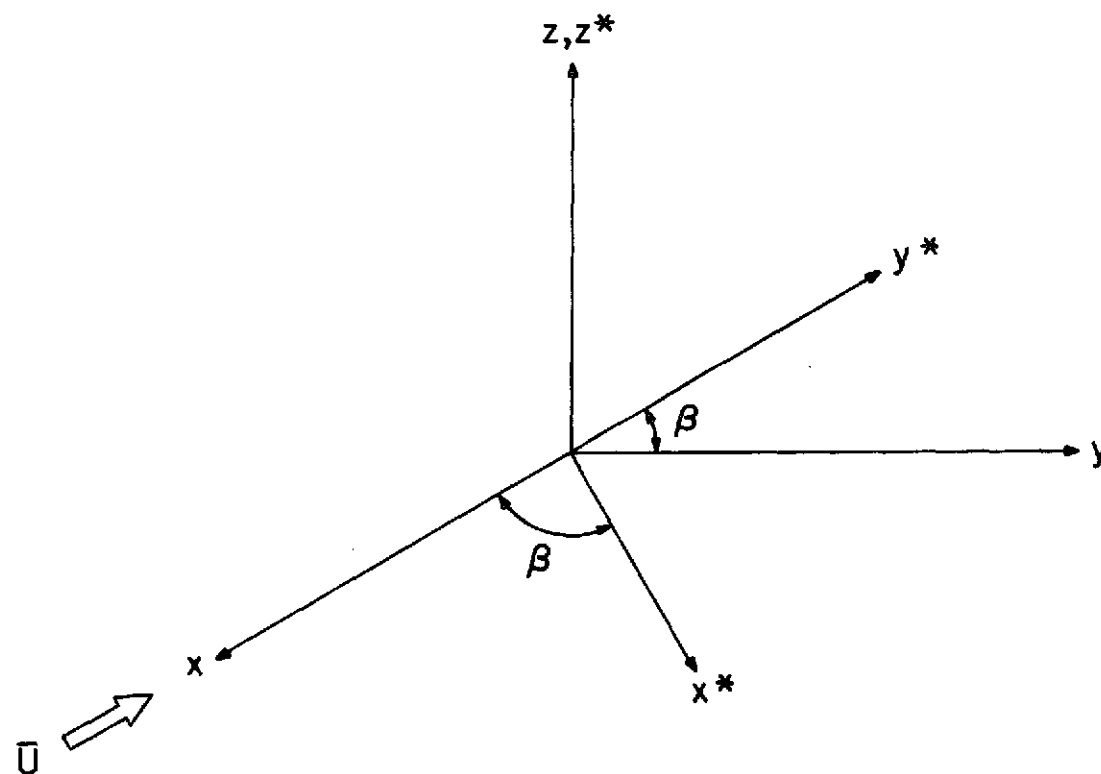
Figure 1-b. Schematic Diagram of the Probe Oriented Coordinate System x*y*z* and the Mean Wind Coordinate System xyz.
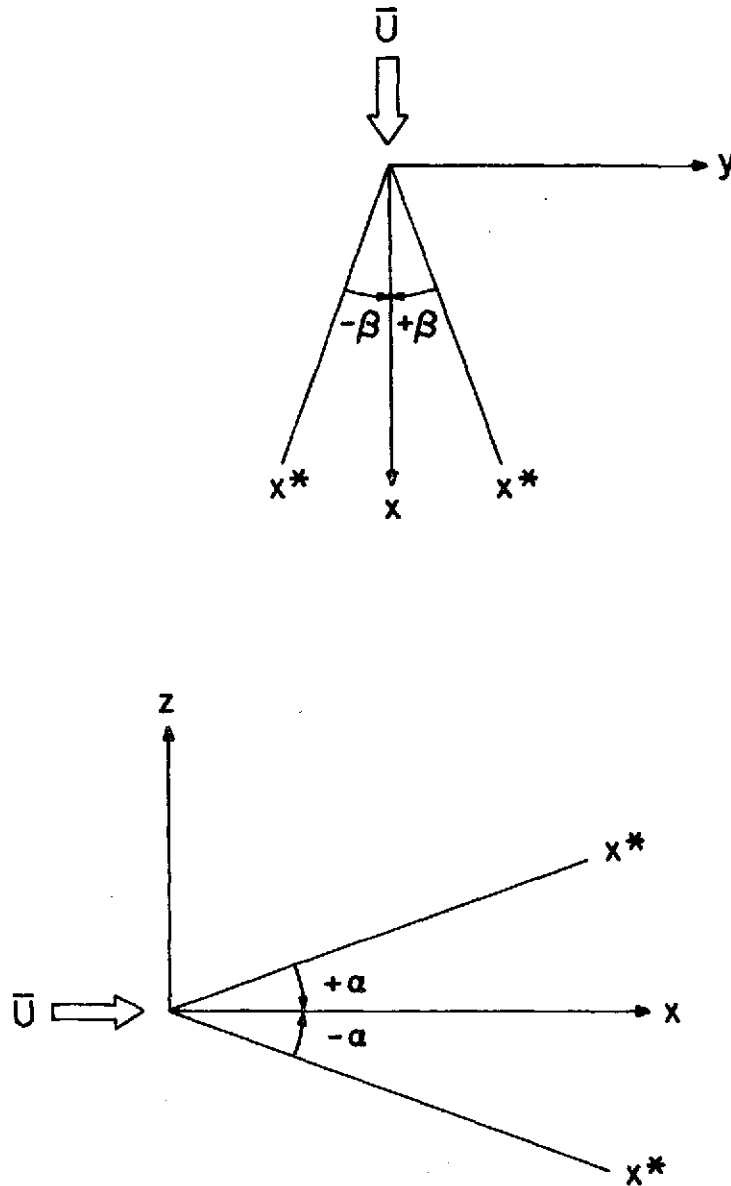
Figure 1-c.   Schematic Diagram of the Probe Yaw
Angle (top) and the Probe Pitch Angle
(bottom) with the Mean Wind Direction.
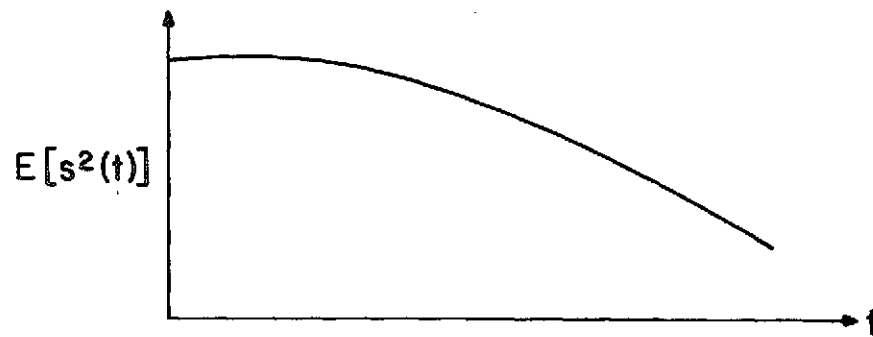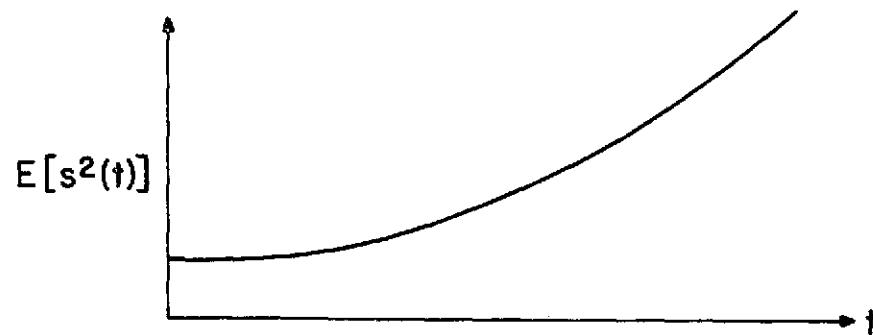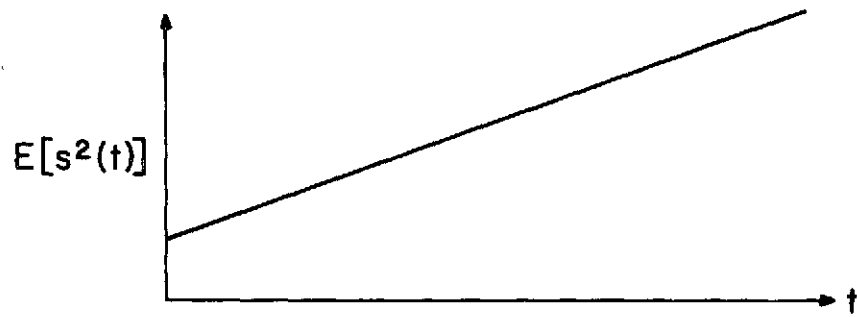
Figure 2. Effectively Removable Trend Types for the Mean
Square Value.
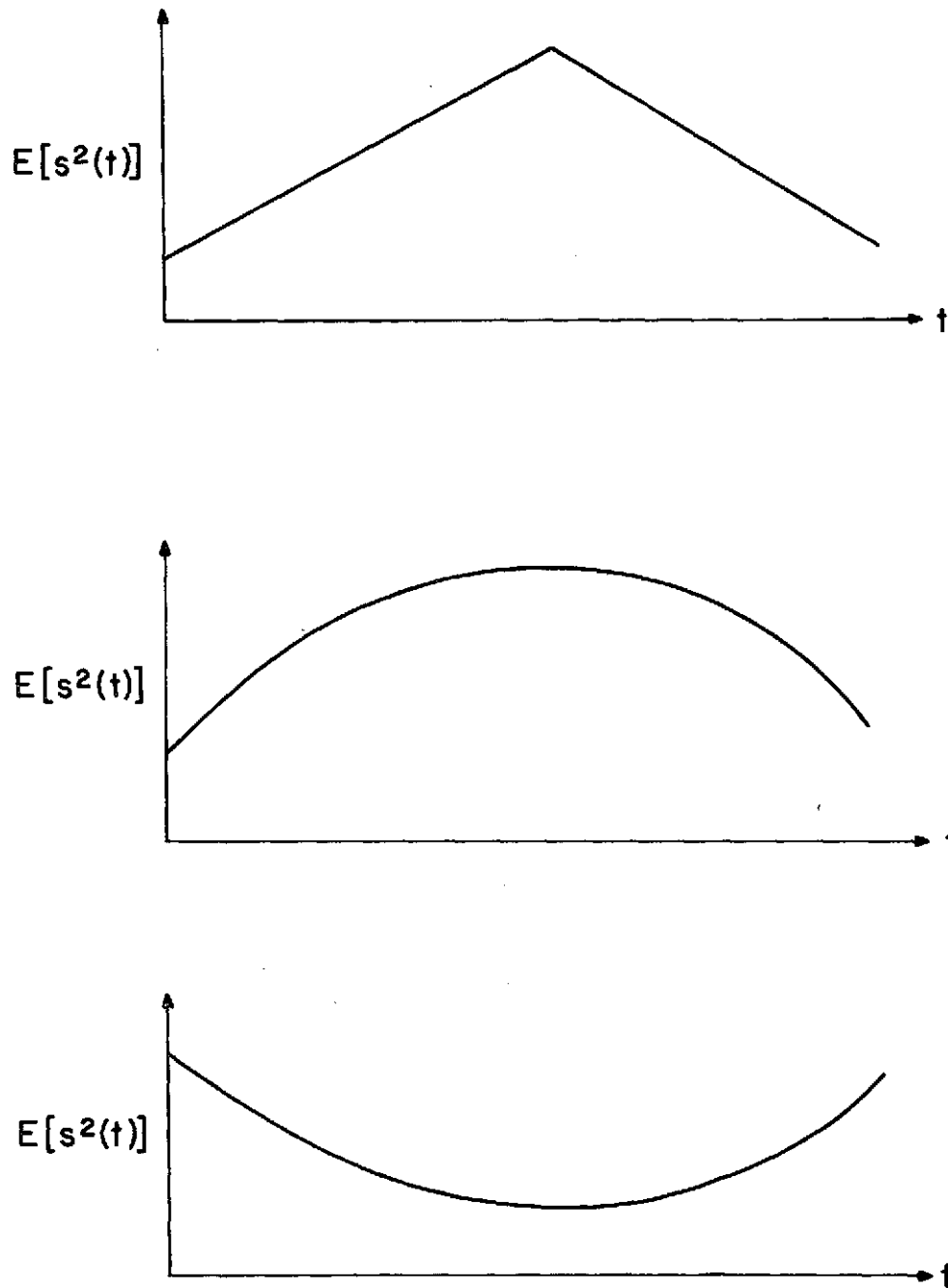
Figure 3. Ineffectively Removable Trend Types for the Mean Square Value.

$E[s^2(t)]$
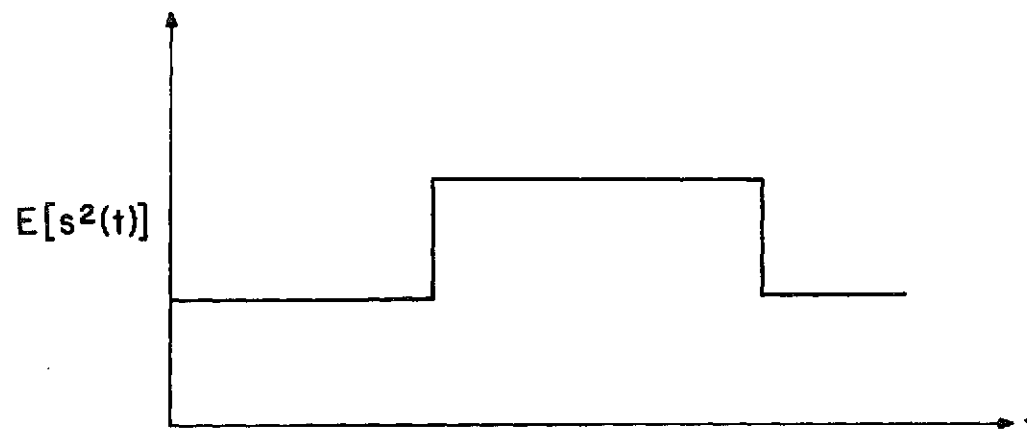
Figure 4. Type of Nonstationary Trend Undetectable by the Trend Test.
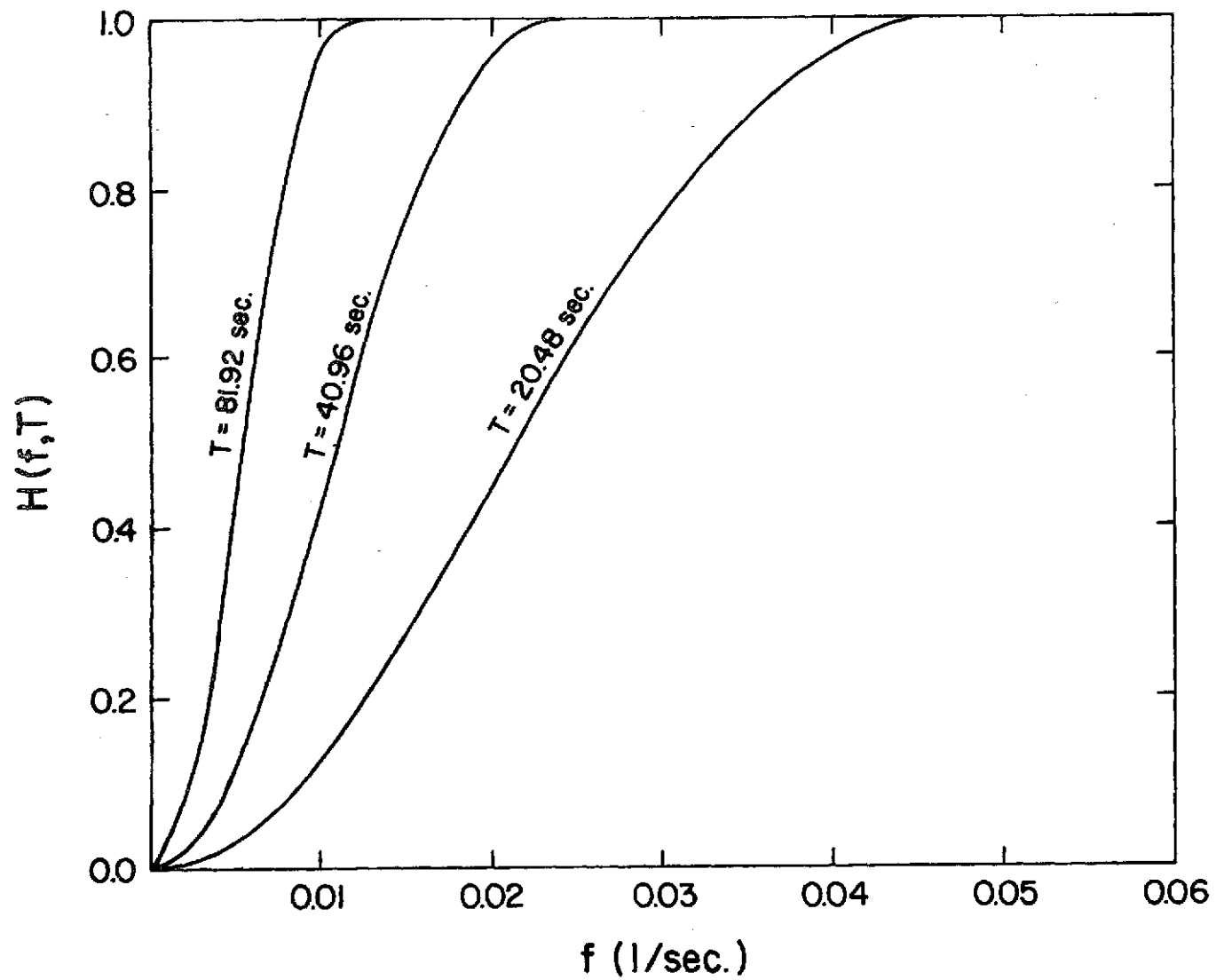
Figure 5.   Filter Shapes for the Moving-Average and High-Pass Filter.
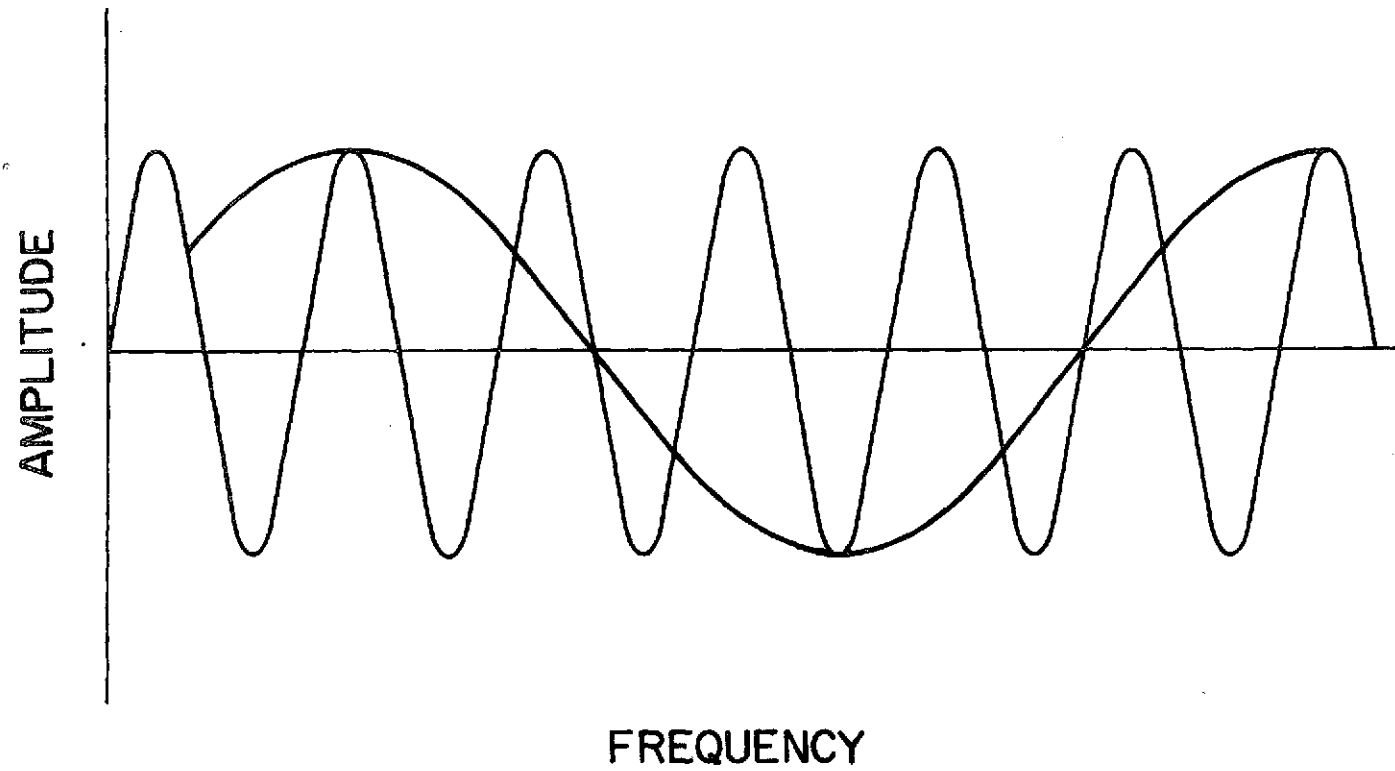
Figure 6.   The Effect of Slow Sampling Rate of a High Frequency Wave.
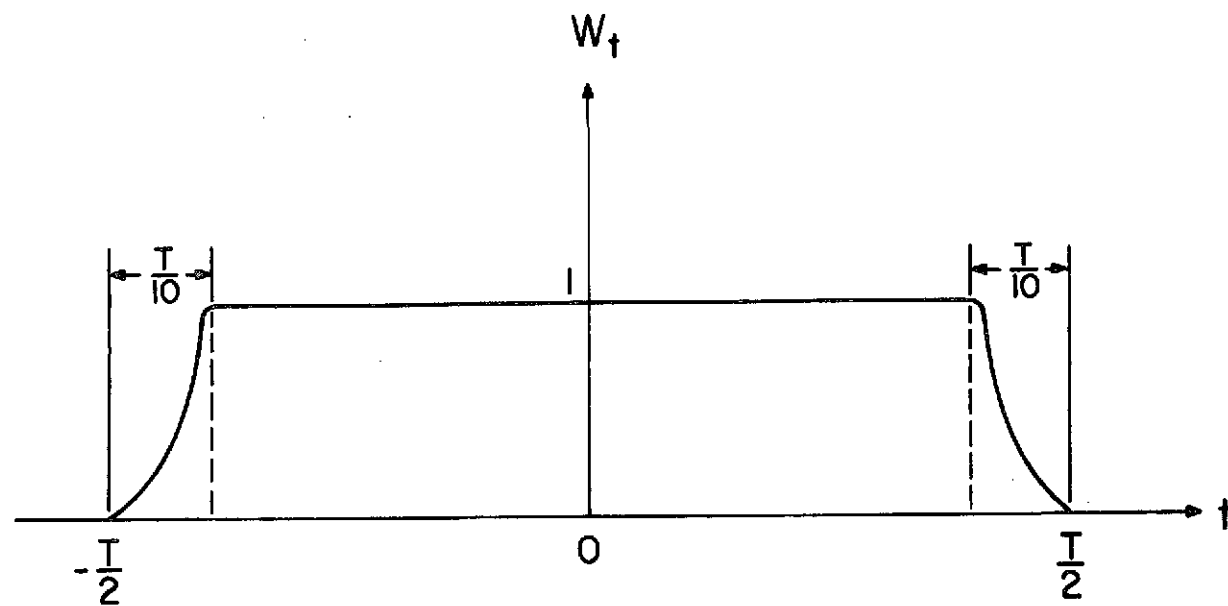
Figure 7. Cosine Taper Data Window.
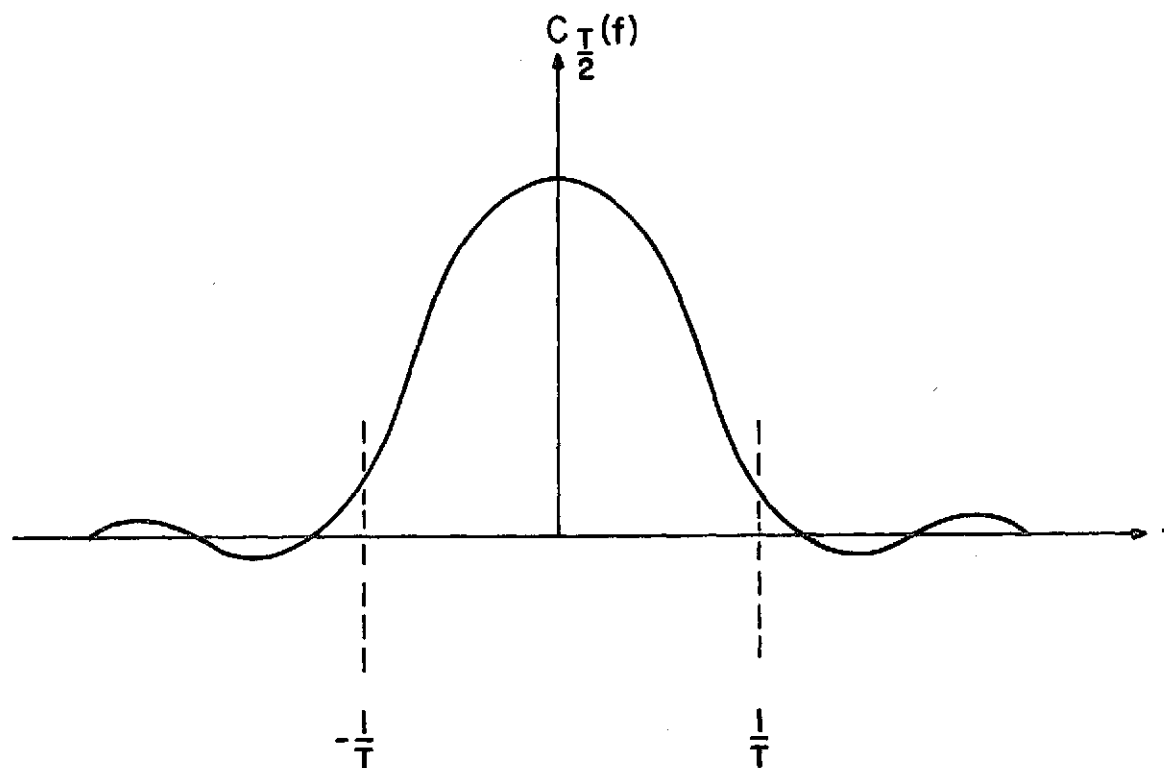
Figure 8.   Smooth Filter Shape Corresponds to the Cosine Taper Data
Window for FFT Estimates.

TRIANGULAR SPECTRAL WINDOW

$$B_e = \frac{1}{T}$$

TRIANGULAR SPECTRAL WINDOW

$$B_e' = \frac{M-1}{T}$$
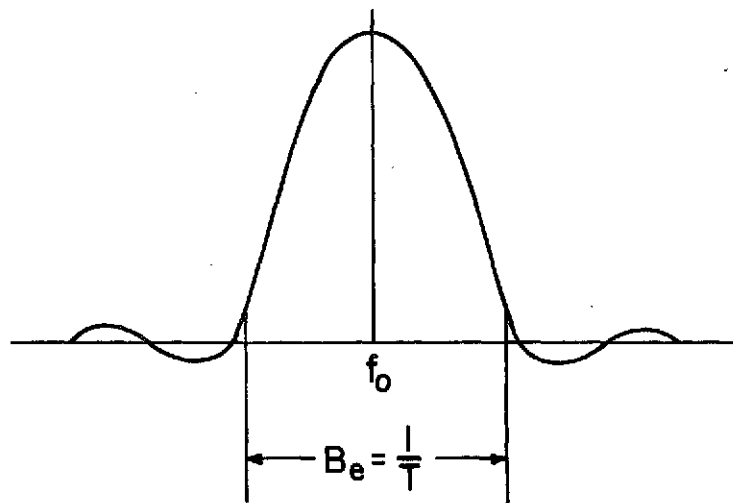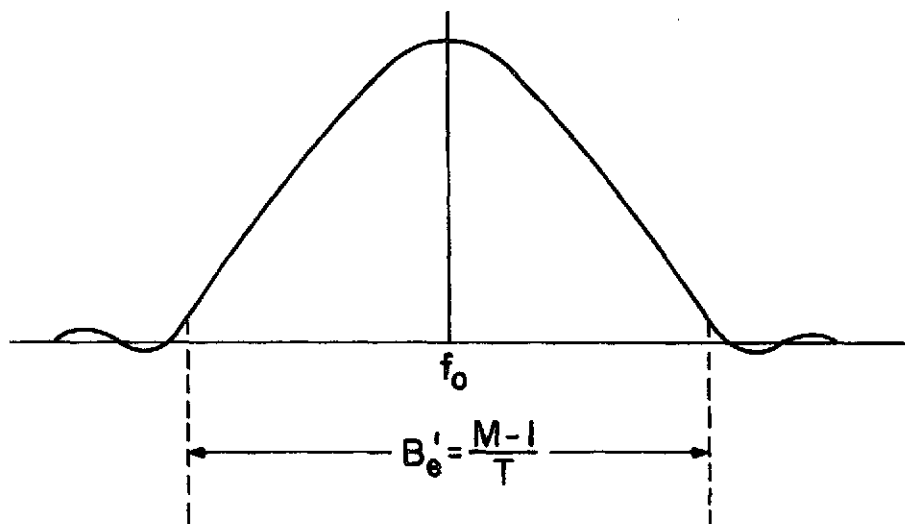
Figure 9. Filter Shape Before (top) and After
(bottom) Segment Smoothing.

INITIAL TRIANGULAR SPECTRAL WINDOW

f_o

$\left|\leftarrow B_e = \dfrac{1}{T} \rightarrow\right|$
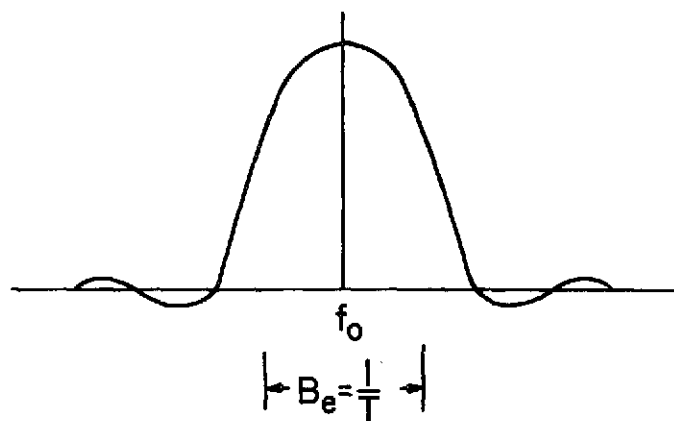
FINAL TRAPEZOIDAL SPECTRAL WINDOW

f_o

$\left|\longleftarrow\quad B_e' = \dfrac{K}{T}\quad\longrightarrow\right|$
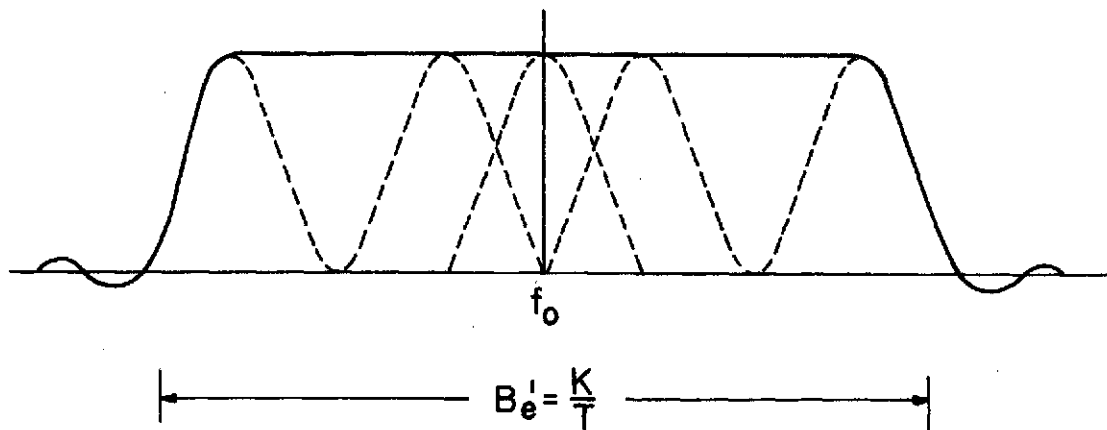
Figure 10. Filter Shape Before (top) and After (bottom) Frequency Smoothing (K is the number of smoothing points).
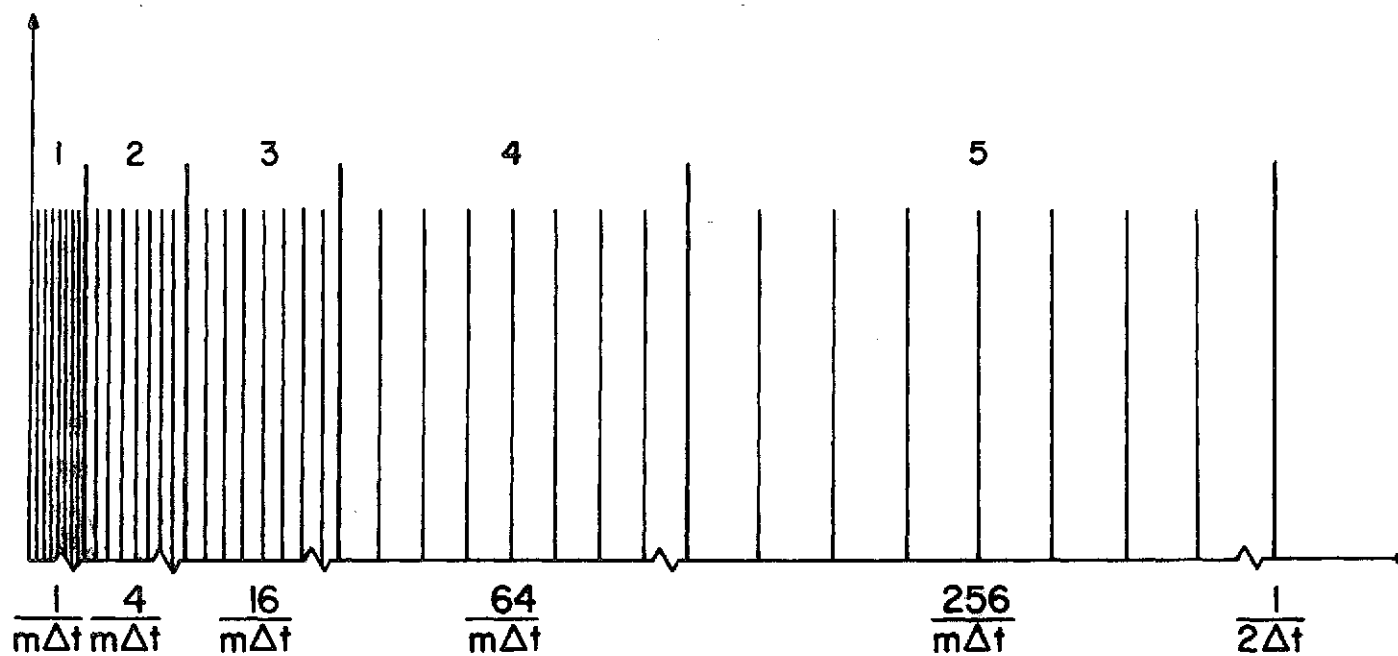
Figure 11. Overall Filter Spacing of the Proposed Frequency Smoothing Technique (m = 8192, Δt = 0.005 second).
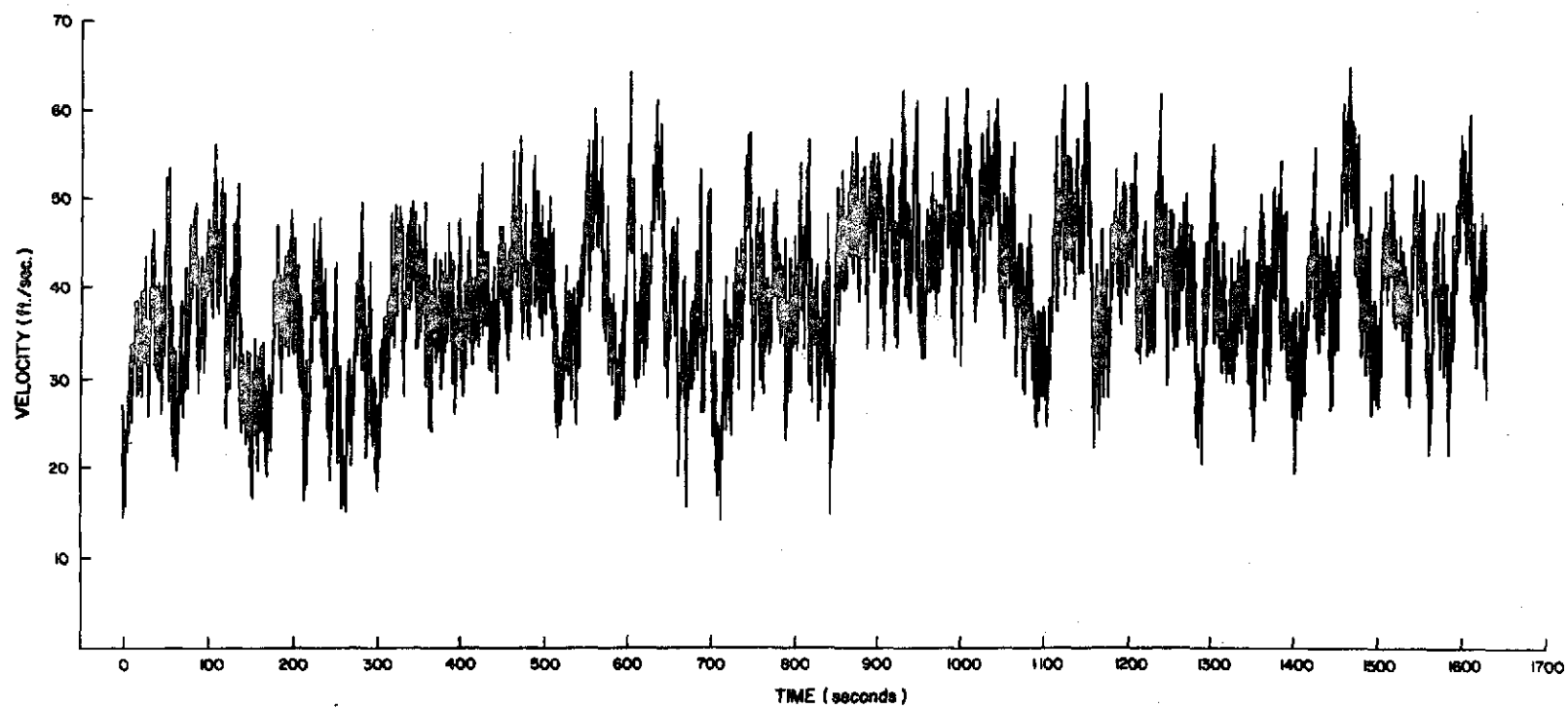
Figure 12. Time Series Simulated from von Karman Spectrum.
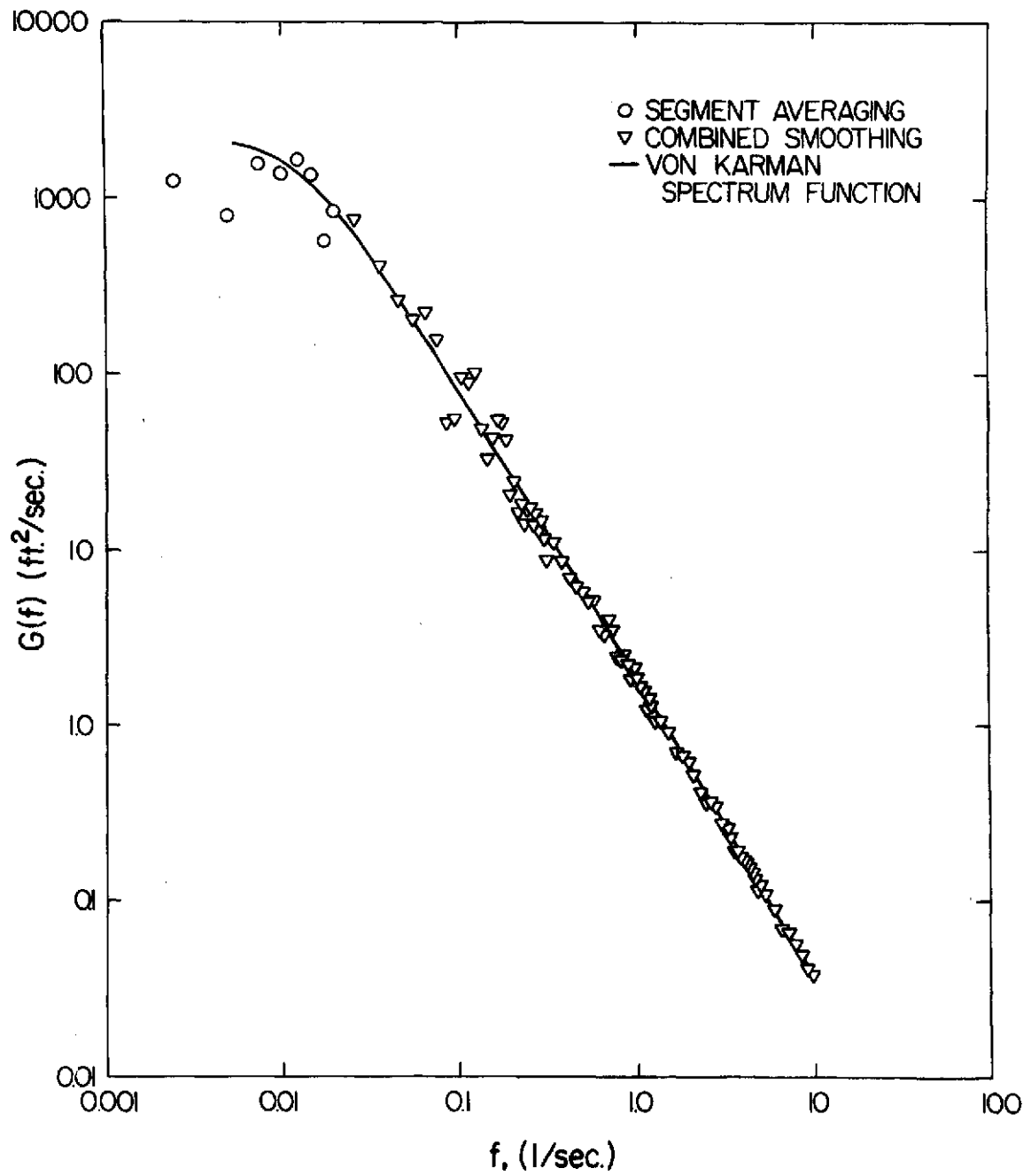
Figure 13.   Power Spectrum of the Simulated Time Series.
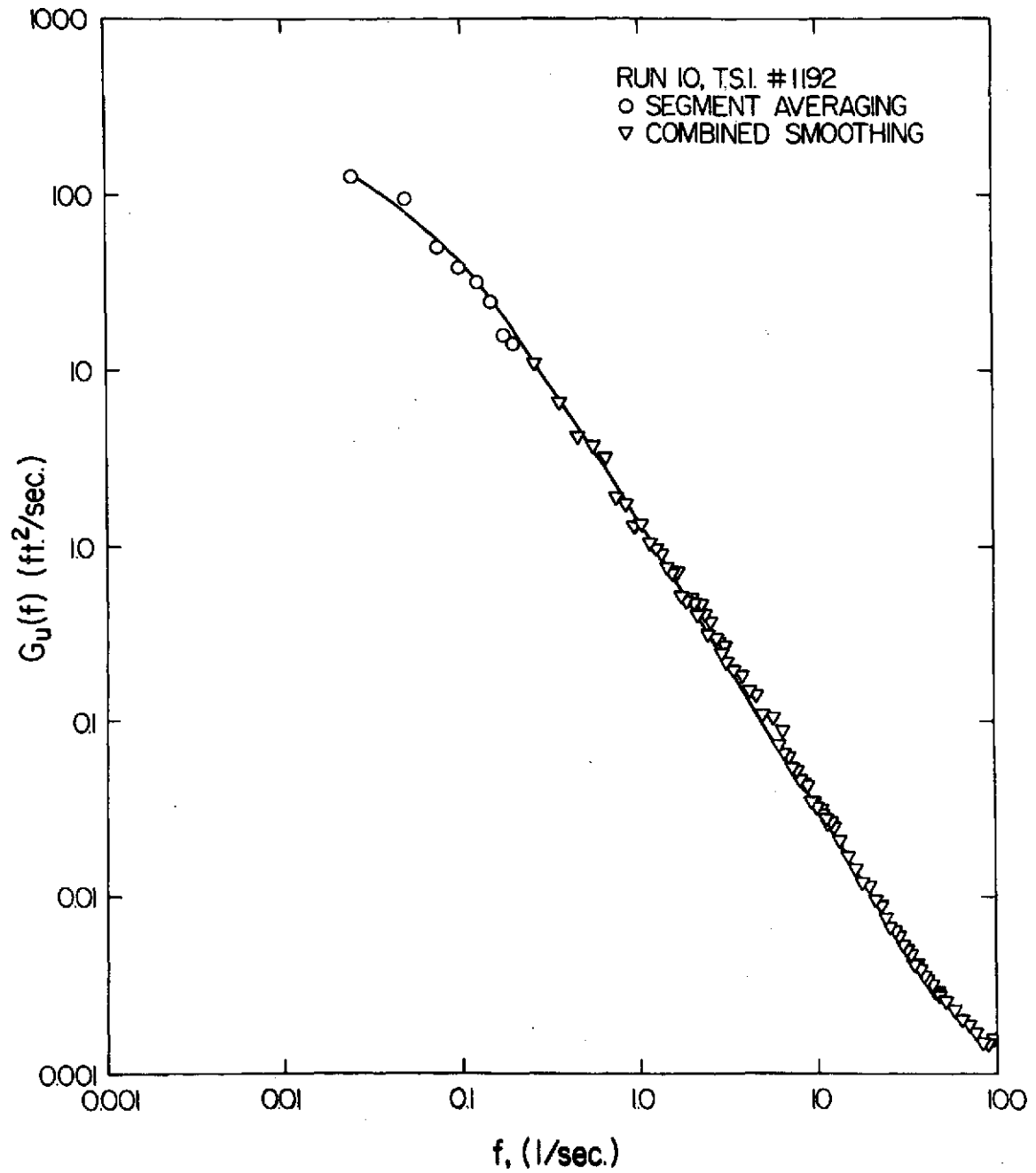
Figure 14. Power Spectrum of the Longitudinal Velocity Component.
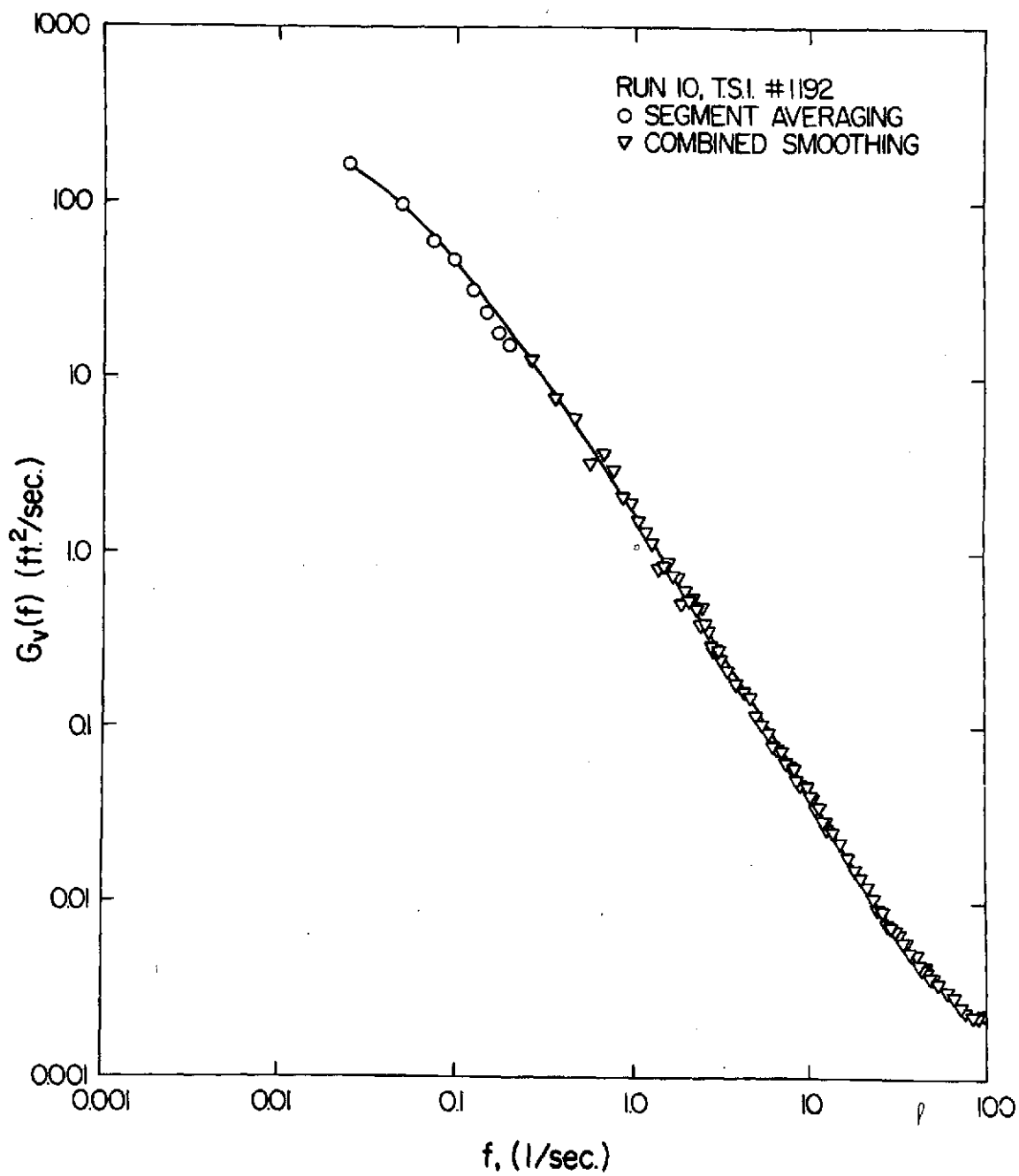
Figure 15.   Power Spectrum of the Lateral Velocity Component.
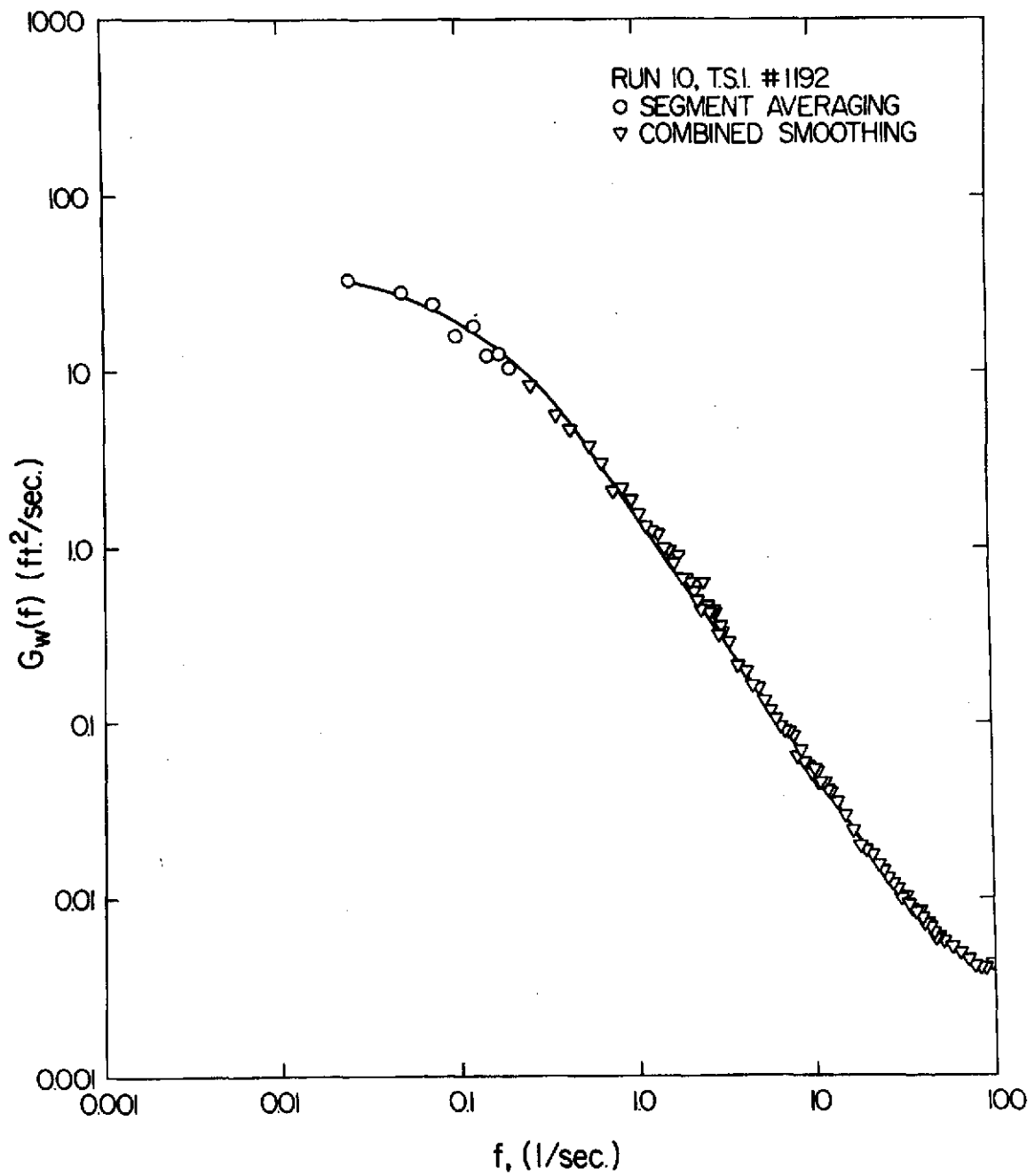
Figure 16.   Power Spectrum of the Vertical Velocity Component.
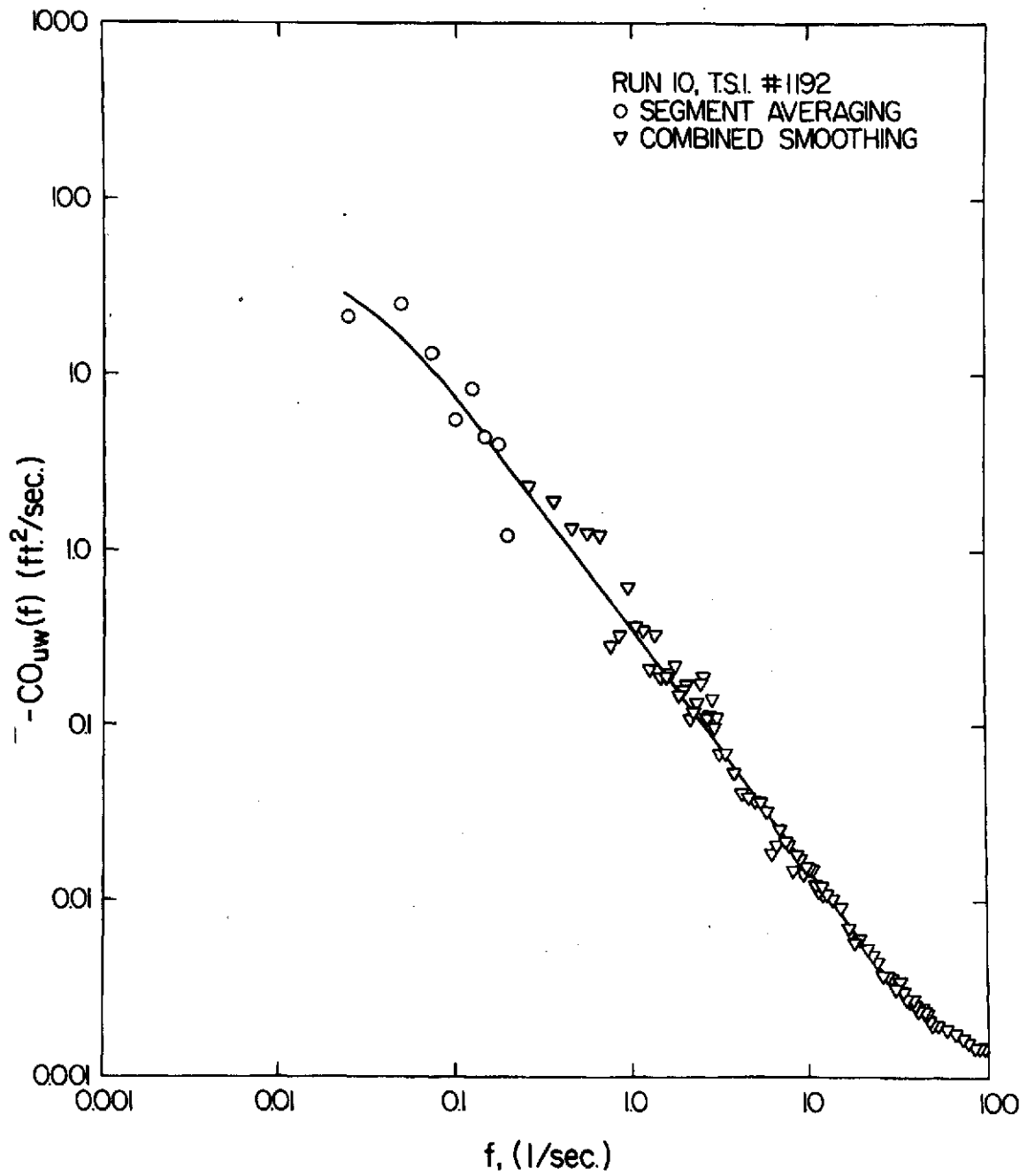
Figure 17. Cospectrum Between Longitudinal and Vertical Velocity Components.
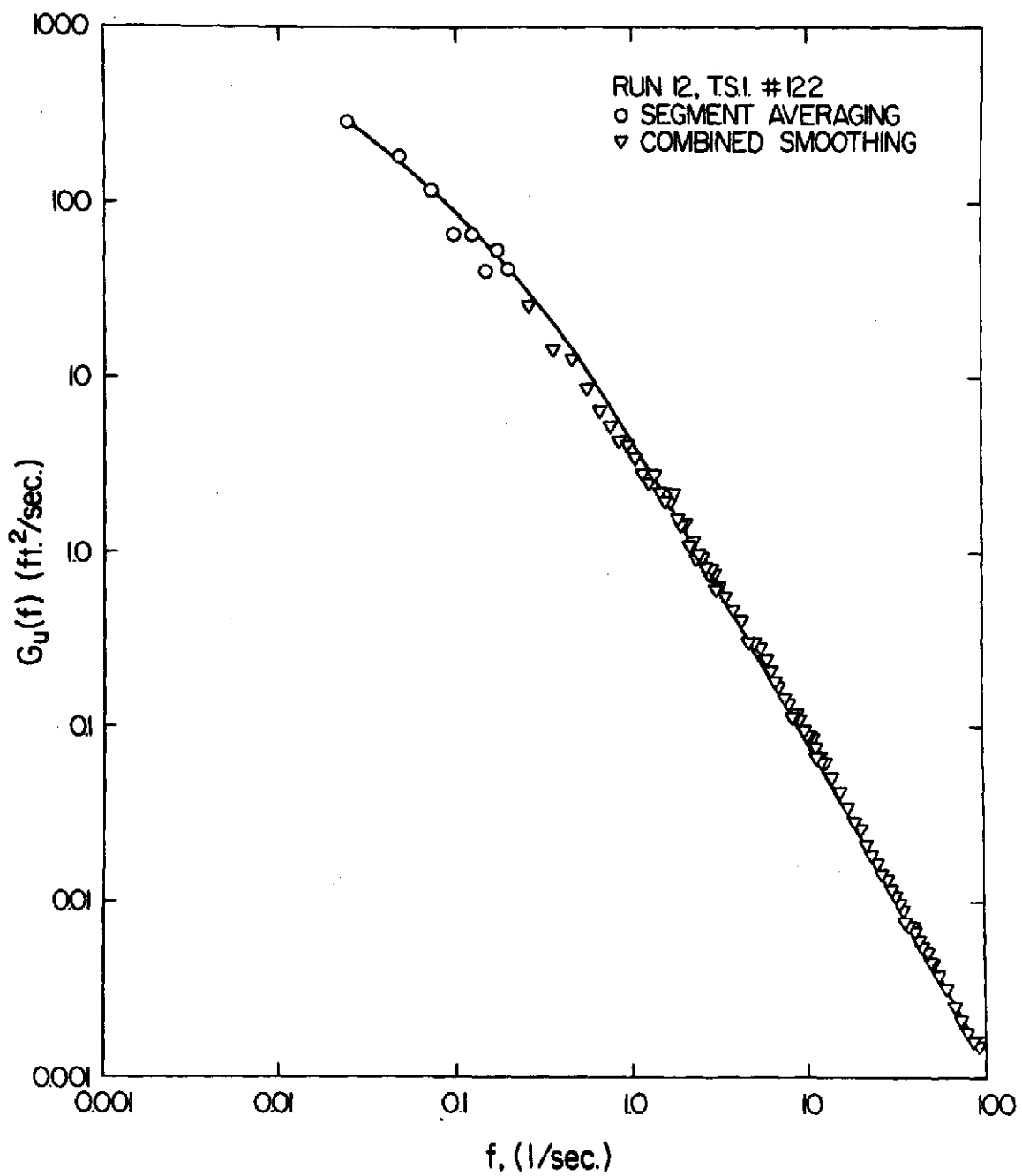
Figure 18.   Power Spectrum of the Longitudinal Velocity Component.
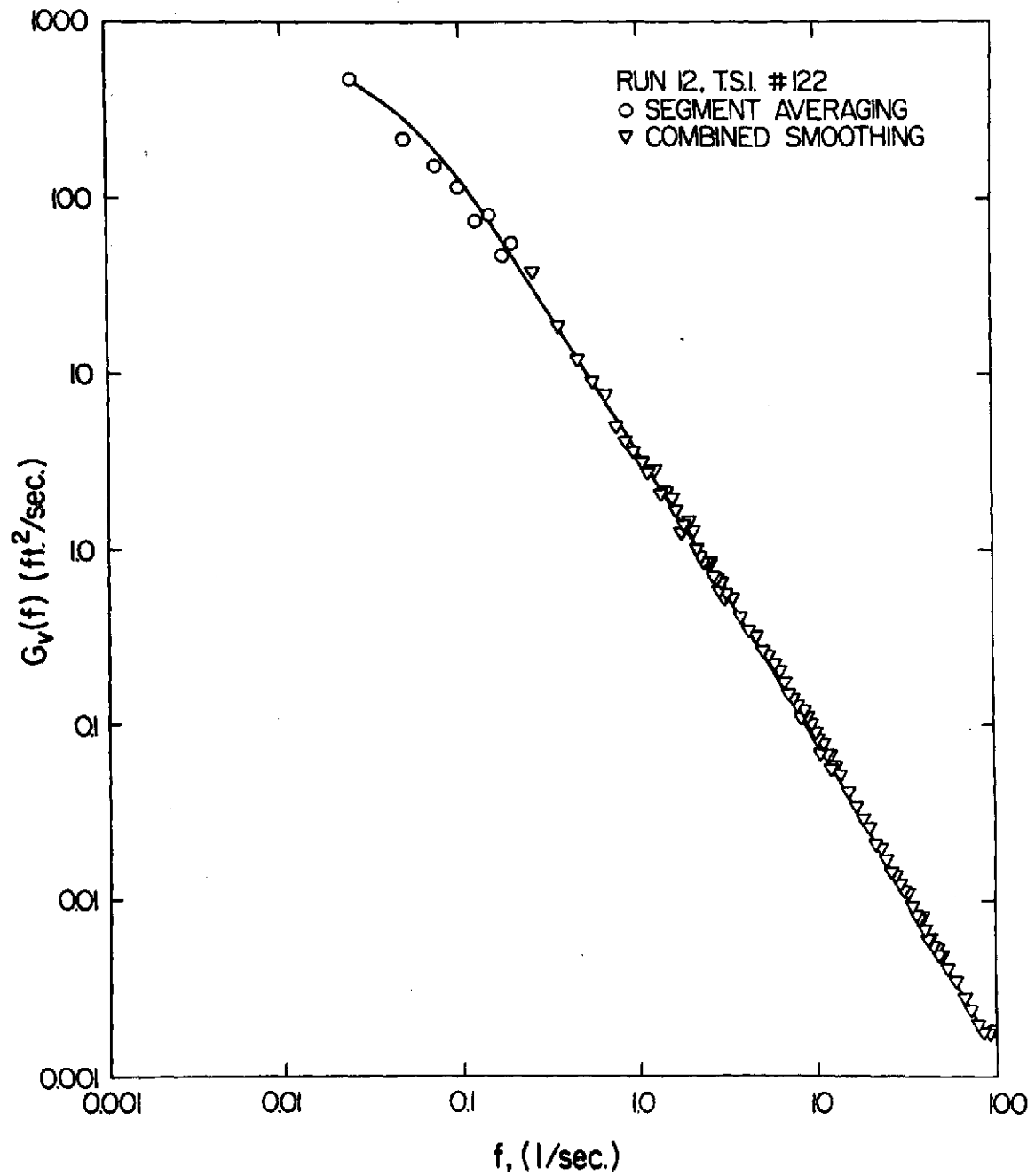
Figure 19.   Power Spectrum of the Lateral Velocity Component.
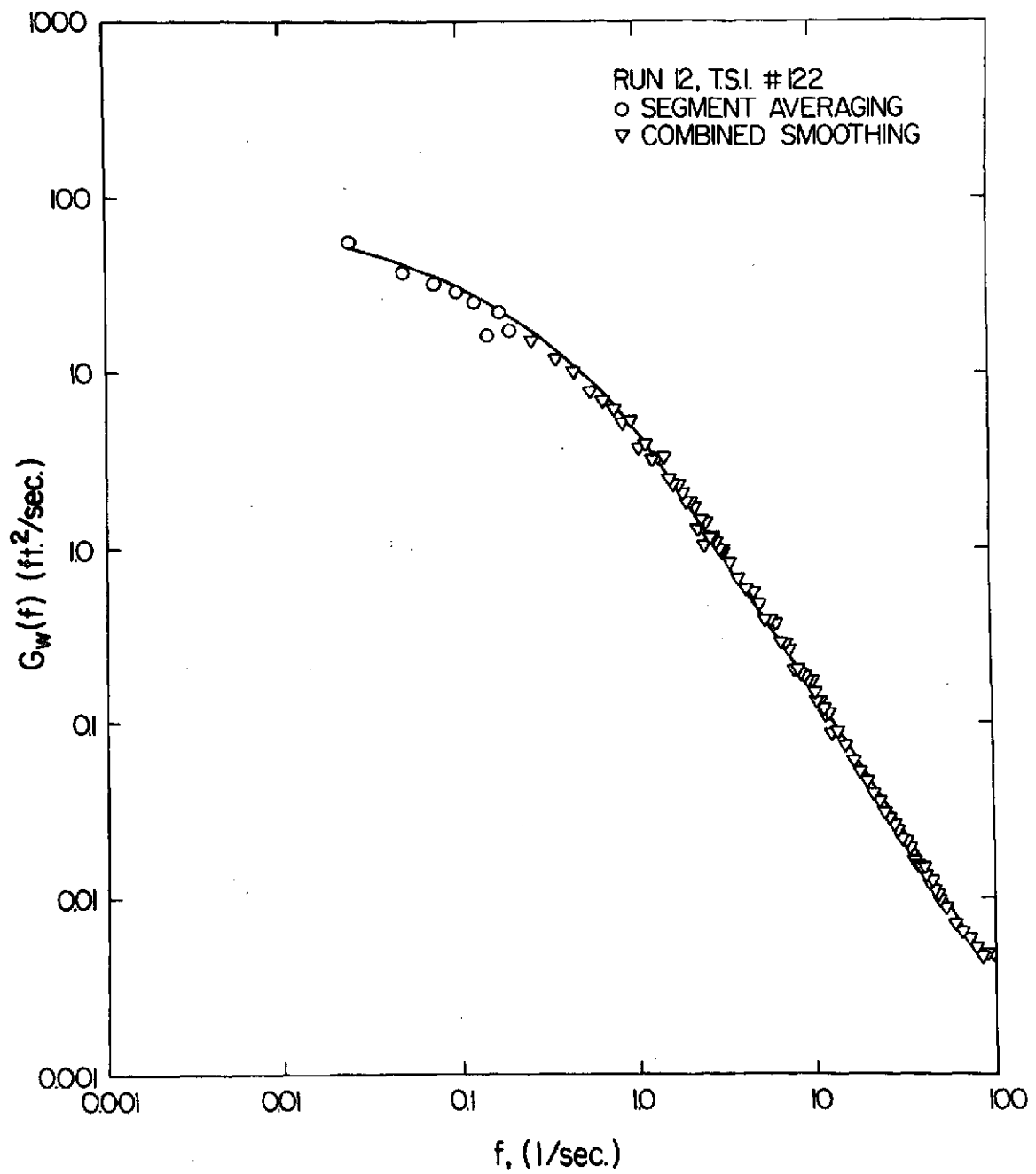
Figure 20. Power Spectrum of the Vertical Velocity Component.
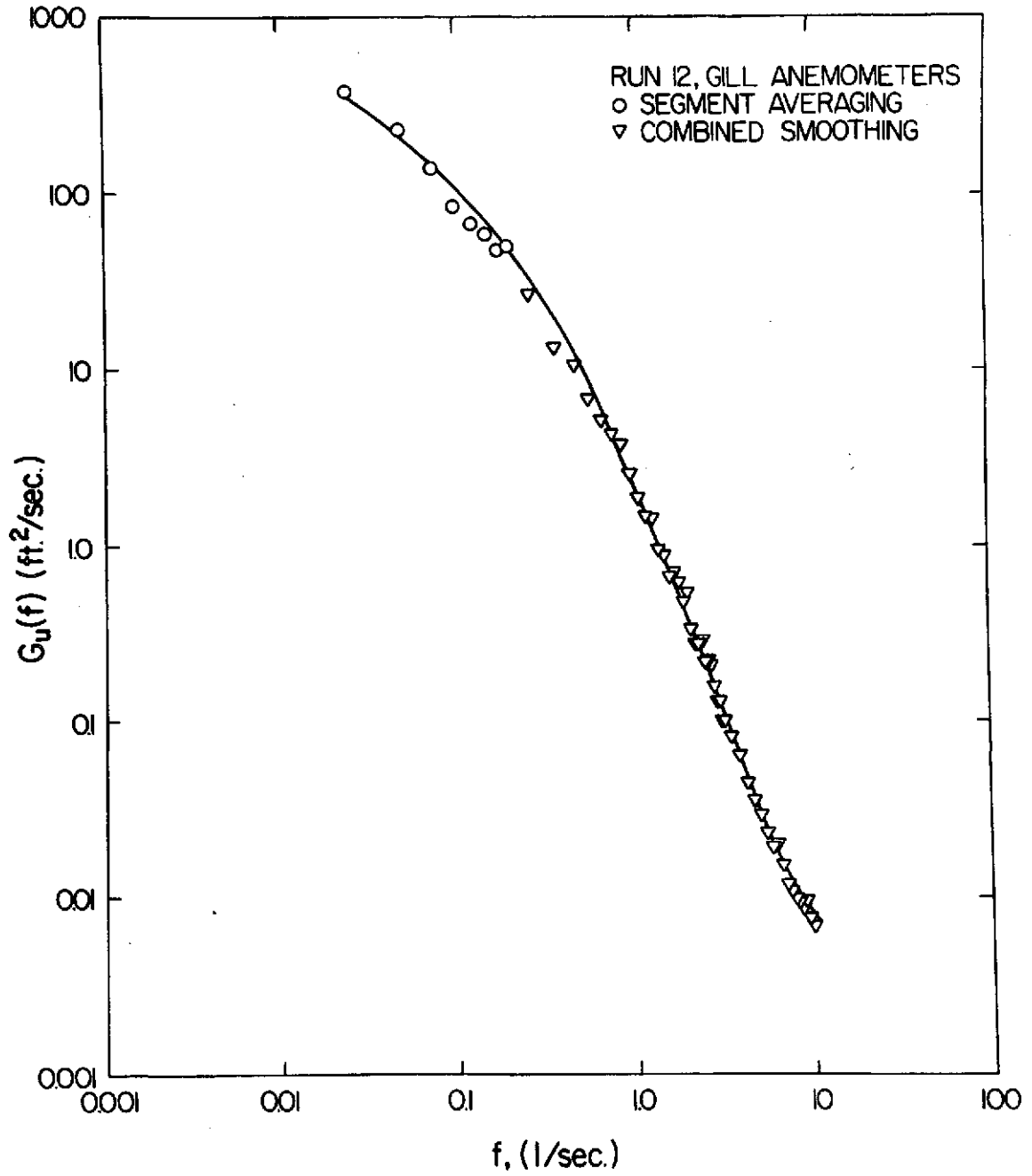
Figure 21.   Power Spectrum of the Longitudinal Velocity Component.
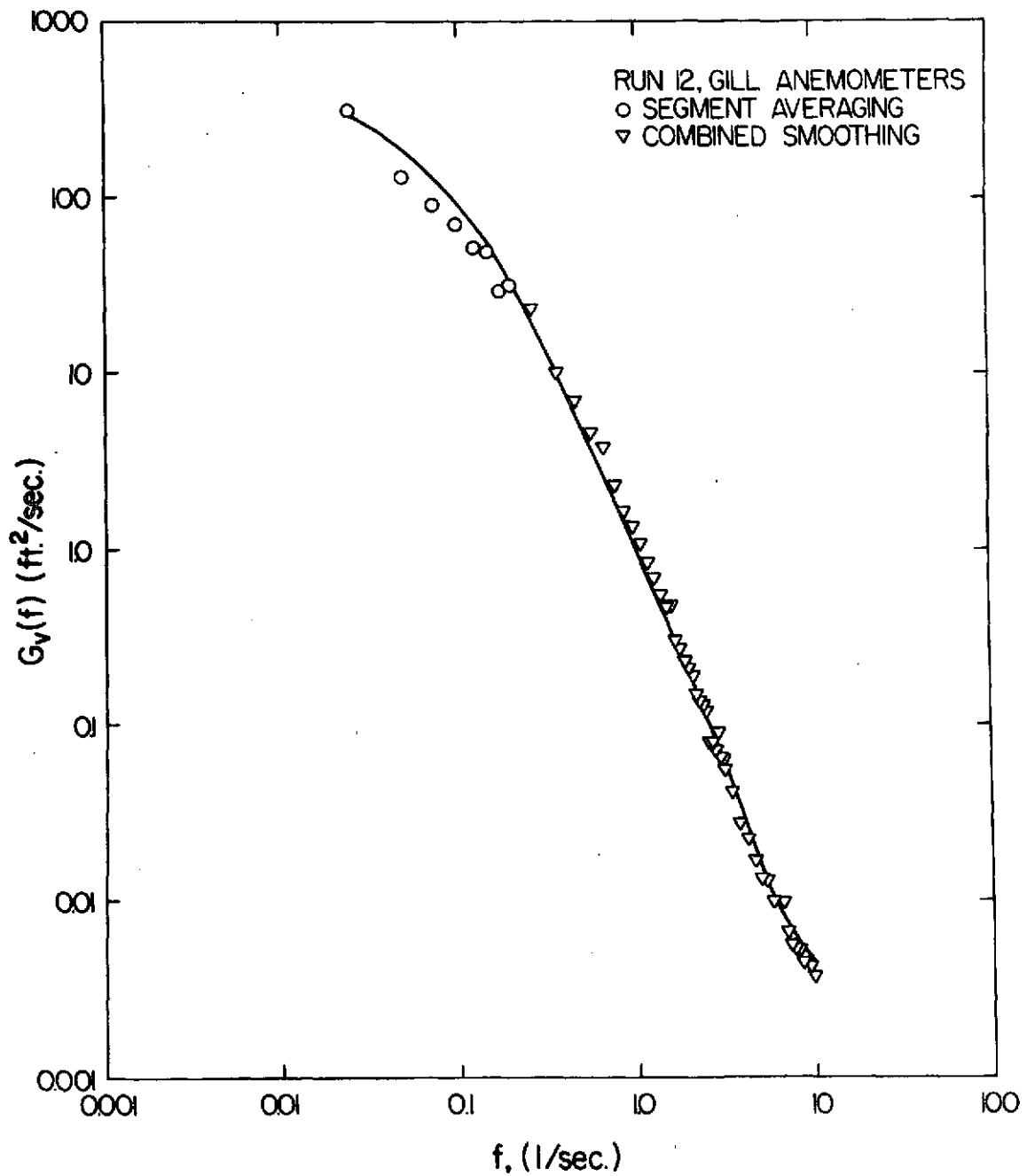
Figure 22. Power Spectrum of the Lateral Velocity Component.
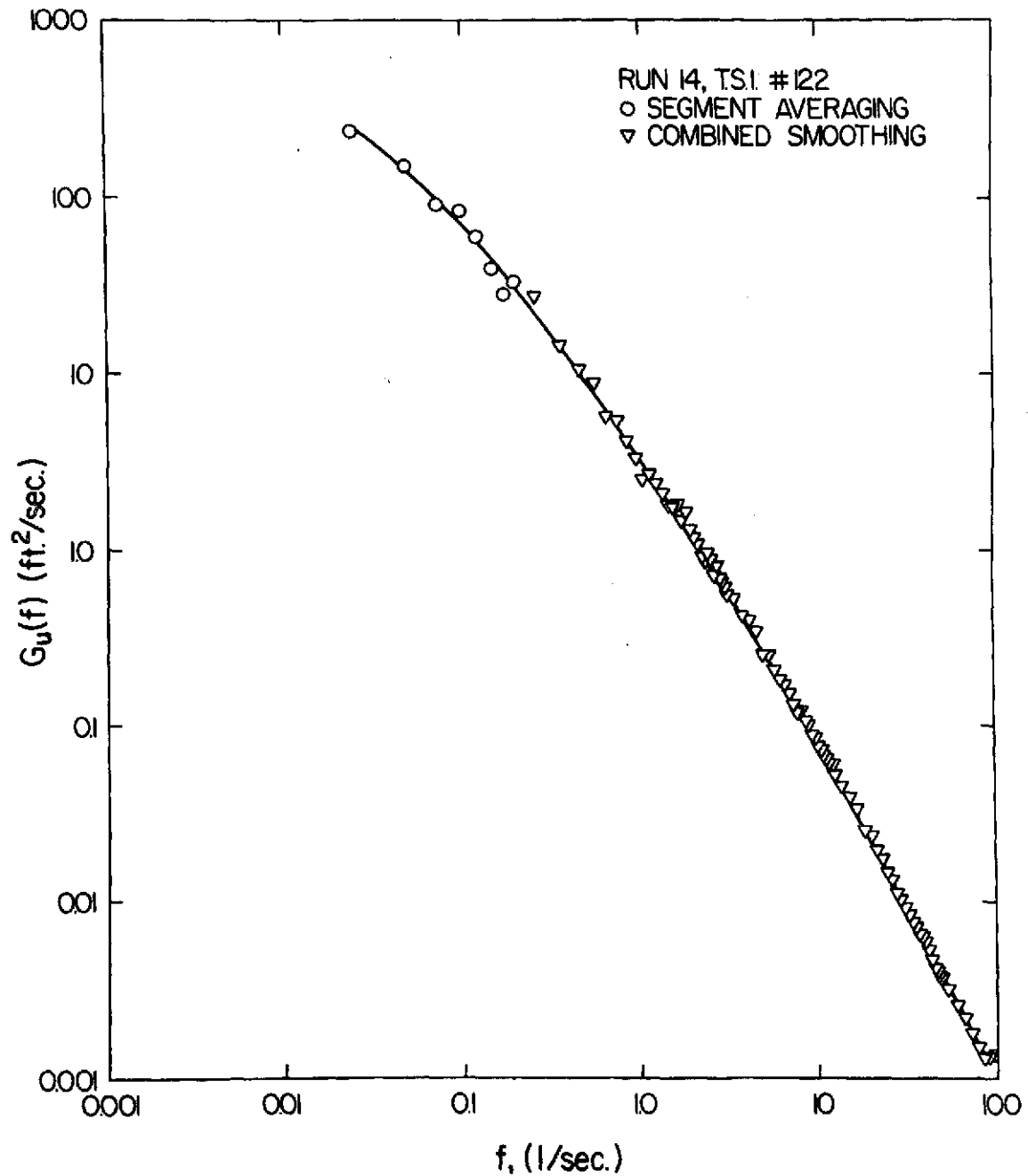
Figure 23. Power Spectrum of the Longitudinal Velocity Component.
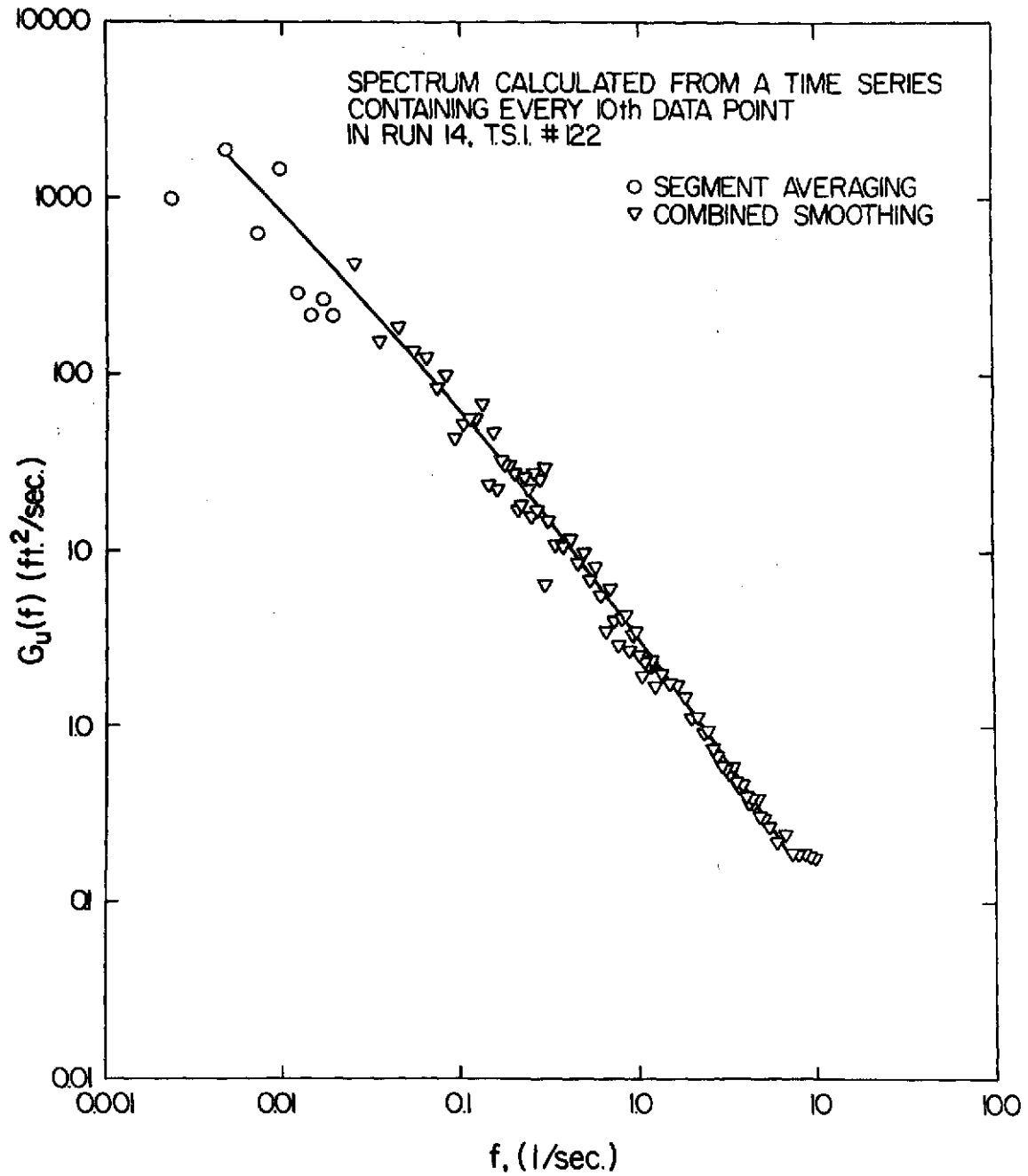
Figure 24. Power Spectrum of the Longitudinal Velocity Component.
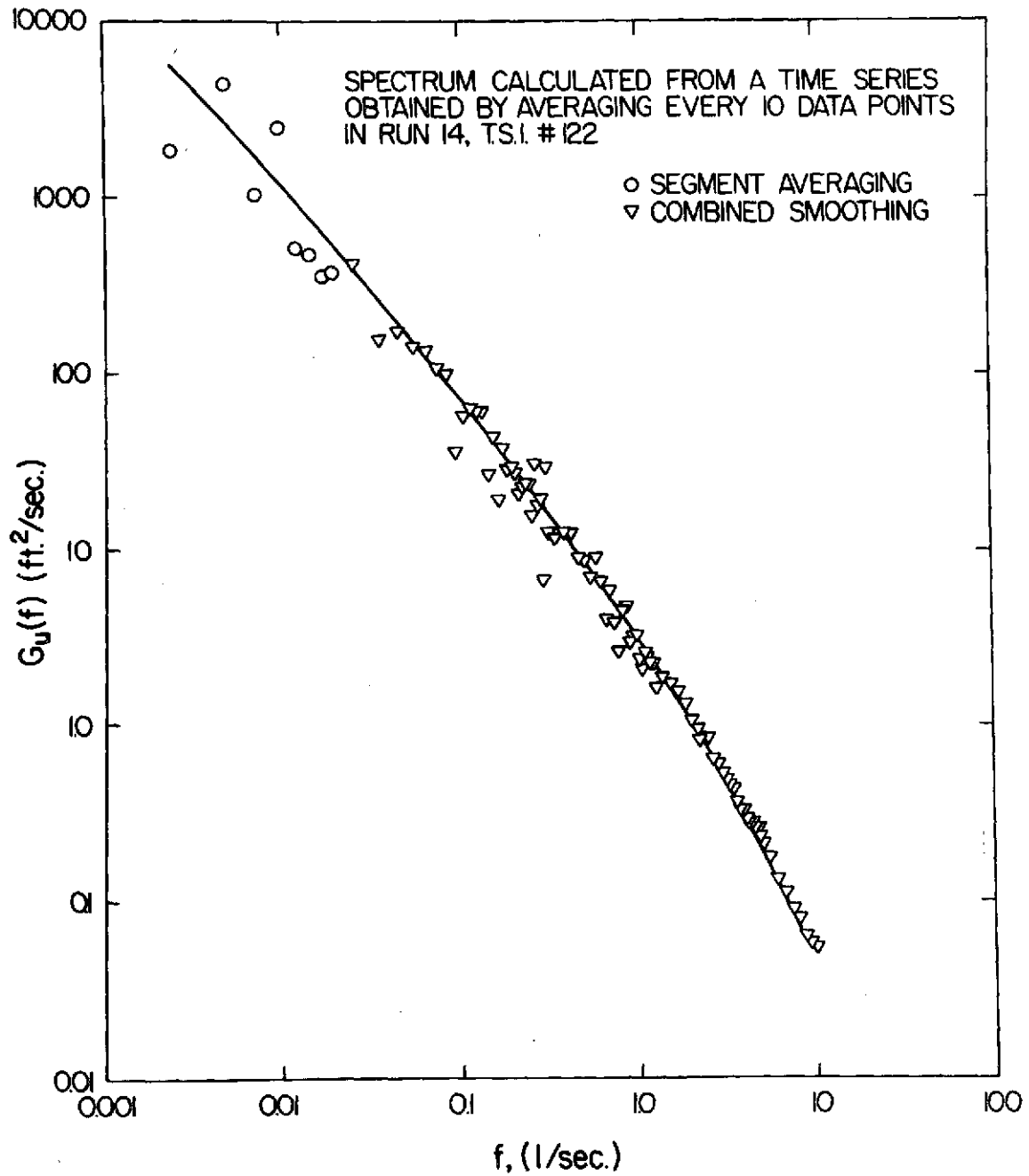
Figure 25. Power Spectrum of the Longitudinal Velocity Component.

TABLE I. PERCENTILES OF THE STANDARD NORMAL
DISTRIBUTION.

$P[T < T_\alpha^*]$	T_α^*	$P[T < T_\alpha^*]$	T_α^*
.001	-3.09	.600	0.25
.005	-2.58	.700	0.52
.010	-2.33	.800	0.84
.020	-2.05	.850	1.04
.025	-1.97	.900	1.28
.030	-1.88	.950	1.645
.040	-1.75	.960	1.75
.050	-1.645	.970	1.88
.100	-1.28	.975	1.97
.150	-1.04	.980	2.05
.200	-0.84	.990	2.33
.300	-0.52	.995	2.58
.400	-0.25	.999	3.09
.500	0		
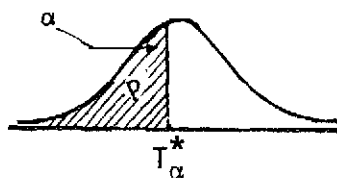
TABLE II. PERCENTAGE POINTS OF REVERSE ARRANGEMENT DISTRIBUTION.[*]

ℓ	α					
	0.99	0.975	0.95	0.05	0.025	0.01
10	9	11	13	31	33	35
11	12	14	16	38	40	42
12	16	18	21	44	47	49
13	19	22	25	52	55	58
14	24	27	30	60	63	66
15	28	32	35	69	72	76
16	34	38	41	78	81	85
17	39	44	48	87	91	96
18	45	50	54	98	102	107
19	52	57	61	109	113	118
20	59	64	69	120	125	130
21	66	72	77	132	137	143
22	74	80	86	144	150	156
23	82	89	95	157	163	170
24	91	98	104	171	177	184
25	100	108	114	185	191	199
26	109	118	125	199	206	215
27	119	128	136	214	222	231
28	130	139	147	230	238	247
29	140	150	159	246	255	265
30	152	162	171	263	272	282
31	163	174	184	280	290	301
32	176	187	197	298	308	319
33	188	200	210	317	327	339
34	201	214	225	335	346	359
35	215	228	239	355	366	379
36	229	243	254	375	386	400
37	243	258	270	395	407	422
38	258	273	286	416	429	444
39	274	289	302	438	451	466
40	290	305	319	460	474	489
41	306	322	336	483	497	513
42	323	340	354	506	520	537
43	340	357	372	530	545	562
44	357	376	391	554	569	588
45	375	394	410	579	595	614
46	394	413	430	604	621	640
47	413	433	450	630	647	667
48	432	453	471	656	674	695
49	452	474	492	683	701	723
50	473	495	514	710	729	751

TABLE II (Continued)

ℓ	α					
	0.99	0.975	0.95	0.05	0.025	0.01
51	494	516	536	738	758	780
52	515	538	558	767	787	810
53	537	561	581	796	816	840
54	559	584	605	825	846	871
55	582	607	629	855	877	902
56	605	631	653	886	908	934
57	628	655	678	917	940	967
58	652	680	703	949	972	1000
59	677	705	729	981	1005	1033
60	702	731	756	1013	1038	1067
61	727	757	782	1047	1072	1102
62	753	784	810	1080	1106	1137
63	780	811	837	1115	1141	1172
64	806	838	866	1149	1177	1209
65	834	866	894	1185	1213	1245
66	861	895	923	1221	1249	1283
67	890	924	953	1257	1286	1320
68	918	953	983	1294	1324	1359
69	948	983	1014	1331	1362	1397
70	977	1014	1045	1369	1400	1437
71	1007	1045	1076	1408	1439	1477
72	1038	1076	1108	1447	1479	1517
73	1069	1108	1141	1486	1519	1558
74	1100	1140	1174	1526	1560	1600
75	1132	1173	1207	1567	1601	1642
76	1165	1206	1241	1608	1643	1684
77	1198	1240	1275	1650	1685	1727
78	1231	1274	1310	1692	1728	1771
79	1265	1309	1346	1734	1771	1815
80	1299	1344	1382	1777	1815	1860
81	1334	1379	1418	1821	1860	1905
82	1369	1415	1455	1865	1905	1951
83	1405	1452	1492	1910	1950	1997
84	1441	1489	1530	1955	1996	2044
85	1478	1526	1568	2001	2043	2091
86	1515	1564	1606	2048	2090	2139
87	1552	1603	1646	2094	2137	2188
88	1590	1642	1685	2142	2185	2237
89	1629	1681	1725	2190	2234	2286
90	1668	1721	1766	2238	2283	2336

TABLE II (Continued)

ℓ	α					
	0.99	0.975	0.95	0.05	0.025	0.01
91	1707	1761	1807	2287	2333	2387
92	1747	1802	1849	2336	2383	2438
93	1787	1843	1891	2386	2434	2490
94	1828	1885	1933	2437	2485	2542
95	1870	1927	1976	2488	2537	2594
96	1911	1970	2020	2539	2589	2648
97	1954	2013	2064	2591	2642	2701
98	1996	2057	2108	2644	2695	2756
99	2040	2101	2153	2697	2749	2810
100	2083	2145	2198	2751	2804	2866

*Values of $t_{\ell;\alpha}$ such that $Prob[t_\ell > t_{\ell;\alpha}] = \alpha$.

TABLE III. PERCENTILES OF THE CHI-SQUARE DISTRIBUTION.*

Degrees of Freedom	$\chi^2_{.99}$	$\chi^2_{.975}$	$\chi^2_{.95}$	$\chi^2_{.90}$	$\chi^2_{.10}$	$\chi^2_{.05}$	$\chi^2_{.025}$	$\chi^2_{.01}$
1	.00016	.00098	.0039	.0158	2.71	3.84	5.02	6.63
2	.020	.051	.103	.211	4.61	5.99	7.38	9.21
3	.115	.216	.352	.584	6.25	7.81	9.35	11.3
4	.297	.484	.711	1.06	7.78	9.49	11.1	13.3
5	.554	.831	1.15	1.61	9.24	11.1	12.8	15.1
6	.872	1.24	1.64	2.20	10.6	12.6	14.4	16.8
7	1.24	1.69	2.17	2.83	12.0	14.1	16.0	18.5
8	1.65	2.18	2.73	3.49	13.4	15.5	17.5	20.1
9	2.09	2.70	3.33	4.17	14.7	16.9	19.0	21.7
10	2.56	3.25	3.94	4.87	16.0	18.3	20.5	23.2
12	3.57	4.40	5.23	6.30	18.5	21.0	23.3	26.2
14	4.66	5.63	6.57	7.79	21.1	23.7	26.1	29.1
16	5.81	6.91	7.96	9.31	23.5	26.3	28.8	32.0
18	7.01	8.23	9.39	10.9	26.0	28.9	31.5	34.8
20	8.26	9.59	10.9	12.4	28.4	31.4	34.2	37.6
22	9.54	11.0	12.3	14.0	30.8	33.9	36.8	40.3
24	10.9	12.4	13.8	15.7	33.2	36.4	39.4	43.0
26	12.2	13.8	15.4	17.3	35.6	38.9	41.9	45.6
28	13.6	15.3	16.9	18.9	37.9	41.3	44.5	48.3
30	15.0	16.8	18.5	20.6	40.3	43.8	47.0	50.9
40	22.1	24.4	26.5	29.0	51.8	55.8	59.3	63.7

TABLE III (Continued)

Degrees of Freedom	$\chi^2_{.99}$	$\chi^2_{.975}$	$\chi^2_{.95}$	$\chi^2_{.90}$	$\chi^2_{.10}$	$\chi^2_{.05}$	$\chi^2_{.025}$	$\chi^2_{.01}$
50	29.7	32.3	24.8	37.7	63.2	67.5	71.4	76.2
60	37.5	40.5	43.2	46.5	74.4	79.1	83.3	88.4

*Values of $\chi^2_{\gamma;\alpha}$ such that Prob $[\chi^2_\alpha > \chi^2_{\gamma;\alpha}] = \alpha$
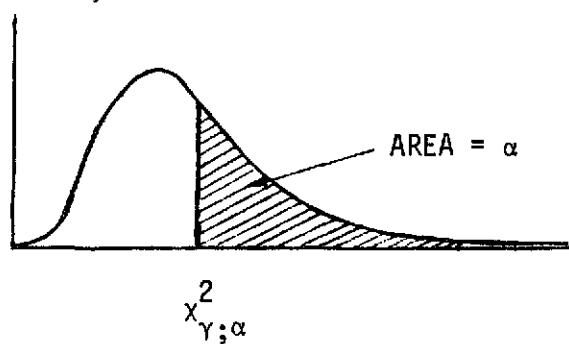
TABLE IV. RESULTS OF RUN 10 MEASUREMENTS: TSI #1192 (TRIPLE SPLIT FILM).

Block Number	Block Means of the Velocity Components in the Sensor Oriented Coordinate System		
	v(A) fps	v(B) fps	v(C) fps
1	7.159	0.315	19.118
2	6.872	1.232	15.274
3	6.664	12.136	10.567
4	7.306	11.930	12.626
5	6.235	5.927	14.096
6	2.369	3.524	10.346
7	4.893	1.206	15.555
8	6.932	-0.821	23.212
9	6.692	-1.322	26.001
10	4.141	2.949	16.273
11	5.224	1.336	16.416
12	5.282	3.082	15.915
13	10.639	14.491	17.574
14	8.049	3.766	21.162
15	8.247	6.195	17.395
16	6.072	0.441	22.161
17	7.211	0.205	22.961
18	7.766	0.980	18.673
19	5.015	-0.723	18.898
20	5.915	-0.143	19.546
21	8.586	2.636	20.457
22	7.390	3.662	15.965
23	4.374	6.836	13.083
24	4.337	-0.866	19.375
25	3.472	-1.763	21.035
26	4.058	-0.796	20.246
27	6.941	1.359	18.494
28	7.503	1.036	20.262
29	9.147	9.244	15.837
30	7.301	10.648	11.629
31	8.605	7.725	12.869
32	7.905	4.548	16.498
33	4.665	1.491	16.278
34	6.505	2.555	16.601
35	7.209	6.773	12.281
36	5.946	5.954	11.613
37	9.551	13.367	13.501
38	7.881	3.950	14.587

TABLE IV (Continued)

Block Number	Block Means of the Velocity Components in the Sensor Oriented Coordinate System		
	v(A) fps	v(B) fps	v(C) fps
39	5.730	1.151	16.624
40	1.979	1.008	11.641
41	2.102	2.806	11.127
42	0.468	3.191	8.227
43	1.599	3.204	7.521
44	7.733	7.867	12.748
Sample Mean	6.129 fps	3.734 fps	16.188 fps
Number of Reverse Arrangements of the Block Means	504.0	424.0	584.0

Means, variances and covariances of the velocity components and temperature in the mean wind coordinate system:

$$U = 17.429 \text{ fps}$$
$$V = 0.0 \text{ fps}$$
$$W = 3.129 \text{ fps}$$
$$T = 39.110 \text{ °F}$$
$$\overline{u^2} = 15.778 \text{ (fps)}^2$$
$$\overline{uv} = -2.474 \text{ (fps)}^2$$
$$\overline{uw} = -3.903 \text{ (fps)}^2$$
$$\overline{u\theta} = -0.205 \text{ fps-°F}$$
$$\overline{v^2} = 18.029 \text{ (fps)}^2$$
$$\overline{vw} = 1.012 \text{ (fps)}^2$$
$$\overline{v\theta} = 0.513 \text{ fps-°F}$$
$$\overline{w^2} = 10.4 \text{ (fps)}^2$$
$$\overline{w\theta} = -0.105 \text{ fps-°F}$$
$$\overline{\theta^2} = 0.455 \text{ (°F)}^2$$

TABLE V. RESULTS OF RUN 11 MEASUREMENTS: TSI #1192 (TRIPLE SPLIT FILM) -- GILL ANEMOMETERS.

Block Number	Block Means of the Velocity Components in the Probe Oriented Coordinate System			
	Gill Anemometers v'(x*)	TSI #1192 v'(x*)	Gill Anemometers v'(y*)	TSI #1192 v'(y*)
1	33.839	31.774	7.490	8.561
2	27.660	25.584	7.645	8.140
3	29.385	26.814	10.668	11.404
4	22.272	18.846	18.131	14.929
5	27.244	23.009	16.073	16.952
6	26.837	22.699	16.747	17.116
7	26.221	22.869	13.638	14.326
8	20.513	18.016	12.177	11.590
9	16.328	14.732	12.509	9.598
10	24.719	21.331	17.402	15.866
11	25.447	22.354	11.876	12.642
12	16.918	15.709	9.262	8.018
13	24.315	20.883	13.089	13.879
14	26.210	22.893	12.069	12.099
15	30.838	27.496	11.497	12.394
16	32.487	28.336	14.951	15.874
17	28.082	25.038	10.749	11.963
18	26.172	24.006	8.004	8.302
19	26.893	25.376	5.158	6.399
20	24.310	22.529	7.533	8.126
21	39.024	37.139	5.112	6.206
22	42.911	40.890	4.986	7.015
23	38.896	36.741	6.889	8.387
24	40.385	38.757	2.037	3.641
25	39.766	38.061	3.621	5.018
26	37.026	36.001	3.353	4.697
27	39.881	38.289	-4.187	-3.475
28	30.765	29.668	-2.398	-1.054
29	28.728	27.510	-1.806	-1.240
30	27.699	26.396	-3.908	-3.883
31	27.268	25.651	1.018	1.411
32	33.251	31.501	6.514	7.734
33	28.653	27.330	2.609	3.478
34	29.494	28.187	5.964	7.159
35	31.008	29.634	5.831	7.159
36	28.059	26.900	3.132	4.153
37	24.640	23.980	-1.387	-1.692

TABLE V (Continued)

Block Number	Block Means of the Velocity Components in the Probe Oriented Coordinate System			
	Gill Anemometers v'(x*)	TSI #1192 v'(x*)	Gill Anemometers v'(y*)	TSI #1192 v'(y*)
38	26.047	25.087	0.799	1.076
39	25.754	24.587	3.797	4.825
40	20.645	19.657	4.591	4.639
41	22.335	21.677	-0.353	-0.153
42	15.381	15.310	-1.259	-1.701
43	17.851	16.315	-4.003	-4.018
44	15.865	15.173	-2.678	-2.659
Number of Reverse Arrangements of the Block Means in Sensor Oriented Coordinate System	512.0	427.0	766.0	671.0

Mean Wind Components in the Probe Oriented Coordinate System

	TSI #1192	Gill Anemometers
U' (fps)	25.93	27.91
V' (fps)	6.70	6.25
T (°F)	33.03	
β (deg.)	-14.49	-12.62

TABLE V (Continued)

Means, Variances and Covariances of the Velocity Components
in the Mean-Wind Coordinate System

	TSI #1192	Gill Anemometers
U (fps)	26.778	28.600
V (fps)	0.0	0.0
W (fps)	5.920	
$\overline{u^2}$ (fps)^2	35.914	26.367
$\overline{uv}$ (fps)^2	2.464	0.319
$\overline{uw}$ (fps)^2	-4.391	
$\overline{u\theta}$ fps-°F	-0.743	
$\overline{v^2}$ (fps)^2	32.931	22.680
$\overline{vw}$ (fps)^2	0.050	
$\overline{v\theta}$ (fps-°F)	-0.242	
$\overline{w^2}$ (fps)^2	25.316	
$\overline{w\theta}$ (fps-°F)	0.040	
$\overline{\theta^2}$ (°F)	0.367	

TABLE VI. RESULTS OF RUN 12 MEASUREMENTS: TSI #122 (DUAL SPLIT FILM) -- GILL ANEMOMETERS.

Block Number	Block Means of the Velocity Components in the Probe Oriented Coordinate System				
	Gill Anemometers $v(x^*)$	TSI #122 $v(x^*)$	Gill Anemometers $v(y^*)$	TSI #122 $v(y^*)$	TSI #122 $v(z^*)$
1	24.132	23.535	-3.656	-0.149	7.976
2	23.528	23.560	-1.027	2.866	8.096
3	28.992	26.246	-9.957	-8.377	6.793
4	32.051	29.115	-3.910	-1.331	7.950
5	32.846	34.792	-5.209	-2.437	7.064
6	28.414	23.290	-18.330	-18.530	7.804
7	30.508	23.050	-24.876	-24.837	7.244
8	26.462	18.599	-24.103	-23.335	5.787
9	22.803	20.223	-22.716	-21.351	6.405
10	22.515	20.223	-7.472	-6.077	6.498
11	32.998	32.323	2.572	5.328	8.175
12	35.420	34.819	1.880	5.312	8.931
13	19.690	18.519	-7.062	-5.419	5.366
14	22.059	17.190	-14.803	-14.636	5.289
15	16.780	14.627	-9.382	-7.963	4.142
16	16.681	17.027	-2.512	0.433	3.971
17	22.781	21.644	-0.704	1.207	6.798
18	25.599	24.852	-0.144	3.554	8.288
19	36.042	32.616	-9.502	-7.801	6.364
20	23.357	21.106	-6.997	-4.233	7.121
21	18.160	15.151	-10.525	-7.953	4.729
22	23.236	14.392	-23.278	-22.111	6.049
23	19.137	16.359	-10.046	-9.157	6.888
24	17.285	16.352	-4.860	-2.812	4.520
25	23.981	23.431	-0.543	2.057	4.589

TABLE VI (Continued)

Block Number	Block Means of the Velocity Components in the Probe Oriented Coordinate System				
	Gill Anemometers v(x*)	TSI #122 v(x*)	Gill Anemometers v(y*)	TSI #122 v(y*)	TSI #122 v(z*)
26	21.584	20.232	-7.411	-5.219	5.268
27	17.827	11.484	-15.543	-14.812	4.806
28	22.796	15.873	-20.170	-19.084	5.593
29	17.114	15.384	-5.864	-3.682	5.430
30	32.880	30.078	-7.292	-5.822	5.836
31	30.316	28.692	-4.863	-1.108	5.683
32	25.317	23.307	-5.360	-2.556	5.693
33	21.278	17.926	-10.252	-8.780	4.413
34	24.692	19.871	-15.139	-14.429	4.395
35	19.140	16.372	-9.616	-7.810	5.104
36	21.599	18.726	-10.101	-7.680	4.837
37	25.766	21.717	-10.178	-6.826	5.813
38	26.900	25.464	-3.067	0.537	5.895
39	39.215	37.735	0.576	5.472	7.868
40	29.653	25.839	-11.967	-10.007	6.523
41	24.603	24.219	-1.600	1.987	6.503
42	23.190	19.188	-13.438	-11.190	6.923
43	23.058	17.221	-16.795	-14.658	3.632
44	17.602	14.790	-11.366	-9.221	5.639
Number of Reverse Arrangements of the Block Means	524.0	523.0	514.0	494.0	601.0

TABLE VI (Continued)

Mean Velocity Components in the Probe Oriented Coordinate System

	§TSI #122	§Gill Anemometers	TSI #122	Gill Anemometers
U' (fps)	21.750	24.772	21.750	24.772
V' (fps)	-6.878	-9.014	-6.878	-9.014
W' (fps)	6.107		6.107	
T (°F)	41.609		41.609	
β (deg.)	17.550	19.995	17.550	19.995

Means, Variances and Covariances of the Velocity Components in the Mean-Wind Coordinate System

	§TSI #122	§Gill Anemometers	TSI #122	Gill Anemometers
U (fps)	22.812	26.361	22.812	26.361
V (fps)	0.0	0.0	0.0	0.0
W (fps)	6.107		6.107	
$\overline{u^2}$ (fps)^2	34.863	27.760	35.559	28.320
$\overline{uv}$ (fps)^2	-0.216	-3.393	-0.116	-3.239
$\overline{uw}$ (fps)^2	-0.282		-0.285	
$\overline{u\theta}$ fps-°F	-1.182		-1.182	
$\overline{v^2}$ (fps)^2	55.290	35.451	57.377	36.160
$\overline{vw}$ (fps)^2	9.241		9.412	
$\overline{v\theta}$ fps-°F	-0.338		-0.298	
$\overline{w^2}$ (fps)^2	20.873		20.983	

TABLE VI (Continued)

	[§]TSI #122	[§]Gill Anemometers	TSI #122	Gill Anemometers
$\overline{w\theta}$ fps-°F	0.219		0.227	
θ^2 (°F)^2	1.452		1.468	

[§]Block means removed.

TABLE VII. RESULTS OF RUN 14 MEASUREMENTS: TSI #122 -- GILL ANEMOMETERS.

Block Number	Block Means of the Velocity Components in the Probe Oriented Coordinate System				
	Gill Anemometers v(x*)	TSI #122 v(x*)	Gill Anemometers v(y*)	TSI #122 v(y*)	TSI #122 v(z*)
1	27.628	26.230	14.520	15.538	6.729
2	27.143	25.422	14.621	15.258	6.440
3	26.295	24.621	13.140	13.171	5.488
4	18.198	18.103	6.020	6.836	4.866
5	25.149	23.531	10.516	11.415	6.182
6	30.664	29.643	14.508	15.209	7.989
7	25.101	24.066	10.748	10.844	5.784
8	26.115	24.250	16.188	16.088	6.887
9	31.156	29.846	10.589	11.733	6.228
10	26.985	24.673	-1.872	-3.296	7.295
11	31.578	29.201	18.478	18.559	7.719
12	35.638	33.469	19.658	20.491	8.862
13	28.971	27.138	9.979	10.512	7.365
14	26.242	24.870	12.074	12.676	6.943
15	23.638	22.676	10.260	10.612	5.101
16	23.057	21.433	13.697	13.658	5.845
17	31.742	28.310	20.198	19.890	7.806
18	33.644	31.865	17.692	17.668	8.193
19	26.085	23.935	15.668	16.013	6.009
20	25.228	24.271	10.891	11.562	6.729
21	25.775	25.187	2.402	2.172	6.951
22	24.197	23.540	7.788	7.601	7.842
23	28.916	27.966	12.146	13.293	7.141
24	23.690	21.835	-2.679	-4.636	6.452
25	24.901	23.608	-4.543	-5.495	7.405
26	20.647	19.645	-5.765	-6.584	7.069

159

TABLE VII (Continued)

Block Number	Block Means of the Velocity Components in the Probe Oriented Coordinate System				
	Gill Anemometers $v(x^*)$	TSI #122 $v(x^*)$	Gill Anemometers $v(y^*)$	TSI #122 $v(y^*)$	TSI #122 $v(z^*)$
27	25.743	24.216	-5.777	-7.872	7.205
28	19.740	17.967	-7.290	-9.133	7.400
29	26.619	24.414	12.687	14.010	7.710
30	26.126	25.368	4.391	4.101	6.598
31	27.358	25.690	-5.627	-7.820	7.291
32	22.217	20.911	-3.553	-4.903	6.867
33	18.328	16.226	-6.596	-8.732	8.258
34	27.728	26.292	2.808	1.939	6.390
35	28.495	26.844	10.775	10.788	6.362
36	28.370	26.843	8.828	9.566	5.420
37	25.417	23.856	11.189	10.961	7.837
38	34.486	32.053	19.427	20.322	8.298
39	45.617	41.982	25.594	25.250	9.975
40	28.522	27.665	13.154	14.080	9.371
41	37.873	35.921	16.237	17.067	9.696
42	32.370	30.956	4.584	3.508	7.454
43	21.294	20.853	4.196	3.971	3.768
44	19.579	18.862	2.896	2.408	6.338
Number of Reverse Arrangements of the Block Mean	472.0	467.0	558.0	564.0	375.0

160

TABLE VII (Continued)

Mean Velocity Components in the Probe Oriented Coordinate System

	§TSI #122	§Gill Anemometers	TSI #122	Gill Anemometers
U' (fps)	25.597	27.142	25.597	27.142
V' (fps)	8.416	8.519	8.416	8.519
W' (fps)	7.035		7.035	
T (°F)	55.000		55.000	
β (deg.)	-18.200	-17.425	-18.200	-17.425

Means, Variances and Covariances of the Velocity Components in the Mean-Wind Coordinate System

	§TSI #122	§Gill Anemometers	TSI #122	Gill Anemometers
U (fps)	26.945	28.448	26.945	28.448
V (fps)	0.0	0.0	0.0	0.0
W (fps)	7.035		7.035	
$\overline{u^2}$ (fps)^2	30.694	27.325	31.365	28.088
$\overline{uv}$ (fps)^2	4.043	2.825	4.231	2.937
$\overline{uw}$ (fps)^2	-0.486		-0.380	
$\overline{u\theta}$ (fps-°F)	0.0		0.0	
$\overline{v^2}$ (fps)^2	50.041	35.886	50.761	36.391
$\overline{vw}$ (fps)^2	2.765		2.776	
$\overline{v\theta}$ (fps-°F)	0.0		0.0	

TABLE VII (Continued)

	[§]TSI #122	[§]Gill Anemometers	TSI #122	Gill Anemometers
$\overline{w^2}$ (fps)^2	17.705		17.758	
$\overline{w\theta}$ (fps-°F)	0.0		0.0	
$\overline{\theta^2}$ (°F^2)	0.0		0.0	

[§]Block means removed.

APPENDIX A

THE RESPONSE CHARACTERISTICS OF THE GILL ANEMOMETERS

Sensor Response

The Gill anemometer utilizes propellers, the shafts of which are parallel to each of the two perpendicular coordinate axes in the horizontal plane. The polystyrene propellers have four blades and are constructed to turn one revolution for each 31.7 cm of air passing the propeller. Each anemometer contains a miniature tachometer generator which is turned by the propeller and produces a voltage that is related to the respective wind components. Since the set of Gill anemometers were rotated with the TSI anemometers, they were oriented in such a fashion that one anemometer was on the average in the direction of the mean wind and the second anemometer perpendicular to the first one both in a horizontal plane. In this orientation both Gill anemometers were calibrated in the wind tunnel for velocities ranging from 10 fps to 70 fps and for various angles of attack varying from -40° to +40° with respect to the mean-velocity direction.

It is therefore suggested that this set of propeller anemometers should not be used when the angle of attack is larger than +40° or less than -40°. The velocities should not go beyond the range as specified.

The velocity components can be obtained from the following empirical relations which fitted the calibration data very well for the above ranges in velocity and angle of attack:

$$v_x' = 0.069 \frac{E_x}{(\cos \beta)^{0.4}} \tag{A-1}$$

and

$$v_y' = 0.085 \, E_y \tag{A-2}$$

where E_x and E_y are the anemometer output voltages and β is the angle of attack. Since the angle β is not known at the outset, a simple iteration procedure is used to calculate the velocity component v_x'. No single empirical relation was attempted to be obtained since the two propellers were always rotated in such a way so that one was along the mean wind and the other one normal to it.

From the empirical equations obtained from the wind-tunnel calibration data one can easily see that these anemometers deviate systematically from the ideal cosine law and no reliance can be placed on just a single calibration with zero angle of attack.

In turbulent conditions, there can be large differences between the indicated speed and the actual velocity. The differences arise from sensor sensitivity to relative wind direction, sensor dynamic characteristics, and to the data averaging procedure. The difference between measurements with various common types of anemometers may exceed 30 percent [62].

The response time of the rotating type of anemometers such as cup anemometers and propeller type anemometers is always obtained by letting the anemometers accelerate from rest to some equilibrium speed of rotation depending on the wind velocity. The response of the anemometers which are allowed to decelerate from some speed of

rotation to rest is very difficult to realize in the wind tunnel.
As a consequence the response time is based on the acceleration of
the anemometers and the response for deceleration is assumed to be
similar. However, the cup anemometers and propeller anemometers are
known to accelerate faster than to decelerate with increasing and
decreasing wind velocities respectively. As a result, the calculated
mean velocity is estimated too high with respect to the actual velocity
when the anemometers are used in turbulent winds. In addition, the
output voltage of the anemometers shows a rectified undulation superimposed
on the mean voltage. The frequency and magnitude of this "ripple" depends
on the rate of rotation of the anemometer. If the propeller anemometers
are used for the measurement of fluctuating velocities the digitized
data will be affected by the presence of this undulation.

The calibration data have indicated that the output of the propeller
anemometer is related directly to the component of the velocity parallel
to its shaft. Because of varying response characteristics when the
propeller operates in a accelerating flow as compared to a decelerating
flow, the mean velocity is overestimated (See results in Tables V, VI,
and VII). Because of the limited response characteristics at frequencies
higher than 1 hertz, the propeller anemometers underestimate the variances
and covariances of the different velocity comopnents. This fact is very
well illustrated if the spectra of the velocity components measured by
the Gill anemometers are compared with those measured by the fast-response
TSI anemometer (compare figure 18 with 21 and figure 19 with 22).

APPENDIX B

LISTING OF FORTRAN PROGRAMS

167

```
C *******************************DATP 1*******************************C
C---------------------------------------------------------------------C
C            PPPPPP      A      RRRRR    TTTTT    11111                C
C            P    P    A  A     R   R      T        1                  C
C            PPPPPP    A    A   RRRRR      T        1                  C
C            P        AAAAA     RR         T        1                  C
C            P        A     A   R RR       T        1                  C
C            P        A     A   R   R      T      11111                C
C---------------------------------------------------------------------C
C    DATA PROCESSING SYSTEM OF A SET OF FOUR  DIGITIZED TIME SERIES    C
C    FOR CALCULATING MEAN,CORRELATION AND TRANSFORMATION MATRIX        C
C            U(1,I)=X-COMPONENTS VELOCITY OF SENSOR 1,V(A)             C
C            U(2,I)=Y-COMPONENTS VELOCITY OF SENSOR 1,V(B)             C
C            U(3,I)=Z-COMPONENTS VELOCITY OF SENSOR 1,V(C)             C
C            U(4,I)=TEMPERATURE OF SENSOR 1                            C
C---------------------------------------------------------------------C
      DIMENSION U(4,8192),UBBK(44,4),BETA1(44),COV(44,4,4),DEG(44)
      DIMENSION UBKT(44),UBTOTL(4),TOTREV(8),TUB(3),STDVIT(44,8,8),
     1REVARR(44,8),BKVAR(44,4,4)
C---------------------------------------------------------------------C
C               CALL DATA FROM MAGNETIC TAPE                          C
C   NDTBK=DATBK=NUMBER OF DATA IN EACH BLOCK                          C
C   NOBLK=IB=NUMBER OF BLOCKS                                         C
C   IX=NDTBK=NUMBER OF DATA IN EACH BLOCK                             C
C   IB=THE BLOCK NUMBER                                               C
C   NTS=NUMBER OF TIME SERIES                                         C
C---------------------------------------------------------------------C
      NTS=4
      NDTBK=8192
      NOBLK=44
      BLKNO=NOBLK
      IB=1
```

```
      IX=NDTBK
5000  DO 7 I=1,NDTBK
    7 READ(10,10) U(4,I),U(1,I),U(2,I),U(3,I)
   10 FORMAT(4A4)
C------------------------------------------------------------------C
C    CALCULATE THE MEAN VALUE IN EACH BLOCK WHICH WE MIGHT CALL     C
C    PIECEWISE MEAN                                                 C
C    UBBK(IB,J)=MEAN VALUE IN EACH BLOCK,IB=1,2,...,NOBLK, J=1,2,...,4   C
C------------------------------------------------------------------C
      DO 11 J=1,NTS
   11 UBBK(IB,J)=0.0
      I=1
   12 DO 13 J=1,NTS
   13 UBBK(IB,J)=UBBK(IB,J)+U(J,I)
      IF(I .EQ. NDTBK) GO TO 14
      I=I+1
      GO TO 12
   14 DATBK=NDTBK
      DO 15 J=1,NTS
   15 UBBK(IB,J)=UBBK(IB,J)/DATBK
      UBKT(IB)=SQRT(UBBK(IB,1)**2+UBBK(IB,2)**2+UBBK(IB,3)**2)
C------------------------------------------------------------------C
C    CALCULATE THE TRANSFORMATION ANGLE BETA1 UN EACH BLOCK         C
C    CALCULATE TNE MEAN SQUARES AND CORRELATIONS IN EACH BLOCK      C
C    COV=MEAN SQUARES AND CORRELATIONS IN A BLOCK                   C
C    BKVAR=BLOCK VARIANCES AND COVARIANCES                          C
C------------------------------------------------------------------C
      BETA1(IB) = ATAN(-1.22475*(UBBK(IB,2)-UBBK(IB,3))/(UBBK(IB,1)
     1+UBBK(IB,2)+UBBK(IB,3)))
      DEG(IB)=(180.0/3.14159)*BETA1(IB)
      DO 16 K=1,NTS
      DO 16 J=1,NTS
```

```
   16 COV(IB,K,J)=0.0
      I=1
   17 DO 18 K=1,NTS
      DO 18 L=1,NTS
   18 COV (IB,K,L)=COV(IB,K,L)+U(K,I)*U(L,I)
      IF(I .EQ. NDTBK) GO TO 191
      I=I+1
      GO TO 17
  191 DO 19 K=1,NTS
      DO 19 L=1,NTS
   19 COV(IB,K,L)=COV(IB,K,L)/DATBK
      DO 192 N=1,NTS
      BKVAR(IB,N,N)=COV(IB,N,N)-UBBK(IB,N)*UBBK(IB,N)
  192 STDVIT(IB,N,N)=SQRT(ABS(BKVAR(IB,N,N)))
      IF (IB .EQ. NOBLK) GO TO 3000
      IB=IB+1
      GO TO 5000
 3000 CONTINUE
      WRITE (6,100)
  100 FORMAT(1H1,1X,'BK NO',2X,'MEAN V(A)',2X,'MEAN V(B)',2X,'MEAN V(C)'
     1,3X,'MAGNITUDE',2X,'MEAN TEMP',2X,'BLK ANG',3X,'STD DIV VA',2X,
     2'STD DIV VB',2X,'STD DIV VC',2X,'STD DIV T'//)
      DO 101 IB=1,NOBLK
  101 WRITE(6,102) IB,UBBK(IB,1),UBBK(IB,2),UBBK(IB,3),UBKT(IB),UBBK(IB,
     14),DEG(IB),STDVIT(IB,1,1),STDVIT(IB,2,2),STDVIT(IB,3,3),STDVIT(IB,
     24,4)
  102 FORMAT(3X,I2,2X,F9.3,3(3X,F9.3),2X,F9.3,3X,F6.2,4(3X,F9.3))
C-----------------------------------------------------------------------C
C    HERE BEGINS THE CALCULATION OF THE MEAN OR WE MIGHT CALL IT THE     C
C    GRAND OR ACCUMULATED MEAN,OR SAMPLE MEAN                            C
C    UBTOTL(J)=ACCUMULATED MEAN,J=1,2,3,4                                C
C-----------------------------------------------------------------------C
```

```
      DO 20 J=1,NTS
   20 UBTOTL(J)=0.0
      J=1
   21 DO 22 IB=1,NOBLK
   22 UBTOTL(J)=UBTOTL(J)+UBBK(IB,J)
      IF(J .EQ. NTS) GO TO 24
      J=J+1
      GO TO 21
   24 DO 23 J=1,NTS
   23 UBTOTL(J)=UBTOTL(J)/BLKNO
      VTOTL1=SQRT(UBTOTL(1)**2+UBTOTL(2)**2+UBTOTL(3)**2)
      WRITE(6,104) ((UBTOTL(J),J=1,NTS),VTOTL1)
  104 FORMAT (///2X,'SAMPLE MEAN=',4F12.6,5X,'TOTAL VEL. MAG.=',F12.6/)
C----------------------------------------------------------------------C
C    HERE BEGINS THE CALCULATIONS OF SAMPLE BETAS                       C
C    BETOL1=THE SAMPLE BETA                                             C
C----------------------------------------------------------------------C
      BETOL1 = ATAN(-1.22475*(UBTOTL(2)-UBTOTL(3))/(UBTOTL(1)+UBTOTL(2)
     1+UBTOTL(3)))
      BEDEG=(180.0/3.14159)*BETOL1
      WRITE(6,103) BETOL1,BEDEG
  103 FORMAT(/2X,'BETOL1=',F18.8,5X,'BEDEG=',F10.5)
C----------------------------------------------------------------------C
C    HERE CALCULATES THE NUMBER OF REVERSE ARRANGEMENTS FOR STD. DEV. C
C    IN EACH BLOCK                                                      C
C----------------------------------------------------------------------C
      NSTD=8
      NTEST=NOBLK-1
      DO 181 IB=1,NOBLK
      DO 181 I=1,3
      K=I+5
  181 STDVIT(IB,K,K)=STDVIT(IB,I,I)
```

```
      DO 182 IB=1,NOBLK
      STDVIT(IB,4,4)=UBKT(IB)
      STDVIT(IB,5,5)=DEG(IB)
      DO 182 I=1,3
182   STDVIT(IB,I,I)=UBBK(IB,I)
      DO 194 IB=1,NOBLK
      DO 194 I=1,NSTD
194   REVARR(IB,I)=0.0
      IB=1
      K=IB+1
195   DO 197 II=1,NSTD
      DO 197 JJ=K,NOBLK
      IF (STDVIT(IB,II,II) .GT. STDVIT(JJ,II,II)) GO TO 196
      GO TO 197
196   REVARR(IB,II)=REVARR(IB,II)+1.0
197   CONTINUE
      IF (IB .EQ. NTEST) GO TO 198
      IB=IB+1
      K=IB+1
      GO TO 195
198   CONTINUE
      DO 190 J=1,NSTD
      TOTREV(J)=0.0
      DO 190 IB=1,NTEST
190   TOTREV(J)=TOTREV(J)+REVARR(IB,J)
      WRITE(6,201) (TOTREV(J),J=1,NSTD)
201   FORMAT(//10X,'TOTAL NO. OF REV. ARR.==',8F10.1)
      STOP
      END
```

```
C ***********************TREND********************************C
C--------------------------------------------------------------C
C       THIS PROGRAM IS USED TO APPLY THE MOVING-AVERAGE AND DIFFERENCING
C       HIGH-PASS FILTER TO THE ORIGINAL TIME SERIES.                    C
C--------------------------------------------------------------C
        DIMENSION U(4,16384),UBBK(4,8192)
C--------------------------------------------------------------C
C       NOBLK=NUMBER OF BLOCKS CONSEQUENTLY FILTERED.                    C
C       NDATA=NUMBER OF DATA POINTS TO BE USED AT THE START OF FILTERING
C       PROCESS.                                                         C
C--------------------------------------------------------------C
        NDATA=16384
        NOBLK=43
        NDTBK=NDATA/2
        NHALF=NDTBK/2
        NTS=4
        IB=1
        DATBK=NDTBK
        NEW=NDTBK+1
        DO 1 I=1,NDATA
      1 READ(10,2) U(4,I),U(1,I),U(2,I),U(3,I)
      2 FORMAT(4A4)
        GO TO 2000
   1000 DO 3 I=NEW,NDATA
      3 READ(10,2) U(4,I),U(1,I),U(2,I),U(3,I)
   2000 DO 4 J=1,NTS
      4 UBBK(J,1)=0.0
        DO 5 J=1,NTS
        DO 5 I=1,NDTBK
      5 UBBK(J,1)=UBBK(J,1)+U(J,I)
        DO 6 I=1,NTS
      6 UBBK(I,1)=UBBK(I,1)/DATBK
```

```
      DO 7 I=1,NTS
      J=NDTBK+1
    7 UBBK(I,1)=UBBK(I,1)+(U(I,J)-U(I,1))/DATBK
      DO 8 J=1,NTS
      DO 8 I=2,NDTBK
      K=I-1
      L=NDTBK+I
    8 UBBK(J,I)=UBBK(J,K)+(U(J,L)-U(J,I))/DATBK
      DO 9 K=1,NTS
      DO 9 I=1,NDTBK
      M=I
      J=NHALF+M
    9 U(K,I)=U(K,J)-UBBK(K,I)
      DO 10 I=1,NDTBK
   10 WRITE(11,2) U(4,I),U(1,I),U(2,I),U(3,I)
      DO 11 LL=1,NTS
      DO 11 I=1,NDTBK
      M=I
      J=NDTBK+M
   11 U(LL,I)=U(LL,J)
      IF (IB .EQ. NOBLK) GO TO 5000
      IB=IB+1
      GO TO 1000
 5000 CONTINUE
      WRITE(6,5050) IB
 5050 FORMAT (20X,'NUMBER OF BLOCKS COMPLETED',I4)
      STOP
      END
```

```
C****************************DATP2**************************************C
C---------------------------------------------------------------------C
C             PPPPPP      A       RRRRR    TTTTT    22222              C
C             P   P      A A       R   R     T       2 2               C
C             PPPPPP     A  A      RRRRR     T       2 2               C
C             P         AAAAA      RR        T       2 2               C
C             P         A    A     R RR      T       2 2               C
C             P         A    A     R   R     T      22222              C
C---------------------------------------------------------------------C
C     DATA PROCESSING SYSTEM CALCULATING VARIANCES AND COVARIANCES    C
C     BASED ON THE DATA READ FROM THE TAPE WITH EQUALLY-WEIGHTED      C
C     RUNNING MEAN APPLIED.  SAMPLE MEAN AND BETA ANGLE ARE READ FROM C
C     PREVIOUS PROGRAM. THE PRINTED VALUES ARE THE STATISTICAL VALUES C
C     IN THE MEAN WIND COORDINATE SYSTEM.                             C
C     THE MEANING OF THE CODE NAMES MAY BE READ FROM DATP1.           C
C---------------------------------------------------------------------C
      DIMENSION U(4,8192),COV(43,4,4),UBTOTL(4),SCOV(4,4),TUB(3)
      DIMENSION E1(4,4),UMEAN(4),COVMEN(4,4),TBINT(4)
      DIMENSION XBAR(4),XSUM(4)
      NTS=4
      NDTBK=8192
      NOBLK=43
      BLKNO=NOBLK
      DATBK=NDTBK
      IB=1
      UBTOTL(1)= 6.128789
      UBTOTL(2)= 3.733873
      UBTOTL(3)=16.187836
      UBTOTL(4)=39.109543
      BETOL1= 0.529701
C---------------------------------------------------------------------C
C     SINCE THE MEAN HAS BEEN REMOVED SO WE CALCULATE THE MEAN SQUARE  C
```

```
C       VALUE WHICH SHOULD BE THE VALUE CLOSE TO THE VARIANCES AND         C
C       COVARIANCES                                                        C
C--------------------------------------------------------------------------C
 5000 DO 7 I=1,NDTBK
    7 READ(10,10) U(4,I),U(1,I),U(2,I),U(3,I)
   10 FORMAT(4A4)
C--------------------------------------------------------------------------C
C       HERE THE SMALL NEAR ZERO MEANS ARE CALCULATED AND SUBTRACTED FROM
C       THE DATAS IN THE BLOCK.                                            C
C--------------------------------------------------------------------------C
      DO 81 I=1,NTS
   81 XSUM(I)=0.0
      DO 82 J=1,NTS
      DO 82 K=1,NDTBK
   82 XSUM(J)=XSUM(J) + U(J,K)
      DO 83 I=1,NTS
   83 XBAR(I)=XSUM(I)/NDTBK
      DO 84 J=1,NTS
      DO 84 I=1,NDTBK
   84 U(J,I)=U(J,I)-XBAR(J)
C--------------------------------------------------------------------------C
C       BLOCK VARIANCES AND COVARIANCES ARE CALCULATED IN THE FOLLOWING    C
C--------------------------------------------------------------------------C
      DO 16 K=1,NTS
      DO 16 J=1,NTS
   16 COV(IB,K,J)=0.0
      I=1
   17 DO 18 K=1,NTS
      DO 18 L=1,NTS
   18 COV (IB,K,L)=COV(IB,K,L)+U(K,I)*U(L,I)
      IF(I .EQ. NDTBK) GO TO 191
      I=I+1
```

```
          GO TO 17
  191 DO 19 K=1,NTS
        DO 19 L=1,NTS
   19 COV(IB,K,L)=COV(IB,K,L)/DATBK
        IF (IB .EQ. NOBLK) GO TO 3000
        IB=IB+1
        GO TO 5000
 3000 CONTINUE
C------------------------------------------------------------------C
C    HERE BEGINS THE CALCULATION OF THE SAMPLE VARIANCES AND COVARIANCES
C    FOR THE WHOLE LENGTH OF THE DATA                              C
C    SCOV=SAMPLE VARIANCES AND COVARIANCES                         C
C------------------------------------------------------------------C
        DO 25 K=1,NTS
        DO 25 J=1,NTS
   25 SCOV(K,J)=0.0
        IB=1
   26 DO 27 K=1,NTS
        DO 27 L=1,NTS
   27 SCOV(K,L)=SCOV(K,L)+COV(IB,K,L)
        IF(IB .EQ. NOBLK) GO TO 28
        IB=IB+1
        GO TO 26
   28 DO 29 K=1,NTS
        DO 29 L=1,NTS
   29 SCOV(K,L)=SCOV(K,L)/BLKNO
C------------------------------------------------------------------C
C    HERE BEGINS THE TRANSFORMATION OF MATRIX                      C
C    E1(4,4) IS THE MATRIX TRANSFORMATION FROM THE SENSOR DIRECTION C
C    TO THE MEAN WIND DIRECTION                                    C
C------------------------------------------------------------------C
        DO 43 I=1,NTS
```

```
      UMEAN(I)=0.0
      DO 43 J=1,NTS
      E1(I,J)=0.0
   43 COVMEN(I,J)=0.0
      E1(1,1)=0.57735*COS(BETOL1)
      E1(1,2)=0.57735*SIN(BETOL1)
      E1(1,3)=-0.81650
      E1(2,1)=0.57735*COS(BETOL1)-0.70711*SIN(BETOL1)
      E1(2,2)=0.57735*SIN(BETOL1)+0.70711*COS(BETOL1)
      E1(2,3)=0.40824
      E1(3,1)=0.57735*COS(BETOL1)+0.70711*SIN(BETOL1)
      E1(3,2)=0.57735*SIN(BETOL1)-0.70711*COS(BETOL1)
      E1(3,3)=C.40824
      E1(4,4)=1.0
C----------------------------------------------------------------------C
C     UMEAN(I) IS THE MEAN WIND VELOCITY COMPONENTS & TEMPERATURE       C
C     COVMEN(I,J)IS THE VARIANCES AND COVARIANCES OF WIND TURBULENCE IN
C     THE MEAN WIND DIRECTION.                                          C
C----------------------------------------------------------------------C
      I=1
   46 DO 45 J=1,NTS
      UMEAN(I)=UMEAN(I)+E1(J,I)*UBTOTL(J)
      DO 45 K=1,NTS
      DO 45 L=1,NTS
   45 COVMEN(I,J)=COVMEN(I,J)+E1(K,I)*E1(L,J)*SCOV(K,L)
      IF (I .EQ. NTS) GO TO 47
      I=I+1
      GO TO 46
   47 CONTINUE
C----------------------------------------------------------------------C
C                          WRITTEN STATEMENTS                          C
C----------------------------------------------------------------------C
```

```
      WRITE(6,105)
105 FORMAT(1H1,4X,'BEFORE TRANSFORMATION',27X,'MEAN WIND DIRECTIONS'/)
      WRITE(6,106)
106 FORMAT(2X,'CORRELATION NO.',3X,'SAMPLE VAR. & COVAR.',10X,'VAR.&
     1COVAR.',5X,'VELOCITIES'/)
      DO 107 K=1,NTS
      DO 107 L=1,NTS
107 WRITE(6,108) K,L,SCOV(K,L),COVMEN(K,L),UMEAN(K)
108 FORMAT (7X,I2,3X,I2,8X,F10.3,15X,F10.3,8X,F8.3)
      VTOTL1=SQRT(UBTOTL(1)**2+UBTOTL(2)**2+UBTOTL(3)**2)
      DO 32 I=1,3
  32 TBINT(I)=SQRT(SCOV(I,I))/VTOTL1
      WRITE(6,207)  (TBINT(I),I=1,3)
207 FORMAT(///2X,'TURBULENT INTENSITIES=',3F10.6)
      DO 113 I=1,3
113 TUB(I)=SQRT(COVMEN(I,I))/VTOTL1
      WRITE(6,114) (TUB(I),I=1,3)
114 FORMAT (///2X,'TURBULENT INTENSITY IN THE MEAN WIND DIRECTION=',
     13F8.4)
      STOP
      END
```

```
C*****************************TRANSFORM******************************C
C-----------------------------------------------------------------------C
C--------TRANSFORM THE DATA FROM THE SENSOR ORIENTED DIRECTION TO THE   C
C -------MEAN WIND DIRECTION FOR SPECTRUM CALCULATIONS-1192 & 1193-----C
C     THE MEANING OF EACH CODE NAME MAY BE SEEN FROM DATP1.            C
C-----------------------------------------------------------------------C
      DIMENSION U(4,8192),V(4,8192),E1(4,4)
      NTS=4
      NDTBK=8192
      NOCHK=1
      NOBLK=38
      BETOL1= 0.6165
C ----------------------------------TRANSFORMATIONS----------------------C
      DO 3 I=1,NTS
      DO 3 J=1,NTS
    3 E1(I,J)=0.0
      E1(1,1)=0.57735*COS(BETOL1)
      E1(1,2)=0.57735*SIN(BETOL1)
      E1(1,3)=-C.81650
      E1(2,1)=0.57735*COS(BETOL1)-0.70711*SIN(BETOL1)
      E1(2,2)=0.57735*SIN(BETOL1)+0.70711*COS(BETOL1)
      E1(2,3)=0.40824
      E1(3,1)=0.57735*COS(BETOL1)+0.70711*SIN(BETOL1)
      E1(3,2)=0.57735*SIN(BETOL1)-0.70711*COS(BETOL1)
      E1(3,3)=0.40824
      E1(4,4)=1.0
 1000 DO 1 I=1,NDTBK
    1 READ(10,10) U(4,I),U(1,I),U(2,I),U(3,I)
   10 FORMAT(4A4)
      DO 2 I=1,NTS
      DO 2 J=1,NDTBK
    2 V(I,J)=0.0
```

```
      I=1
   46 DO 45 K=1,NOTBK
      DO 45 J=1,NTS
   45 V(I,K)=V(I,K) + E1(J,I)*U(J,K)
      IF (I .EQ. NTS) GO TO 47
      I=I+1
      GO TO 46
   47 CONTINUE
      DO 9 I=1,NOTBK
    9 WRITE(11,11) V(4,I),V(1,I),V(2,I),V(3,I)
   11 FORMAT (4A4)
      IF (NOCHK .EQ. NOBLK)   GO TO 2000
      NOCHK=NOCHK+1
      GO TO 1000
 2000 CONTINUE
      WRITE(6,999) NOCHK
  999 FORMAT(5X,'NUMBER OF BLOCKS TRANSFORMED',I5)
      STOP
      END
```

```
C*****************************POWER  SPECTRUM***********************************C
C-----------------------------------------------------------------------------C
C     THIS PROGRAM CALCULATES THE POWER SPECTRAL DENSITY ESTIMATES        C
C     INCLUDING THE DATA TAPERING, FAST FOURIER TRANSFORM AND SMOOTHING
C     TECHNIQUES.                                                         C
C-----------------------------------------------------------------------------C
      DIMENSION U(8192),SP1(4097),SP2(4097),PS11(94),SPP(4097)
      DIMENSION FLEQ(94),FNEQ(94),FMEQ(94)
      DIMENSION F(8192),D(820),H(820)
      DIMENSION C(2049),X(8192),Z(2048),V(8192)
      DIMENSION FREQ(94),FLOG(94),PNORM(94)
      COMPLEX*8 E,X,Z
C-----------------------------------------------------------------------------C
C     NDTBK=NUMBER OF DATA POINTS IN EACH BLOCKED TIME SERIES             C
C     DATBK=NDTBK                                                         C
C     NOBLK=NUMBER OF BLOCKS USED IN THE SPECTRAL ESTIMATE.              C
C     MAVE=NUMBER OF SPECTRAL VALUES AS A RESULT OF COMBINED SMOOTHING C
C     NTS=NUMBER OF TIME SERIES TO BE PRECESSED                          C
C     NOWID=NUMBER OF DIFFERENT DATA WINDOWS TO BE TAPERED               C
C     NCK=CONTROL NUMBER USED FOR NUMBER OF DATA WINDOWS                  C
C     KOUNT=THE CONTROL NUMBER DEPENDS ON THE TIME SERIES NEEDED.        C
C     DIVIS=MONDO=1/10 NUMBER OF TAPERING POINTS                         C
C-----------------------------------------------------------------------------C
      NDTBK=8192
      DATBK=NDTBK
      NHALF=NDTBK/2
      HALFN=NHALF
      MAVE=94
      NP=94
      CN=MAVE
      CC=CN
      CD=CN
```

```
      DT=0.CC5
      NOBLK=43
      BLKNO=NCBLK
      NTS=2
      NCK=1
      NOWID=1
      KOUNT=1
      PI=3.14159
      MODNO=820
      DIVIS=MCDNO
      NHF=NHALF+1
      WRITE(6,201)
  201 FORMAT(1H1,50X,'COSINE TAPERING WINDOW'//)
C-------------------------------------------------------------------C
C     D(I) AND H(I) ARE THE END TAPERING FUNCTION IN COSINE TAPER DATA C
C     WINDOW.  F(I) IS THE NUMBER ONE DATA WINDOW USED FOR TAPERING    C
C-------------------------------------------------------------------C
      DO 12 I=1,NDTBK
      P=I
   12 F(I) = 1.0-((P-(DATBK-1.0)/2.0)/((DATBK+1.0)/2.0))**2
      DO 14 I=1,MCDNO
      P=I
   14 D(I)=C.5*(1.0-CCS(PI*P/DIVIS))
      DO 16 I=1,MCDNO
      P=I
   16 H(I)=C.5*(1.0-CCS(PI*(DATBK-P)/DIVIS))
C-------------------------------------------------------------------C
C     THIS PART CALCULATES THE FREQUENCIES,DF IS THE LOWEST           C
C     CNYC IS THE NYQUIST FREQUENCY.  BANDWD=BANDWIDTH                 C
C     FLEQ=FREQ=FNEQ=FMEQ=DIFFERENT REPRESENTATIONS OF FREQUENCY VALUES
C-------------------------------------------------------------------C
      DF=1.0/((DATBK*DT)
```

```
      DNYQ=1.C/(2.0*DT)
      BANDWD=CN*DF
      D1=DF
      D2=D1
      D3=D2
      DO 66  I=1,8
      P=I
   66 FLEQ(I)=P*DF
      DO 61  I=9,38
      P=I
      Q=P-6.0
   61 FLEQ(I)= (4.0*(Q-1.0) + 2.5)*DF
      DO 62  I=39,62
      Q=I
      P=Q-6.0
   62 FLEQ(I)=(16.0*(P-25.0) +9.5)*D1
      DC 63  I=63,86
      P=I
      R=P-6.0
   63 FLEQ(I)= (64.0*(R-49.0) +33.5)*D2
      DO 64  I=87,94
      R=I
      SS=R-6.0
   64 FLEQ(I)= (256.0*(SS-73.0) +129.5)*D3
      DO 65  I=1,NP
      FREQ(I)=FLEQ(I)
      FNEQ(I)=FLEQ(I)
   65 FMEQ(I)=FLEQ(I)
C-----------------------------------------------------------------C
C     DATA READING FROM TAPE                                      C
C     KOUNT=THE CONTROL VALUES USED TO READ DIFFERENT DATA SETS   C
C-----------------------------------------------------------------C
```

```
      DO 104 I=1,NHF
  104 SP2(I)=C.0
 4000 IB=1
      GO TO (1,2,3), KOUNT
    1 READ (10,11) U
   11 FORMAT(A4)
      GO TO 1CCC
    2 REWIND 1C
    4 READ(10,21) U
   21 FORMAT(4X,A4)
      GO TO 1000
    3 REWIND 10
    5 READ(1C,31) U
   31 FORMAT(12X,A4)
 1000 CONTINUE
C------------------------------------------------------------------C
C     FILTERING OF THE TIME SERIES WITH MOVING AVERAGE ALREADY APPLIED C
C     TO ADJUST THE TIME SERIES TC NEAR ZERO MEAN.  SMALL MEAN VALUES  C
C     ARE AGAIN CALCULATED AND SUBTRACTED FRCM THE VALUES OF DATA POINTS
C     IN EACH BLOCK.
C------------------------------------------------------------------C
      XSUM=0.0
      DO 81 I=1,NDTBK
   81 XSUM =U(I) +XSUM
      XBAR=XSUM/DATBK
      DO 82 I=1,NDTBK
   82 U(I)=U(I) -XBAR
C------------------------------------------------------------------C
C     STATEMENTS USED TC MULTIPLY DIFFERENT WINDOWS                  C
C------------------------------------------------------------------C
      GO TO (144,145),NCWID
  144 DO 15 I=1,MCDNO
```

```
   15 U(I)=U(I)*C(I)
      DO 17 I=1,MCDNO
      K=I+7372
   17 U(K)=U(K)*H(I)
      GO TO 500
  145 DO 18 K=1,NDTBK
   18 U(K)=U(K)*F(K)
  500 CONTINUE
C----------------------------------------------------------------------C
C        CALCULATE THE FOURIER COEFFIENTS BY USING FAST FOURIER TRANSFORM C
C----------------------------------------------------------------------C
      DO 99 K=1,NDTBK
   99 V(K) = 0.0
      CALL FFT (U,V,X)
C----------------------------------------------------------------------C
C        CALCULATE THE SPECTRAL VALUES TOTALING 4097 POINTS.  THESE VALUES
C        ARE ADJUSTED BY A SCALE FACTOR DUE TO COSINE TAPERING. LOOP 103   C
C        IS TO SUMMING SEGMENTLY ALL THE BLOCKED SPECTRAL VALUES.  LOOP 109
C        IS TO AVERAGE THEM.  SPP(I) ARE THE VALUES SAME AS SP2(I).        C
C----------------------------------------------------------------------C
      DO 102 I=1,NHF
  102 SP1(I)=2.0*DT*(REAL( X ( I ))**2+AIMAG( X ( I ))**2)/DATBK
      IF (NOWID .NE. 1) GO TO 98
      DO 101 K=1,NHF
  101 SP1(K) =(1.0/0.875)*SP1(K)
   98 DO 103 I=1,NHF
  103 SP2(I)=SP2(I)+SP1(I)
      IF (IB .EQ. NCBLK) GO TO 6000
      IB=IB+1
      GO TO (1,4,5), KCUNT
 6000 CONTINUE
      DO 109 I=1,NHF
```

```
139 SP2(I)=SP2(I)/BLKNO
    DO 121 I=1,NHF
121 SPP(I)=SP2(I)
    WRITE(6,222)  (SP2(I),I=1,NHF)
222 FORMAT(5X,10F10.4)
C--------------------------------------------------------------------C
C      FOR FREQUENCY SMOOTHING,THE ESTIMATED SPECTRUM MAY BE CONSIDERED C
C      AS REPRESENTING THE MIDPOINT OF THE FREQUENCY INTERVAL
C      SINCE ONLY HALF NUMBER OF THE POINTS ARE UNIQUE AFTER TRASFORM   C
C      THE SPECTRAL AVERAGE IS PERFORMED BASED UPON THE TOTAL OF 4096   C
C      VALUES.  CONSEQUENTLY 94 SMOOTHED SPECTRAL VALUES ARE CALCULATED.
C--------------------------------------------------------------------C
    DO 22 I=9,94
 22 PS11(I)=0.0
    DO 71 K=2,9
    J=K-1
 71 PS11(J)=SP2(K)
    L=10
    MA=13
    M4=4
    K=9
 24 DO 23 I=L,MA
 23 PS11(K)=PS11(K)+SPP(I)
    IF (K .EQ. 38) GO TO 25
    K=K+1
    L=L+M4
    MA=MA+M4
    GO TO 24
 25 CONTINUE
    DO 42 J=9,38
 42 PS11(J)=PS11(J)/4.0
    L=130
```

```
      MB=145
      M16=16
      K=39
   52 DO 53 I=L,MB
   53 PS11(K)=PS11(K)+SPP(I)
      IF (K .EC. 62) GO TO 54
      K=K+1
      L=L+M16
      MB=MB+M16
      GO TO 52
   54 CONTINUE
      DO 43 J=39,62
   43 PS11(J)=PS11(J)/16.C
      L=514
      MC=577
      M64=64
      K=63
   55 DO 56 I=L,MC
   56 PS11(K)=PS11(K)+SPP(I)
      IF (K .EC. 86) GC TO 57
      K=K+1
      L=L+M64
      MC=MC+M64
      GO TO 55
   57 CONTINUF
      DO 44 J=63,86
   44 PS11(J)=PS11(J)/64.0
      L=2050
      MD=2305
      M256=256
      K=87
   58 DO 59 I=L,MD
```

```
   59 PS11(K)=PS11(K)+SPP(I)
      IF (K .EQ. 94) GO TO 60
      K=K+1
      L=L+M256
      MD=MD+M256
      GO TO 58
   60 CONTINUE
      DO 45 J=87,94
   45 PS11(J)=PS11(J)/256.C
      DO 27 LL=1,NP
   27 FLOG(LL)=ALCG(FREG(LL))
      DO 28 I=1,NP
   28 PNORM(I)=FREQ(I)*PS11(I)
C----------------------------------------------------------------------C
C      ALL THE WRITTEN STATEMENT                                        C
C----------------------------------------------------------------------C
      IF (NOWID .EQ. 2 .AND. KCUNT .EQ. 1) GO TO 32
      GO TO 36
   32 WRITE(6,33)
   33 FORMAT(1H1,50X,'WINDOW NUMBER 1'//)
   36 CONTINUE
      WRITE(6,1C6)
  106 FORMAT (10X,'SMOOTHED SPECTRUM',5X,'FREQUENCY',5X,'FREQ. MULTPID
     1SPECTRUM',5X,'LOG CF FREQ.'/)
      DC 107 I=1,NP
  107 WRITE (6,1C8) PS11(I),FREQ(I),PNORM(I),FLCG(I)
  108 FORMAT (14X,F10.4,8X,F8.4,14X,F10.4,8X,F8.4)
C----------------------------------------------------------------------C
C      THE CONTROLLED VALUE CF NTS WILL CBTAIN THE CALCULATICNS OF      C
C      DIFFERENT NUMBER CF TIME SERIES.  THE CONTROLLED VALUE UF NCK    C
C      WILL CALCLLATE DIFFERENT DATA WINDCWS.                           C
C----------------------------------------------------------------------C
```

```
      IF (KCUNT .EQ. NTS) GO TO 3000
      KCUNT=KCUNT+1
      DO 110 I=1,NHF
  110 SP2(I)=0.0
      GO TO 4000
 3000 CONTINUE
      IF (NCWID .EQ. NCK) GO TO 37
      NOWID=NCWID+1
      DO 111 I=1,NHF
  111 SP2(I)=0.0
      REWIND 10
      KOUNT=1
      GO TO 4000
   37 CONTINUE
      STOP
      END
      SUBROUTINE FFT (U,V,X)
      IMPLICIT REAL*4(A-H,P-Z)
      DIMENSION C(2049),X(8192),Z(2048),U(8192),V(8192)
      COMPLEX*8 E,X,Z
C-----------------------------------------------------------------C
C     N = TOTAL NO. CF DATA
C     NS =   STAGE NO .
C     NJ = TOTAL NO. OF ADDITION ( AND SUBTRACTION ) STEPS IN EACH STAGE
C     NU = TOTAL NO. OF ADDITIONS ( OR SUBT. ) IN ONE ADDITION STEP
C     IA = STARTING NO. OF EACH ADDITION STEP
C     NT = ENDING NC. OF EACH ADDITION STEP
C     J = ADDITION STEP NC. IN EACH STAGE
C     I , KA = SUBSCRIPT OF NEW X IN EACH STAGE
C       INVERT=1 IS USED TO OBTAIN THE INVERSE FOURIER TRANSFORM. FOR ANY
C       OTHER NUMBERS OF INVERT INDICATES FOURIER TRANSFORM.           C
C-----------------------------------------------------------------C
```

```
      INVERT=3
      N=8192
      NN=N/2
      NM=NN/2
      KK=NN+1
      MM=NM+1
      CALL COSINE (N,NN,NM,C)
      DO 12 I=1,N
   12 X(I)=CMPLX(U(I),V(I))
      NS=1
      NJ=NN
      NU=1
    1 NI=NJ/2
      IA=1
      NT=NU
      DO 71 L=1,NM
      LA=L+NM
   71 Z(L)=X(LA)
C------------------------------------------------------------------C
      NA=MM
      NB=1
      KA=KK
C
      DO 2 J=1,NJ
      NA=NA-NU
      NB=NB+NU
      IF (J-NI) 41,42,43
   41 E=CMPLX(C(NA),-C(NB))
      GO TO 42
   43 E=CMPLX(-C(NA),-C(NB))
   42 DO 9 I=IA,NT
      IF (J.LE.NI) GO TO 81
```

```
      IC=I-NM
      IB=I+NN
      KA=KA+1
      K=KA+NU
      X(KA)=Z(IC)+X(IB)
      X(K )=(Z(IC)-X(IB))*E
      GO TO 9
81    IC=MM-I
      IB=IC+NN
      KA=KA-1
      K=KA-NU
      IF (J.EC.NI) GO TC 82
      X(KA)=(X(IC)-X(IB))*E
      GO TO 83
82    X(KA)=X(IC)-X(IB)
83    X(K)=X(IC)+X(IB)
 9    CONTINUE
      IA=IA+NU
      NT=NT+NU
      IF (J.NE.NI) GO TO 22
      NA=MM+NU
      NB=1-NU
      KA=NN
      GO TO 2
22    KA=K
 2    CONTINUE
C-----------------------------------------------------------------C
      IF (NJ.EQ.2) GO TO 11
      NU=2**NS
      NS=NS+1
      NJ=NI
      GO TO 1
```

```
   11 DO 21 I=1,NN
      IB=I+NN
      E=X(I)+X(IB)
      X(IB)=X(I)-X(IB)
   21 X(I)=E
C-------------------------------------------------------------------C
C     THE NEXT EIGHT CARDS ARE USED CNLY IF INVERSE FOURIER TRANSFORM IS
C     NECESSARY. IN THIS CASE, THIS SUBROUTINE IS USED TO OBTAIN A REAL
C     TIME SERIES U(I) INSTEAD OF USING FOR SPECTRAL CALCULATIONS.     C
C-------------------------------------------------------------------C
      IF (INVERT .EQ. 1) GO TO 27
      GO TO 28
   27 DO 23 I=1,N
   23 X(I)=X(I)/N
      U (1) = REAL (X(1))
      DO 25 I=2,N
   25 U (I) =REAL(X(N-I+2))
   28 CONTINUE
      RETURN
      END
      SUBROUTINE COSINE (N,NN,NM,C)
      DIMENSION C(2049)
      TN=NN
      ANG=3.1415927/TN
      INTB=N/8
      CS=COS (ANG)
      SN=SIN (ANG)
      C(1)=1.
      II=NM+1
      C(II)=0.
      DO 39 J=1,INTB
      JI=J+1
```

```
      JJ=NM+2-J
      C(JI)=C(J)*CS-C(JJ)*SN
      JM=NM+1-J
   39 C(JM)=C(J)*SN+C(JJ)*CS
      RETURN
      END
```

```
C*******************************CROSS SPECTRUM*****************************
C-------------------------------------------------------------------------C
C      THIS PROGRAM CALCULATES THE POWER SPECTRUM, CO-SPECTRUM, QUADRATU-
C      RE SPECTRUM, CROSS SPECTRUM, PHASE ANGLE AND COHERENCY FUNCTION   C
C      BY GOING THROUGH DATA TAPERING, SPECTRAL SMOOTHING TECHNIQUES.    C
C-------------------------------------------------------------------------C
       DIMENSION U(8192),V(8192),SPA(4097),SPB(4097),SPC(4097),SPD(4097),
      1SP1(4097),SP2(4097),CSP(4097),QSP(4097),FREQ(94),FLOG(94)
       DIMENSION AA(1),BB(1),URE(4097),UIM(4097),VRE(4097),VIM(4097)
       DIMENSION F(8192),D(820),H(820)
       DIMENSION C(2049),X(8192),Z(2048)
       DIMENSION PS11(94),PS22(94),CS12(94),QS12(94)
       DIMENSION AMP12(94),COH12(94),PHS(94),DEGPS(94)
       DIMENSION PNOM1(94),PNOM2(94),CSNOM(94),QSNOM(94)
       DIMENSION FLEQ(94),FNEQ(94),FMEQ(94)
       DIMENSION CROS(94),CRSNM(94),CRS(10)
       COMPLEX AA,BB
       COMPLEX*8 E,X,Z
C-------------------------------------------------------------------------C
C      EXPLANATION OF THE DIFFERENT SYMBOLS USED IN THIS PROGRAM CAN BE C
C      OBTAINED FROM THE POWER SPECTRUM PROGRAM.                         C
C-------------------------------------------------------------------------C
       NDTBK=8192
       DATBK=NDTBK
       NHALF=NDTBK/2
       HALFN=NHALF
       NHF=NHALF+1
       MAVE=54
       NP=94
       CN=MAVE
       NOBLK=43
       BLKNO=NOBLK
```

```
      NTS=1
      NCK=1
      NOWID=1
      KOUNT=1
      DT=0.005
      PI=3.14159
      MCDNO=820
      DIVIS=MCDNC
      WRITE(6,201)
  201 FORMAT(1H1,50X,'COSINE TAPERING WINDOW'//)
C---------------------------------------------------------------C
C     WINDOW CALCULATIONS                                       C
C---------------------------------------------------------------C
      DO 12 I=1,NDTBK
      P=I
   12 F(I) = 1.0-((P-(DATBK-1.0)/2.0)/((DATBK+1.0)/2.0))**2
      DO 14 I=1,MCDNO
      P=I
   14 D(I)=C.5*(1.0-COS(PI*P/DIVIS))
      DO 16 I=1,MCDNO
      P=I
   16 H(I)=0.5*(1.0-COS(PI*(DATBK-P)/DIVIS))
C---------------------------------------------------------------C
C     THIS PART CALCULATES THE FREQUENCIES                      C
C---------------------------------------------------------------C
      DF=1.0/(DATBK*DT)
      CNYQ=1.C/(2.0*DT)
      BANDWC=CN*DF
      C1=DF
      C2=C1
      D3=D2
      DO 66 I=1,8
```

```
      P=I
   66 FLEQ(I)=P*DF
      DO 61 I=5,38
      PPP=I
      Q=PPP-6.0
   61 FLEQ(I)= (4.0*(Q-1.0) + 2.5)*DF
      DO 62 I=39,62
      SS=I
      P=SS-6.0
   62 FLEQ(I)=(16.0*(P-25.0) +9.5)*D1
      DO 63 I=63,86
      RLP=I
      R=RLP-6.0
   63 FLEQ(I)= (64.0*(R-49.0) +33.5)*D2
      DO 64 I=87,94
      PQR=I
      SS=PQR-6.0
   64 FLEQ(I)= (256.0*(SS-73.0) +129.5)*D3
      DO 65 I=1,NP
      FREQ(I)=FLEC(I)
      FNEQ(I)=FLEC(I)
   65 FMEQ(I)=FLEC(I)
      DO 27 LL=1,NP
   27 FLOG(LL) = ALOG(FREQ(LL))
C-----------------------------------------------------------C
C     DATA READING FROM TAPE                                C
C-----------------------------------------------------------C
      DO 104 I=1,NHF
      SP1(I)=0.0
      SP2(I)=0.0
      CSP(I)=0.0
  104 QSP(I)=0.0
```

```
4000 IB=1
     GO TO (1,2,3), KOUNT
C----------------CROSS SPECTRUM FOR U AND W ----------------------C
   1 DO 10 I=1,NCTBK
  10 READ (10,11) U(I),V(I)
  11 FORMAT(4X,A4,4X,A4)
     GO TO 1000
C----------------CROSS SPECTRUM FOR U AND V ----------------------C
   2 REWIND 10
   4 DO 20 I=1,NCTBK
  20 READ(10,21) U(I),V(I)
  21 FORMAT(4X,2A4)
     GO TO 1000
C----------------CROSS SPECTRUM FOR T AND W ----------------------C
   3 REWIND 10
   5 DO 30 I=1,NCTBK
  30 READ(10,31) U(I),V(I)
  31 FORMAT(A4,8X,A4)
1000 CONTINUE
C---------------------------------------------------------------C
C    NEAR ZERO MEAN VALUES ARE REMOVED FROM THE FILTERED TIME SERIES. C
C---------------------------------------------------------------C
     XSUMU=0.0
     XSUMV=0.0
     DO 81 I=1,NDTBK
     XSUMU =U(I) +XSUMU
  81 XSUMV =V(I) +XSUMV
     XBARU=XSUMU/DATBK
     XBARV=XSUMV/DATBK
     DO 82 I=1,NDTBK
     U(I) =U(I) -XBARU
  82 V(I)=V(I) -XBARV
```

```
C-----------------------------------------------------------------------C
C      APPLY DIFFERENT DATA WINDOWS TC THE DATA POINTS.                  C
C-----------------------------------------------------------------------C
       GO TO (144,145),NCWID
  144  DO 15 I=1,MCCNC
       V(I)=V(I)*D(I)
   15  U(I)=U(I)*D(I)
       DO 17 I=1,MCDNO
       K=I+7372
       V(K)=V(K)*H(I)
   17  U(K)=U(K)*H(I)
       GO TO 5CC
  145  DO 18 K=1,NDTBK
       V(K)=V(K)*F(K)
   18  U(K)=U(K)*F(K)
  500  CONTINUE
C-----------------------------------------------------------------------C
C      THE FAST FOURIER TRANSFORM IS CALCULATED BY STORING U(I) IN THE   C
C      REAL PART AND V(I) IN THE IMAGINARY PART.                         C
C-----------------------------------------------------------------------C
       CALL FFT (U,V,X)
       AA(1)=CMPLX( REAL(X(1)),0.0)
       BB(1)=CMPLX(AIMAG(X(I)),0.0)
       URE(1)=REAL(AA(1))
       UIM(1)=AIMAG(AA(1))
       VRE(1)=REAL(BB(1))
       VIM(1)=AIMAG(BB(1))
       DO 444 I=2,NHF
       K=NDTBK-I+2
       URE(I) = REAL(( X ( I ) + X (K) )/2.0)
       UIM(I) =AIMAG(( X ( I ) - X (K) )/2.C)
       VRE(I) =AIMAG(( X ( I ) + X (K) )/2.0)
```

```
  444 VIM(I) =-REAL(( X ( I ) - X (K) )/2.0)
      DO 102 I=1,NHF
      SPA(I)=2.0*DT*(URE(I)**2 + UIM(I)**2)/DATBK
      SPB(I)=2.0*DT*(VRE(I)**2 + VIM(I)**2)/DATBK
      SPC(I)=2.0*DT*(URE(I)*VRE(I) + UIM(I)*VIM(I))/DATBK
  102 SPD(I)=2.0*DT*(URE(I)*VIM(I) - UIM(I)*VRE(I))/DATBK
      IF (NOWID .NE. 1) GO TO 98
      DO 101 K=1,NHF
      SPA(K)=(1.0/0.875)*SPA(K)
      SPB(K)=(1.0/0.875)*SPB(K)
      SPC(K)=(1.0/0.875)*SPC(K)
  101 SPD(K)=(1.0/0.875)*SPD(K)
   98 DO 103 I=1,NHF
      SP1(I)=SP1(I) + SPA(I)
      SP2(I)=SP2(I) + SPB(I)
      CSP(I)=CSP(I) + SPC(I)
  103 QSP(I)=QSP(I) + SPD(I)
      IF (IB .EQ. NOBLK) GO TO 6000
      IB=IB+1
      GO TO (1,4,5), KOUNT
 6000 CONTINUE
C----------------------------------------------------------------------C
C     FOR SEGMENT SMOOTHING, SUMMING NUMBER OF THE CORRESPONDING POINTS
C     IN EACH DESIGNATED BLOCKS. ALSO AVERAGED THE SUMMED VALUES.      C
C----------------------------------------------------------------------C
      DO 109 I=1,NHF
      SP1(I)=SP1(I)/BLKNO
      SP2(I)=SP2(I)/BLKNO
      CSP(I)=CSP(I)/BLKNO
  109 QSP(I)=GSP(I)/BLKNO
C----------------------------------------------------------------------C
C     FOR FREQUENCY SMOOTHING,THE ESTIMATED SPECTRUM MAY BE CONSIDERED C
```

```
C       AS REPRESENTING THE MIDPOINT OF THE FREQUENCY INTERVAL
C       SINCE ONLY HALF NUMBER OF THE POINTS ARE UNIQUE AFTER TRASFORM   C
C       THE SPECTRAL AVERAGE IS PERFORMED BASED UPON THE TOTAL OF 4096   C
C       POINTS AND TOTAL OF 94 POINTS ARE OBTAIED                        C
C----------------------------------------------------------------------C
        DO 113 I=1,10
  113 CRS(I) = SQRT(CSP(I)**2 + QSP(I)**2)
        DO 8888 I=1,10
 8888 WRITE(6,9999)  SP1(I),SP2(I),CRS(I),CSP(I),QSP(I)
 9999 FORMAT(10X,5F16.4)
        DO 22 I=9,NP
        PS11(I)=0.0
        PS22(I)=0.0
        CS12(I)=C.0
   22 QS12(I)=0.0
        DO 71 K=2,9
        J=K-1
        PS11(J)=SP1(K)
        PS22(J)=SP2(K)
        CS12(J)=CSP(K)
   71 QS12(J)=QSP(K)
        L=10
        MA=13
        M4=4
        K=9
   24 DO 23 I=L,MA
        PS11(K)=PS11(K)+SP1(I)
        PS22(K)=PS22(K)+SP2(I)
        CS12(K)=CS12(K)+CSP(I)
   23 QS12(K)=QS12(K)+QSP(I)
        IF (K .EQ. 38) GO TO 25
        K=K+1
```

```
      L=L+M4
      MA=MA+M4
      GO TO 24
 25 CONTINUE
      DO 42 J=9,38
      PS11(J)=PS11(J)/4.0
      PS22(J)=PS22(J)/4.0
      CS12(J)=CS12(J)/4.0
 42 QS12(J)=QS12(J)/4.0
      L=130
      MB=145
      M16=16
      K=39
 52 DO 53 I=L,MB
      PS11(K)=PS11(K)+SP1(I)
      PS22(K)=PS22(K)+SP2(I)
      CS12(K)=CS12(K)+CSP(I)
 53 QS12(K)=QS12(K)+QSP(I)
      IF (K .EQ. 62) GO TO 54
      K=K+1
      L=L+M16
      MB=MB+M16
      GO TO 52
 54 CONTINUE
      DO 43 J=39,62
      PS11(J)=PS11(J)/16.0
      PS22(J)=PS22(J)/16.0
      CS12(J)=CS12(J)/16.0
 43 QS12(J)=QS12(J)/16.0
      L=514
      MC=577
      M64=64
```

```
      K=63
55 DO 56 I=L,MC
   PS11(K)=PS11(K)+SP1(I)
   PS22(K)=PS22(K)+SP2(I)
   CS12(K)=CS12(K)+CSP(I)
56 QS12(K)=QS12(K)+QSP(I)
   IF (K .EQ. 86) GO TO 57
   K=K+1
   L=L+M64
   MC=MC+M64
   GO TO 55
57 CONTINUE
   DO 44 J=63,86
   PS11(J)=PS11(J)/64.0
   PS22(J)=PS22(J)/64.0
   CS12(J)=CS12(J)/64.C
44 QS12(J)=QS12(J)/64.0
   L=2050
   MD=2305
   M256=256
   K=87
58 DO 59 I=L,MD
   PS11(K)=PS11(K)+SP1(I)
   PS22(K)=PS22(K)+SP2(I)
   CS12(K)=CS12(K)+CSP(I)
59 QS12(K)=QS12(K)+QSP(I)
   IF (K .EQ. 94) GO TO 60
   K=K+1
   L=L+M256
   MD=MD+M256
   GO TO 58
60 CONTINUE
```

```
      DO 45 J=87,94
      PS11(J)=PS11(J)/256.0
      PS22(J)=PS22(J)/256.0
      CS12(J)=CS12(J)/256.0
   45 QS12(J)=QS12(J)/256.0
      DO 114 I=1,NP
  114 CROS(I)=SQRT(CS12(I)**2 + QS12(I)**2)
      DO 265 I=1,NP
      AMP12(I)=CS12(I)*CS12(I) + QS12(I)*QS12(I)
  265 PHS(I) = + ATAN(QS12(I)/CS12(I))
      DO 266 I=1,NP
      COH12(I)=AMP12(I)/(PS11(I)*PS22(I))
  266 DEGPS(I)=180.0*PHS(I)/(2.0*PI)
      DO 28 I=1,NP
      PNOM1(I)=FREQ(I)*PS11(I)
      PNOM2(I)=FREQ(I)*PS22(I)
      CRSNM(I) =FREQ(I)*CROS(I)
      CSNOM(I)=FREQ(I)*CS12(I)
   28 QSNOM(I)=FREQ(I)*QS12(I)
C----------------------------------------------------------------------C
C     ALL THE WRITTEN STATEMENT                                        C
C----------------------------------------------------------------------C
      IF (NOWID .EQ. 2 .AND. KOUNT .EQ. 1) GO TO 32
      GO TO 36
   32 WRITE(6,33)
   33 FORMAT(1H1,50X,'WINDOW NUMBER 1'//)
   36 CONTINUE
      WRITE(6,106)
  106 FORMAT(5X,'SMOD PCWER SPECT 1',5X,'SMOD POWER SPECT 2',5X,'COSPEC'
     1,5X,'QUADSPEC',5X,'COHERENCY',5X,'PHASE(DEG)',5X,'FREQ',2X,'CROSS
     2SPEC'/)
      DO 107 I=1,NP
```

```
  107 WRITE(6,108) PS11(I),PS22(I),CS12(I),QS12(I),COH12(I),DEGPS(I),
     1FREQ(I),CROS(I)
  108 FORMAT(10X,F10.4,10X,F10.4,6X,F8.4,6X,F8.4,6X,F8.4,6X,F8.2,4X,F8.4
     1,3X,F8.3)
      WRITE(6,203)
  203 FORMAT(//5X,'FREQ MTPD SPEC 1',5X,'FREQ MUTLD SPEC 2',5X,'FREQ MUT
     1LD COSPEC',5X,'FREQ MUTLD QUADSPEC',5X,'LOG OF FREQ',5X,'FREQ MULT
     2CROSS'/)
      DO 204 I=1,NP
  204 WRITE(6,205) PNOM1(I),PNOM2(I),CSNOM(I),QSNOM(I),FLOG(I),CRSNM(I)
  205 FORMAT(10X,F10.4,15X,F10.4,10X,F10.4,10X,F10.4,10X,F8.4,10X,F8.4)
C-------------------------------------------------------------------------C
C       NTS CONTROLS THE NUMBER OF TIME SERIES BEING CALCULATED.   NCK    C
C       CONTROLS THE NUMBER OF DATA WINDOWS TO BE USED.                   C
C-------------------------------------------------------------------------C
      IF (KOUNT .EQ. NTS) GO TO 3000
      KOUNT=KOUNT+1
      DO 110 I=1,NHF
      SP1(I)=0.0
      SP2(I)=0.0
      CSP(I)=0.0
  110 QSP(I)=0.0
      GO TO 4000
 3000 CONTINUE
      IF (NCWID .EQ. NCK) GO TO 37
      NOWID=NOWID+1
      DO 111 I=1,NHF
      SP1(I)=0.0
      SP2(I)=0.0
      CSP(I)=0.0
  111 QSP(I)=0.0
      REWIND 10
```

```
      KOUNT=1
      GO TO 4000
   37 CONTINUE
      STOP
      END
      SUBROUTINE FFT (U,V,X)
      IMPLICIT REAL*4(A-H,P-Z)
      COMPLEX*8 E,X,Z
      DIMENSICN C(2049),X(8192),Z(2048),U(8192),V(8192)
C                                                                        C
C------------------------------------------------------------------------C
C------------------------------------------------------------------------C
C    N = TOTAL NO. OF DATA
C    NS =   STAGE NC .
C    NJ = TOTAL NO. OF ADDITION ( AND SUBTRACTION ) STEPS IN EACH STAGE
C    NU = TOTAL NO. OF ADDITIONS ( CR SUBT. ) IN ONE ADDITION STEP
C    IA = STARTING NO. OF EACH ADDITION STEP
C    NT = ENDING NO. OF EACH ADDITION STEP
C    J = ADDITION STEP NO. IN EACH STAGE
C    I , KA = SUBSCRIPT OF NEW X IN EACH STAGE
C------------------------------------------------------------------------C
      INVERT=3
      N=8192
      NN=N/2
      NM=NN/2
      KK=NN+1
      DO 12 I=1,N
   12 X(I)=CMPLX(U(I),V(I))
      MM=NM+1
      CALL CCSINF (N,NN,NM,C)
      NS=1
      NJ=NN
```

```
      NU=1
   1  NI=NJ/2
      IA=1
      NT=NU
      DO 71 L=1,NM
      LA=L+NM
  71  Z(L)=X(LA)
C------------------------------------------------------------------------C
      NA=MM
      NB=1
      KA=KK
C------------------------------------------------------------------------C
      DO 2 J=1,NJ
      NA=NA-NU
      NB=NB+NU
      IF (J-NI) 41,42,43
  41  E=CMPLX(C(NA),-C(NB))
      GO TO 42
  43  E=CMPLX(-C(NA),-C(NB))
  42  DO 9 I=IA,NT
      IF (J.LE.NI) GO TO 81
      IC=I-NM
      IB=I+NN
      KA=KA+1
      K=KA+NU
      X(KA)=Z(IC)+X(IB)
      X(K )=(Z(IC)-X(IB))*E
      GO TO 9
  81  IC=MM-I
      IB=IC+NN
      KA=KA-1
      K=KA-NU
```

```
      IF (J.EQ.NI) GO TO 82
      X(KA)=(X(IC)-X(IB))*E
      GO TO 83
   82 X(KA)=X(IC)-X(IB)
   83 X(K)=X(IC)+X(IB)
    9 CONTINUE
      IA=IA+NU
      NT=NT+NU
      IF (J.NE.NI) GO TO 22
      NA=MM+NU
      NB=1-NU
      KA=NN
      GO TO 2
   22 KA=K
    2 CONTINUE
C-----------------------------------------------------------------C
      IF (NJ.EQ.2) GO TO 11
      NU=2**NS
      NS=NS+1
      NJ=NI
      GO TO 1
   11 DO 21 I=1,NN
      IB=I+NN
      E=X(I)+X(IB)
      X(IB)=X(I)-X(IB)
   21 X(I)=E
C-----------------------------------------------------------------C
C     THE FOLLOWING EIGHT STATEMENTS ARE USED ONLY IF INVERSE FOURIER  C
C     TRANSFORM IS NECESSARY IN THIS FFT PROGRAM.                      C
C-----------------------------------------------------------------C
      IF (INVERT .EQ. 1) GO TO 27
      GO TO 28
```

```
27 DO 23 I=1,N
23 X(I)=X(I)/N
   U (1) = REAL (X(1))
   DO 25 I=2,N
25 U (I) =REAL(X(N-I+2))
28 CONTINUE
   RETURN
   END
   SUBROUTINE COSINE (N,NN,NM,C)
   DIMENSION C(2049)
   TN=NN
   ANG=3.1415927/TN
   INTB=N/8
   CS=COS (ANG)
   SN=SIN (ANG)
   C(1)=1.
   II=NM+1
   C(II)=0.
   DO 39 J=1,INTB
   JI=J+1
   JJ=NM+2-J
   C(JI)=C(J)*CS-C(JJ)*SN
   JM=NM+1-J
39 C(JM)=C(J)*SN+C(JJ)*CS
   RETURN
   END
```

```
C**********************SIMULATION*******************************C
C-------------------------------------------------------------C
C       THIS PROGRAM SIMULATES A TIME SERIES BY USING THE VON KARMAN SEMI-
C       EMPIRICAL SPECTRUM BY USING FAST FOURIER TRANSFORM METHOD.      C
C       THE SAMPLING RATE IS 20 SAMPLES PER SECOND TO CREATE THE 32768  C
C       TOTAL NUMBER OF DATA POINTS FOR APPROXIMATELY OF 1638 SECONDS   C
C-------------------------------------------------------------C
        DIMENSION A(32768,1,1), M(3), INV(8192), S(8192), PP(32768)
        COMPLEX A
        UBAR = 40.0
        COEF = SQRT(32768.0*20.0/2.0)
C-------------------------------------------------------------C
C                    THE VON KARMAN SEMI-EMPIRICAL SPECTRUM          C
C       BOTH GAUSS AND HARM ARE SCIENTIFIC SUBROUTINE IN THE IBM PACKAGE
C-------------------------------------------------------------C
        DO 100 I = 2,16384
        AI = I
        FREQ = (AI-1.0)/1638.4
        SPECT = (57.6*UBAR)/
      1 ((1.0+70.78*((360.0*FREQ/UBAR)**2))**(5.0/6.0))
        H = SQRT(SPECT)
        CALL GAUSS (19,0.707,0.0,XI)
        CALL GAUSS (13,0.707,0.0,ETA)
        XREAL = COEF*H*XI
        XIMAG = COEF*H*ETA
        A(I,1,1) = CMPLX(XREAL,XIMAG)
  100 CONTINUE
        DO 200 J = 1,16383
        K = 16385 + J
        L = 16385 - J
        A(K,1,1) = CONJG(A(L,1,1))
  200 CONTINUE
```

```
      A(1,1,1) = CMPLX (32768.0*UBAR,0.0)
      A(16385,1,1) = CMPLX(0.0,0.0)
      M(1) = 15
      M(2) = 0
      M(3) = 0
      CALL HARM(A,M,INV,S,-1,IFERR)
      DO 400 I=1,32768
 400  PP(I)=REAL(A(I,1,1))
      DO 300 N = 1,32768
 300  WRITE(10,50) PP(N)
  50  FORMAT (A4)
      WRITE(6,3000) (PP(I),I=1,32768,32)
3000  FORMAT(5X,12F10.2)
      STOP
      END
```

Dr. Jan N. Yang
Air Force Materials Laboratory
Wright Patterson Air Force Base
Dayton, Ohio, 45433   1 copy

Dr. L. Wittig
Bolt, Beranek and Newman
Accoustic Consultants
50 Moulton Street
Cambridge, Mass 02138   2 copies

Thermo-Systems, Inc.
2500 Cleveland Avenue North
St. Paul, Minnesota 55113

    Dr. L. M. Fingerson   1 copy
    Mr. R. B. Kiland   1 copy

Dr. H. McMahon
Georgia Institute of Technology
School of Aerospace Engineering
Atlanta, Georgia   30332   1 copy

Mr. R. M. Henry
ESSD Planetary Atmospheres Section
National Aeronautics and Space Administration
Langley Research Center-Mail Stop 160
Hampton, Virginia   23365   1 copy